

**MATHEMATICAL MODELLING OF VERTICAL ROLLER
MILLS**

**DİK VALSLİ DEĞİRMENLERİN MATEMATİKSEL
MODELLEMESİ**

DENİZ ALTUN

Prof. Dr. A. HAKAN BENZER

Supervisor

Submitted to Graduate School of Science and Engineering of Hacettepe University

as a Partial Fulfillment to the Requirements

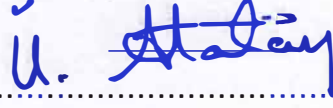
for the Award of the Degree of Doctor of Philosophy

in Mining Engineering

2017

This work named "**Mathematical Modelling of Vertical Roller Mills**" by **DENİZ ALTUN** has been approved as a thesis for the degree of **DOCTOR OF PHILOSOPHY in MINING ENGINEERING** by the below mentioned Examining Committee Members.

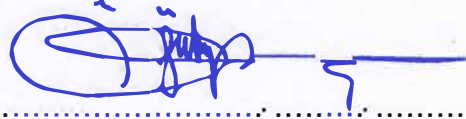
Prof. Dr. M. Ümit ATALAY
Head



Prof. Dr. A. Hakan BENZER
Supervisor



Prof. Dr. Özcan Y. GÜLSOY
Member



Prof. Dr. Volkan BOZKURT
Member



Asst. Prof. Dr. N. Metin CAN
Member



This thesis has been approved as a thesis for the degree of **DOCTOR OF PHILOSOPHY in MINING ENGINEERING** by the Board of Directors of the Institute for Graduate School of Science and Engineering.

Prof. Dr. Menemşe GÜMÜŞDERELİOĞLU
Director of the Institute of
Graduate School of Science and Engineering

YAYINLAMA VE FİKRİ MÜLKİYET HAKLARI BEYANI

Enstitü tarafından onaylanan lisansüstü tezimin/raporumun tamamını veya herhangi bir kısmını, basılı (kağıt) ve elektronik formatta arşivleme ve aşağıda verilen koşullarla kullanıma açma iznini Hacettepe üniversitesine verdiğimi bildiririm. Bu izinle Üniversiteye verilen kullanım hakları dışındaki tüm fikri mülkiyet haklarım bende kalacak, tezimin tamamının ya da bir bölümünün gelecekteki çalışmalarda (makale, kitap, lisans ve patent vb.) kullanım hakları bana ait olacaktır.

Tezin kendi orijinal çalışmam olduğunu, başkalarının haklarını ihlal etmediğimi ve tezimin tek yetkili sahibi olduğumu beyan ve taahhüt ederim. Tezimde yer alan telif hakkı bulunan ve sahiplerinden yazılı izin alınarak kullanması zorunlu metinlerin yazılı izin alarak kullandığımı ve istenildiğinde suretlerini Üniversiteye teslim etmeyi taahhüt ederim.

- Tezimin/Raporumun tamamı dünya çapında erişime açılabilir ve bir kısmı veya tamamının fotokopisi alınabilir.**

(Bu seçenekle teziniz arama motorlarında indekslenebilecek, daha sonra tezinizin erişim statüsünün değiştirilmesini talep etmeniz ve kütüphane bu talebinizi yerine getirirse bile, tezinin arama motorlarının önbelleklerinde kalmaya devam edebilecektir.)

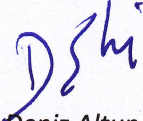
- Tezimin/Raporumun 30.01.2020 tarihine kadar erişime açılmasını ve fotokopi alınmasını (İç Kapak, Özet, İçindekiler ve Kaynakça hariç) istemiyorum.**

(Bu sürenin sonunda uzatma için başvuruda bulunmadığım takdirde, tezimin/raporumun tamamı her yerden erişime açılabilir, kaynak gösterilmek şartıyla bir kısmı ve ya tamamının fotokopisi alınabilir)

- Tezimin/Raporumun tarihine kadar erişime açılmasını istemiyorum, ancak kaynak gösterilmek şartıyla bir kısmı veya tamamının fotokopisinin alınmasını onaylıyorum.**

- Serbest Seçenek/Yazarın Seçimi**

31 / 01 / 2017


Deniz Altun



In loving memory of my father

ETHICS

In this thesis study, prepared in accordance with the spelling rules of Graduate School of Science and Engineering of Hacettepe University,

I declare that

- all the information and documents have been obtained in the base of the academic rules
- all audio-visual and written information and results have been presented according to the rules of scientific standards
- in case of using other works, related studies have been cited in accordance with the scientific standards
- all cited studies have been fully referenced
- I did not do any distortion in the data set
- And any part of this thesis has not been presented as another thesis study at this or any other university

27 / 01 / 2017

Deniz ALTUN

ABSTRACT

MATHEMATICAL MODELLING OF VERTICAL ROLLER MILLS

Deniz Altun

Doctor of Philosophy, Department of Mining Engineering

Supervisor: Prof. Dr. A. Hakan Benzer

January 2017, 148 pages

In this study, it was aimed to develop a mathematical model of vertical roller mills which have found an application in the industry with high energy efficiency. With this aim, pilot scale and industrial scale grinding tests were performed for various materials. During the pilot scale studies, mobile vertical roller mill unit and conventional vertical roller mill were used. Mobile unit has two grinding mode: overflow and airswept. In overflow mode, there is a two-stage air classification system, which is separate from grinding part. This design enables to collect samples from grinding and separation parts, individually. Data obtained from overflow mode grinding tests provided the basis of the modelling studies.

After grinding tests, particle size distributions of the collected samples during the sampling studies and fresh feed samples were subjected to bed breakage tests under compression. As a result of the characterization tests, breakage distribution functions and material indices of the samples calculated to use in the model.

Within the context of the modelling studies, vertical roller mill was divided into two section as grinding and separation. Model parameters were back calculated for each operation. Then, relationships between model parameters and operational variables were investigated. Obtain correlations were defined by mathematical equations and new modelling approach was developed for vertical roller mills. Developed model structure were tested on pilot scale grinding test data by simulation. In consequence of the simulation studies, it was concluded that the estimation accuracy of the developed modelling approach is successful.

Keywords: Vertical roller mill, grinding, size reduction, modelling, simulation

ÖZET

DİK VALSLİ DEĞİRMENLERİN MATEMATİKSEL MODELLEMESİ

Deniz Altun

Doktora, Maden Mühendisliği Bölümü

Tez Danışmanı: Prof. Dr. A. Hakan Benzer

Ocak 2017, 148 sayfa

Bu çalışmada, endüstride yüksek enerji verimliliği ile yer bulan dik valsli değirmenlerin matematiksel modelinin geliştirilmesi amaçlanmıştır. Bu amaçla, farklı malzemeler kullanılarak pilot ve endüstriyel ölçekli öğütme testleri gerçekleştirilmiştir. Pilot ölçekli testlerde, mobil dik değirmen ünitesi olmak ve geleneksel dik valsli değirmen kullanılmıştır. Mobil ünite, geleneksel hava süpürmeli ve üst akımlı öğütme şeklinde çalıştırılmaktadır. Üst akımlı öğütme tipinde, iki aşamalı sınıflandırma sistemi bulunmakta ve sınıflandırıcı öğütme kısmından ayrı olmaktadır. Bu dizayn da öğütme ve sınıflandırma kısımlarından ayrı olarak numune alınmasına olanak sağlamaktadır. Üst akımlı öğütme testlerinden elde edilen veriler modelleme çalışmalarının temelini oluşturmaktadır.

Öğütme testlerinin ardından, örnekleme sırasında devre etrafından alınan numunelerin tane boyu dağılımları belirlenmiş ve taze besleme numuneleri basınç altında yatak kırma testlerine tabi tutulmuşlardır. Karakterizasyon testleri sonucunda

modelde kullanılmak üzere malzemelerin kırılma dağılım fonksiyonları ile malzeme sabiti hesaplanmıştır.

Modelleme çalışmaları kapsamında, dik valsli değirmen öğütme ve sınıflandırma kısımları olmak üzere ikiye ayrılmıştır. Her bir operasyon için model parametreleri hesaplanmıştır. Daha sonra hesaplanan model parametreleri ile operasyonel değişkenler arasındaki ilişkiler incelenmiştir. Kurulan ilişkiler matematiksel eşitliklerle ifade edilerek yeni model yapısı geliştirilmiştir. Geliştirilen model yapısı, pilot ölçekli test verileri üzerinde simülasyon yolu ile test edilmiştir. Simülasyon sonucunda model yaklaşımının tahmin gücünün başarılı olduğu sonucuna varılmıştır.

Anahtar Kelimeler: Dik valsli değirmen, öğütme, boyut küçültme, modelleme, simülasyon

ACKNOWLEDGEMENTS

I would like to express my sincere gratitude to;

My supervisor Prof. Dr. A. Hakan Benzer for his constant encouragement, intellectual guidance, critical comments, valuable suggestions and contributions during this study,

Prof. Dr. Özcan Y. Gülsoy and Asst. Prof. N. Metin Can, the members of the thesis monitoring committee for their valuable contributions,

Dr. Carsten Gerold, the head of Loesche GmbH Ore & Minerals Technology/Process Technology for providing the equipment and his technical contributions, Dr. Mathis Reichert from Loesche GmbH Process Tehnology for his constant support. Assoc. Prof. Dr. Namık Aydoğan for his excellent advises and supports during data collection stage. Assist. Prof. Hakan Dündar and Dr. N. Alper Toprak, my valuable colleagues for helping me in my thesis studies and friendship. Prof. Dr. Abdullah OBUT, for their valuable contributions during thesis writing process.

Fırat Atalay, Emre Yılmazkaya, Özgür Özcan, Güneş Ertunç for their friendship and support. Mustafa Yılmaz department technician, Birgül Atay and Sıddık Yılmazoğlu department secretaries for their help in many ways.

Deepest appreciation to Okay Altun, my husband for patient motivation, believing in me and his enduring love. Aras Altun, my son, my ray of sunshine. My mother, brother and sister for their unrequited love and support. My precious father who is forever in my heart.

TABLE OF CONTENTS

ABSTRACT	i
ÖZET	iii
ACKNOWLEDGEMENTS.....	v
TABLE OF CONTENTS	vi
1. INTRODUCTION.....	1
2. COMPRESSED BED BREAKAGE TECHNOLOGIES	3
2.1. High Pressure Grinding Roll (HPGR)	4
2.2. Horomill®	6
2.3. Vertical Roller Mill (VRM)	7
2.3.1. Chronology of Vertical Roller Mill Development.....	7
2.3.2. Current State of Vertical Roller Mill Technology	15
2.3.3. The Significant Features of Vertical Roller Mills.....	23
2.3.3.1. Specific Energy Consumption	24
2.3.3.2. Feed Particle Size and Moisture Content.....	25
2.3.3.3. Floor Space.....	25
2.3.3.4. Product Quality.....	26
2.3.3.5. Wear	27
2.3.4. Working Principle of Vertical Roller Mills	29
2.3.5. Elements of Vertical Roller Mills	30
2.3.5.1. Grinding Elements.....	30
2.3.5.2. Nozzle Ring.....	31
2.3.5.3. Classifier	32
2.3.6. Design and Operating Parameters Affecting the Vertical Roller Mill Performance.....	33
2.3.7. Modelling Approaches of Vertical Roller Mills	36

3.	EXPERIMENTAL STUDIES	42
3.1.	Pilot Scale Studies	42
3.1.1.	Grinding Tests with OGP _{mobile}	43
3.1.2.	Grinding Tests with LM 3,6	51
3.2.	Industrial Scale Tests	54
3.3.	Material Characterization Studies	58
4.	MASS BALANCE STUDIES	69
4.1.	Pilot Scale Mass Balancing	69
4.2.	Industrial Scale Mass Balancing	83
5.	MODELLING STUDIES	87
5.1.	Modelling of Grinding Section	87
5.1.1.	Application Of Grinding Model To Industrial Scale Data	94
5.2.	Modelling of Separation Section	96
6.	SIMULATION STUDIES	103
6.1.	Simulations for Loesche OGP _{Mobile}	104
6.2.	Simulations for LM 3,6	108
7.	RESULTS AND DISCUSSION	113
8.	CONCLUSIONS	121
9.	RECOMENDATIONS	123
	REFERENCES	124
	APPENDICES	132
	CURRICULUM VITAE	136

1. INTRODUCTION

Comminution is the process by which particles are reduced in size to liberate the valuable minerals for subsequent unit operations e.g., leaching or flotation is produced. The size reduction process is highly energy consuming and is a remarkable component of the world electricity consumption. It is estimated that up to 2-3% of the world's energy is used for crushing and grinding [1]. This ratio has a tendency to increase with the increasing demand for minerals and finer product size [2]. With the introduction of high pressure grinding rolls (HPGRs), high compression technology has become the main interest of the industry because of the positive effects on energy efficiency and downstream processes. Thus, vertical roller mills come to the fore again. Design and introduction of the Horomills into the market in 1993 followed this development in high compression milling technology. Among these equipment, vertical roller mills have an important position in cement and mining industry.

Vertical roller mills are widely used for especially grinding of coal, cement raw materials, clinker and minerals like bauxite, phosphate, magnesite, etc. These machines consist of grinding and separation parts. Grinding operation takes place between the grinding table and the rollers by compression force. Classification operation is carried out by high efficiency dynamic air classifiers inside the vertical roller mill shell. Also, vertical roller mills combine drying, grinding and separation operations in one unit. Beside this property of this system, other features like low specific energy consumption, low wear rates, handling material with high moisture, coarser feed cause gaining an advantage of vertical roller mills over conventional grinding systems.

Control and optimization of the vertical roller mill systems have become important with the widespreading application. Consequently, operational principles and their effects should be analyzed in detail. Conducting modelling and simulation studies are one of the ways of improving the overall efficiency of the circuits. Initially, relationships between operational parameters and outputs like size and flowrate should be investigated to develop a model. Most of the studies intended for filling this gap conducted in this area, were carried out theoretically and at laboratory scale. Also, approaches were developed based on cement grinding data. In a study presented by Kersting [3], a model for vertical roller mill was developed theoretically.

Musto and Dunn [4] carried out laboratory scale tests and investigated the relationships between operational parameters but this approach remained insufficient for industrial scale mills. Material properties and particle size distributions were used in an approach developed by Wang et al. [5], but operating parameters of vertical roller mill were not taken into consideration. When all these studies on vertical roller mill modelling were evaluated, need for developing new approaches by using pilot and industrial data for different materials has risen because of the insufficiency of the existing models.

The main objective of this study determined on the basis of the requirements, is developing mathematical relationships between operational parameters and performance of the vertical roller mill systems. On this opportunity, efficient operation of vertical roller mill systems will be possible by comprehending the process. With this aim, pilot scale and industrial scale tests were performed for various materials such as gold, copper, platinum, polymetallic ores to investigate the relationships between operational parameters. Two different pilot scale vertical roller mills were used in this study. Initially, a new pilot plant vertical roller mill concept developed by Loesche GmbH was used to investigate the process inside the vertical roller mill system. This unit has two grinding mode as airswept and overflow. Airswept mode is similar to congenital vertical roller mills. But, in overflow grinding mode, each operation inside the vertical roller system as grinding and classification was separated and designed as a closed circuit. This concept enables to collect samples around the grinding and classification systems. It makes possible to evaluate the performance of each operation, individually. As a second step of the study, certain parts of pilot scale grinding tests were performed by conventional airswept vertical mills with smaller grinding table diameter. Material properties plays a crucial role in reliable models as design and operational parameters. On the basis of this, material characterization studies were performed for tested materials. First basis of the relationships was developed by pilot scale grinding tests. In the modelling studies, vertical roller mill system was separated into the two sections: grinding and separation. Then, models developed for these operations, individually. Applicability of the developed model to industrial vertical roller mills were tested with industrial scale tests performed with cement clinker. At the end of the study, simulation studies were performed for the verification of the developed model.

2. COMPRESSED BED BREAKAGE TECHNOLOGIES

Energy consumption of comminution circuits is a major problem of the industry. Latest innovations showed that it is possible to reduce the energy consumption of comminution circuits by using energy efficient equipment. Up to now, various types of equipment have been developed. These size reduction equipments are generally classified according to working principle. Particle breakage in size reduction processes are performed by different mechanisms of impact, compression, abrasion and attrition. Breakage mechanisms are illustrated in Figure 2.1.

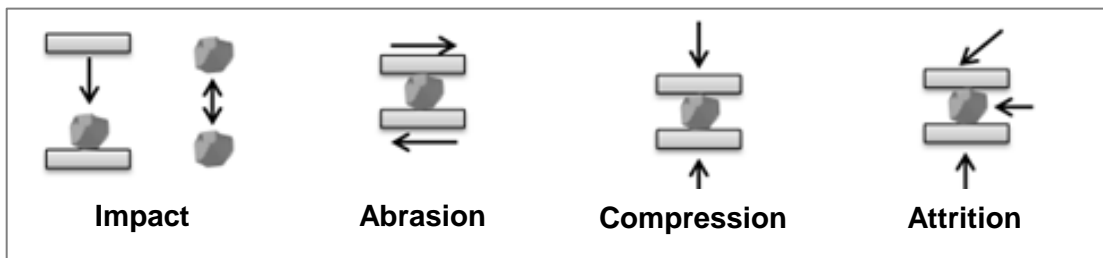


Figure 2.1 Breakage mechanisms

Impact breakage is defined as collision of a particle with other particle or object. Compression breakage occurs by applying compression force to particle bed. Abrasion breakage occurs by rubbing and attrition breakage generally occurs when smaller particles are trapped between coarse particles. Breakage mechanisms affect the particle size distributions of the product. Impact and compression are generally effective on coarse particles while attrition and abrasion mechanisms are effective on fine particles. Among these mechanisms, compression breakage is the most efficient size reduction method. Schönert [6] proposed that energy used for size reduction transferred to material efficiently as a result of the breakage by compression between two plates. For this reason, breakage by compression provide an advantage in terms of energy utilization. On the basis of this, compressed bed breakage technologies as high pressure grinding Rolls, Horomills and vertical roller mills have become more popular. These grinding technologies are explained in the following section. Among these, vertical roller mills are explained more comprehensively because of the scope of this thesis.

2.1. High Pressure Grinding Roll (HPGR)

Schönert and Knobloch [7] stated that the applicability of compression breakage mechanism for high throughputs can be achieved by compressing the particles between two counter rotating rolls. On the basis of this, high pressure grinding roll was developed and the first industrial scale application was carried out in cement industry [8,9]. With the introduction of HPGRs, high compression technology has become the main interest of the industry because of the positive effects on energy efficiency and downstream processes [10-13]. Remarkable features of HPGRs can be listed as below.

- HPGR produces more fine material at a given crush size than in conventional crushers
- At higher pressures, HPGR creates micro-fractures in the crushed rock particles
- Greater fines in a crushed product and micro fractures allow process solutions to come into contact with more surface area of the mineral being processed and thus help metal extraction
- HPGR crushers, compared to conventional cone crushers, generate less noise and dust
- HPGR crushing typically consumes approximately 20% less power per ton than conventional crushing plants producing the same product.

HPGR mainly consists of two counter-rotating rolls (Figure 2.2). Pressure is applied to one of the rolls by means of a hydro-pneumatic spring system, while the other roll is held in a fixed position in the frame. Feed to the rolls is provided by means of a hopper mounted above the rolls equipped with level control to ensure that the rolls are continuously choke-fed. Because, interparticle breakage in the compression zone between the rollers is achieved by choke feeding the material to the HPGR, otherwise the HPGR runs like a conventional roll crusher [8].

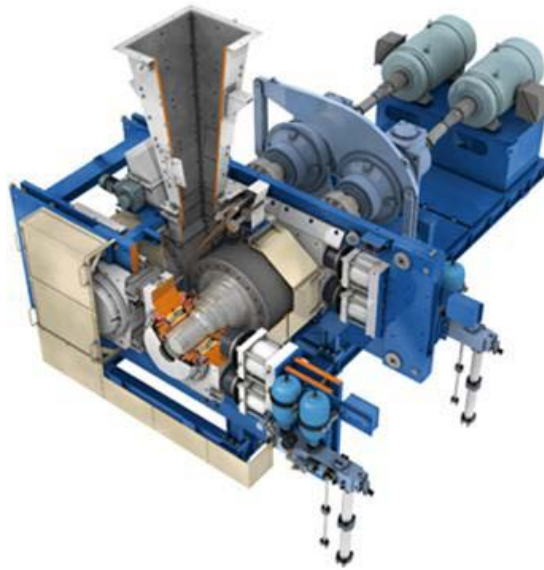


Figure 2.2 General view of HPGR [14]

The output of HPGR mainly depends on the specific energy consumption and the distribution of applied energy in the material bed according to the composition of the bed in terms of the particle size fractions [15]. For best utilization of the comminution energy during the operation of HPGR, some portion of the HPGR discharge material is recycled back to HPGR to ensure a uniform material bed and higher pressure gradient along the roller width. Basically, five circuit configurations of HPGR (Figure 2.3) can be used in grinding [16]:

1. Open circuit HPGR – closed circuit ball milling
2. Open circuit HPGR with partial recycling – closed circuit ball milling
3. Hybrid grinding
4. Closed circuit HPGR closed circuit ball milling
5. Semi-finish grinding

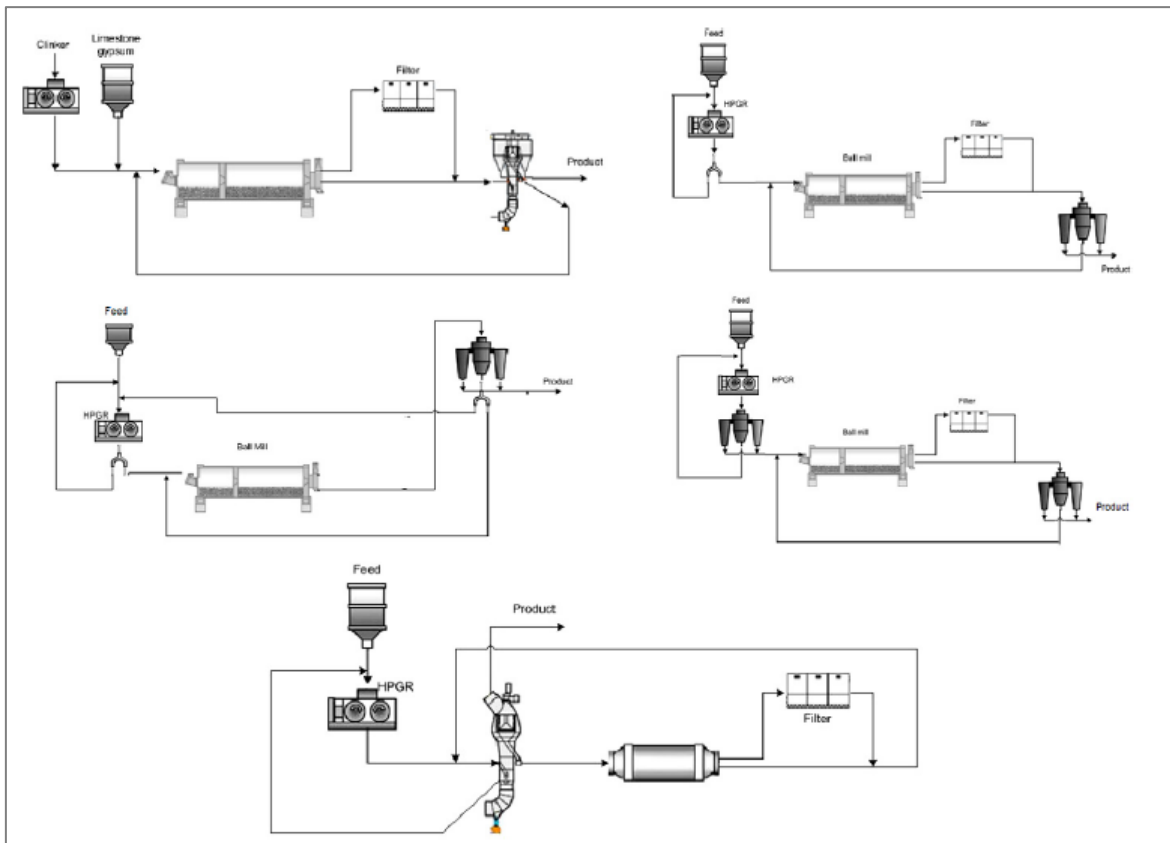


Figure 2.3 HPGR circuit configuration [16]

2.2. Horomill®

Energy efficient grinding technologies have become the main interest of the industry with the development of roller presses. Therefore, the Horomill (Horizontal roller mill) has been designed by the FCB Research Centre and introduced to the market in 1993 [17]. This technology is used for pre grinding, hybrid grinding and finish grinding operations in cement grinding circuits. Basically, advantages of the Horomill are listed below [13,18]:

- Low specific energy consumption
- Low operating wear rates
- Feed material with high moisture
- High drying capacity
- External circulation
- Process stability and low vibration
- Easy maintenance

The Horomill® consists of a horizontal shell equipped with a grinding track in which a roller exerts grinding force. The shell rotates faster than the critical speed which

leads to centrifuging of the material. Main feature is the roller inside the shell which is rotated by the material freely on its shaft without a drive. Operating principle is schematically shown in Figure 2.4.

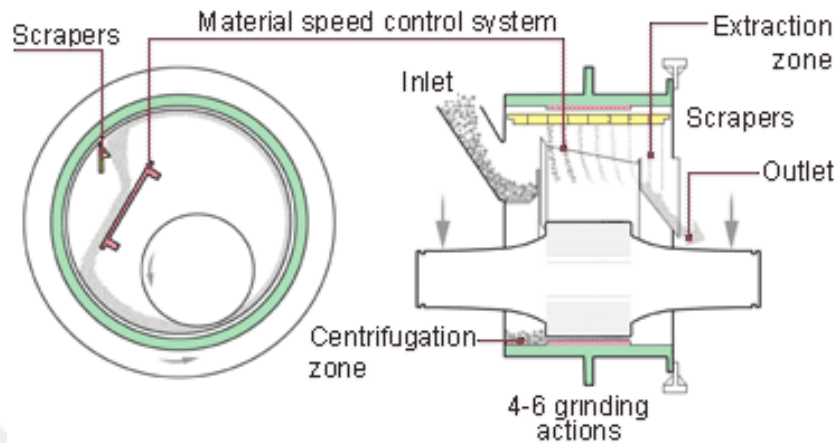


Figure 2.4 Operating principle of Horomill® [19]

Material is fed to the mill by gravity. There are scrapers located in the upper part of the shell. Scrapers cover the entire length of the mill and scrape off the material which falls onto the adjustable panel of the material advance system. Position of the material advance system which is sloping towards the discharge end could be changed in such a way that material could advance slower or faster and thus it determines the number of passage of material under the roller which means the adjustment of the circulating load. Concave and convex geometries of the grinding surfaces lead to angles of nip two or three, 41 times higher than in roller presses resulted in a thicker layer of ground material [20]. Horomill mainly consists of three zones: Feeding, grinding and discharging. In the grinding zone, the cylindrical roller transfers the grinding power onto the material. Material bed in the mill is generated by the centrifugal effect.

2.3. Vertical Roller Mill (VRM)

2.3.1. Chronology of Vertical Roller Mill Development

The basic principles of vertical roller mills have been well-known since the 2nd century. Up to now, many different types of vertical roller mills have been developed to meet the industry's demands.

Edge mills, which comprises of one or more stone grinding rollers and circular grinding surface, are one of the oldest versions of these mills. In the 19th century,

iron and steel took the place of stone with the developments in the industry. This mill was called as the Chilean mill (Figure 2.5). **The Chilean mill** had two or more (3 and 4) rollers, which rotated round a plane ring race by means of a vertical shaft.

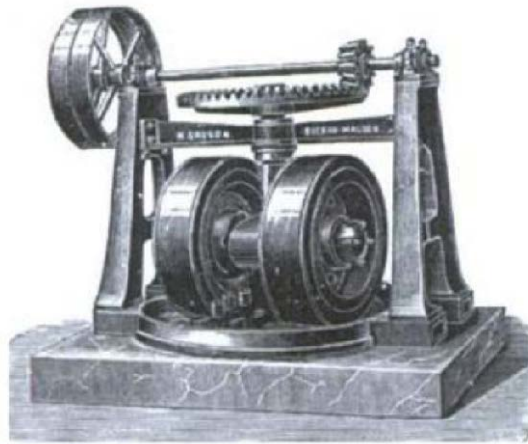


Figure 2.5 The Chilean mill [21]

The Huntington mill (Figure 2.6) was the first developed in 1883 and used for grinding of quartz and valuable metal-bearing rocks. It had three or four rollers that were suspended by yokes from arms attached to the revolving spindle. The rollers could swing freely in a radial direction and were pressed outwards against the ring die for centrifugal action. The ore was fed to the drive wheel's path and the scrapers lifted the material from the bottom then the material ground between the rollers and the die. Product size was controlled by the curved screens, which placed to the discharge of the mill [21]. The mill was produced in three sizes as 3.5, 5 and 6 ft. Literature reported that average capacity of a 5-foot (1.5 m) mill was between 10 to 30 tph [22].

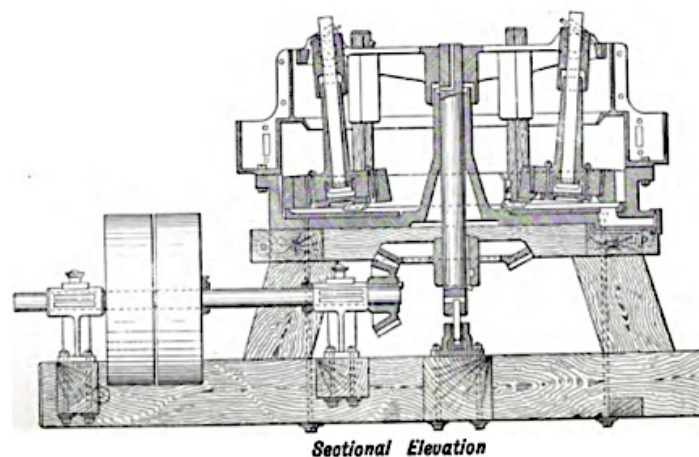


Figure 2.6 The Huntington mill [21]

The Maxecon mill (Figure 2.7) introduced into the market in 1906. The mill had a rotating vertical grinding ring suspended in the chamber by three rollers that were offset by 120° to one another and rotated independently. Ore was fed pneumatically via a curved chute in front of the second roller. After pre crushing, ore was carried to the next two rollers by centrifugal force for further comminution. Ground ore was discharged from sideways of the mill.



Figure 2.7 The Maxecon mill [23]

The Maxecon mills found applications in phosphate and limestone grinding. In 1924, these mills were used as coal pulverisers in Germany [24] with average capacities ranging between 2 to 5 tph. The improvements in cement kiln technology together with increased demand on power required higher coal milling capacities; however, because of the geometrical restrictions, these mills were unable to meet the demand.

The Raymond mill (Figure 2.8) was developed as centrifugal ring roller mill with the aim of handling higher capacities. With its development, production rates were increased up to 10-12 tph for raw coal.

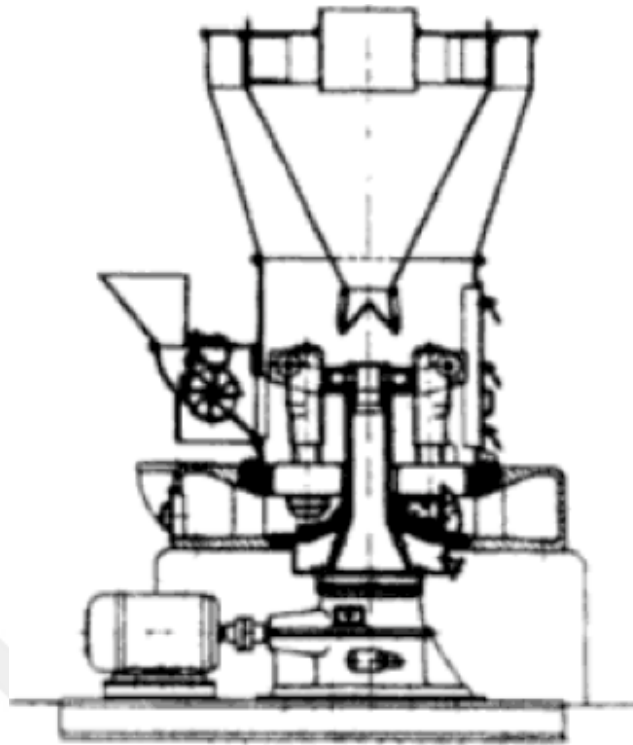


Figure 2.8 The Raymond mill [25]

Grinding operation was obtained by centrifugal forces acting on rollers, which were attached to the vertical shaft of the mill. Ore was fed to the grinding zone between the rollers and ring. Ground product was extracted pneumatically.

In spite of the advantage of capacity advantage, these mills did not perform well in Germany, since they were designed to grind soft coals. Consequently, higher grinding forces were not achieved due to the high vibrations [9].

The Maximal mill (Figure 2.9) was developed in 1925 by Ernst Curt Loesche. This mill was the Loesche's first grinding mill using a rotating bowl as the grinding surface. In contrast to the spinning rollers and fixed bowl designs of the Raymond mill, the Maximal mill had fixed rollers and a spinning bowl to carry the material under the rollers by centrifugal force [26].

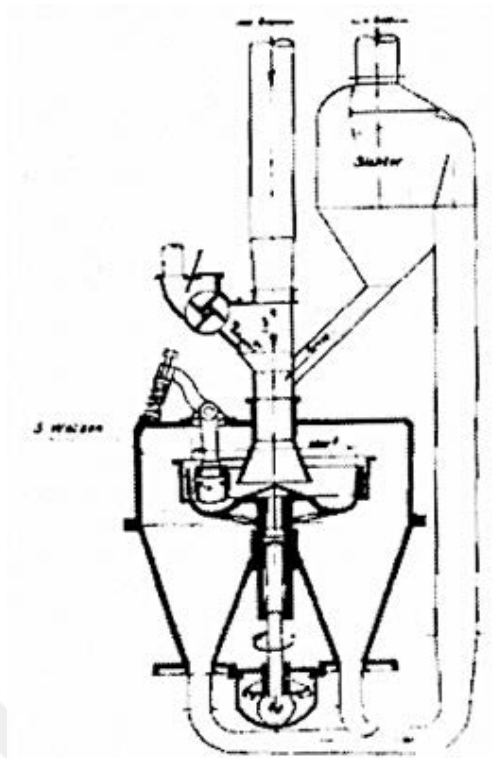


Figure 2.9 The Maximal mill [26]

Capacity improvement was still a problem due to the geometrical restrictions of the Maximal mill. Hence, the dimensions of both the rollers and the grinding surface were modified. In addition, the wall of the grinding bowl was inclined backwards to overcome capacity issues (Figure 2.10).

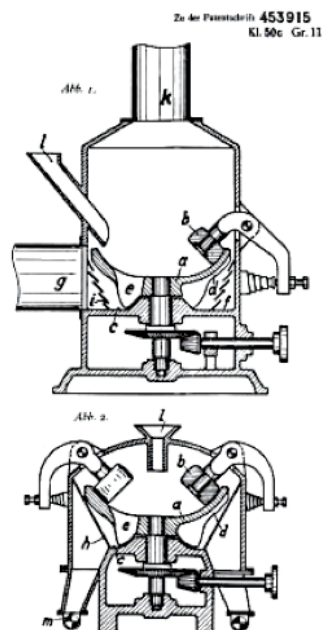


Figure 2.10 The vertical roller mill in 1927 [25]

The Loesche mill was developed in 1928 with a flatter grinding surface [26]. Main purpose of the flatter surface was to increase the diameters of the rollers and to provide material flow on the grinding bowl. Loesche mills were designed with three rollers as the Raymond mills. But the rollers were held by rocker arms. Then, Loesche mills were produced with two rollers to grip the coarse particles in the feed. In 1935, 15° angle for the roller axle was being used to increase the amount of fine materials in the product. The first Loesche mill is shown in Figure 2.11.

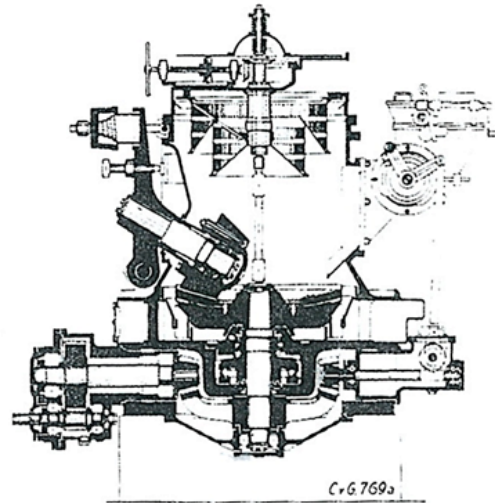


Figure 2.11 The first Loesche mill [26]

Loesche was the first manufacturer of spring-loaded vertical roller grinding mills [10]. The steel spring loading system was used to link rocker arms to one another. This system enabled distributing the grinding forces independently from the rollers to the grinding bed.

The size and the capacity of Loesche mills have increased gradually over the years. In 1960, the largest mill had 2 m grinding surface diameter with 50 tph capacity. In this date, it is possible to achieve 1200 tph production rate for coarse grinding compact structure as they combine grinding and classification actions in a single unit.

The Berz (MB) mill was developed in 1947 (Figure 2.12). The Berz mill had three rollers pressed down onto the grinding surface by a thrust ring. The grinding surface had tracking grooves for the rollers. The rollers were not fixed and driven by the grinding table. Although the Berz mill was used for coal grinding purposes, they were

unable to be marketed widely in cement plants, because of its limited speed and capacity [26].

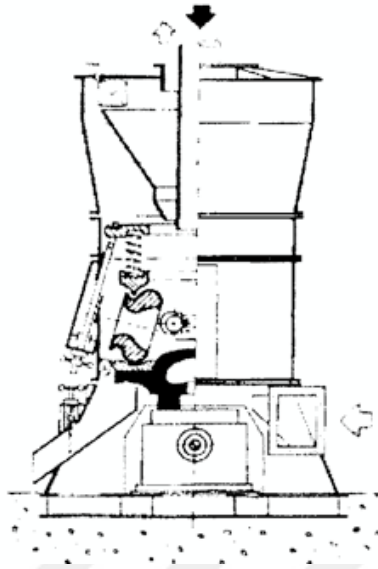


Figure 2.12 The Berz mill [25]

The MPS mill (Figure 2.13) was redesigned version of the Berz mill. The MPS mill had three rollers with tracking groove but differently from the Berz mill, the rollers were fixed with bearings. The rollers were pressed down onto the grinding surface. In small mills, grinding force was generated by a thrust ring while in larger mills thrust frame coupled to tensioning rods. “Lift and swing” system was used to change the rollers [26].

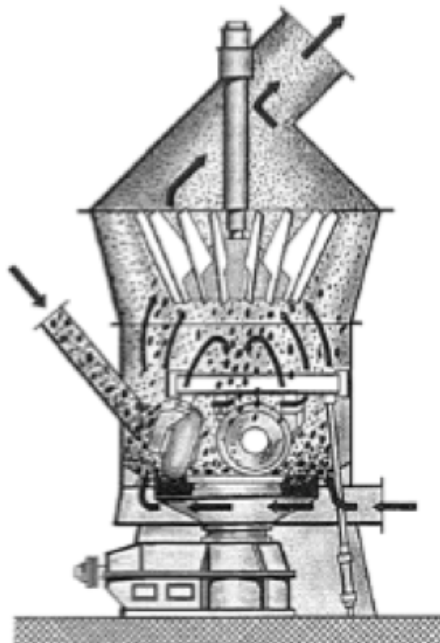


Figure 2.13 The MPS mill [27]

The Polysius vertical roller mill was developed by Krupp-Polysius AG (Figure 2.14). The mill was designed with two sets of double rollers. The roller profiles were rounded and had fixed roller carriers. Polysius mill had double tracking groove in the grinding surface to stabilize the grinding bed. Because of the smaller running diameter of the rollers on grinding table, velocity of the inner roller, that is closer to the mill center, was lower than the outer roller. Force was applied to each roller by hydraulic cylinders [26].

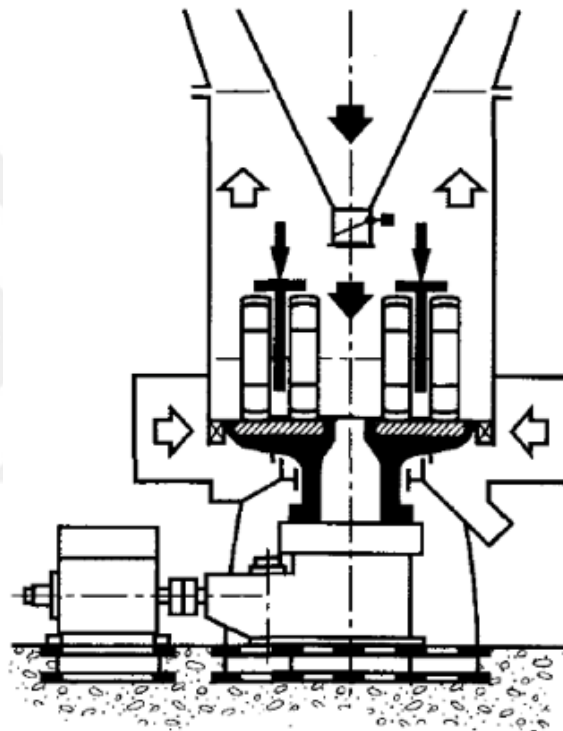


Figure 2.14 The Polysius mill [22]

The Atox mill was developed by FL Smidth after the expiry of the license of the MPS mill. The Atox mill (Figure 2.15) had similar principle with MPS mill. This mill had three grinding rollers, which were connected to one another. The three roller shafts were bolted to a centerpiece. The rollers rotated around their axles but not around center of the bowl. Tension rods connected the outer ends of the shafts to the hydraulic cylinder. The force transmission was very compact and whole design is simple.

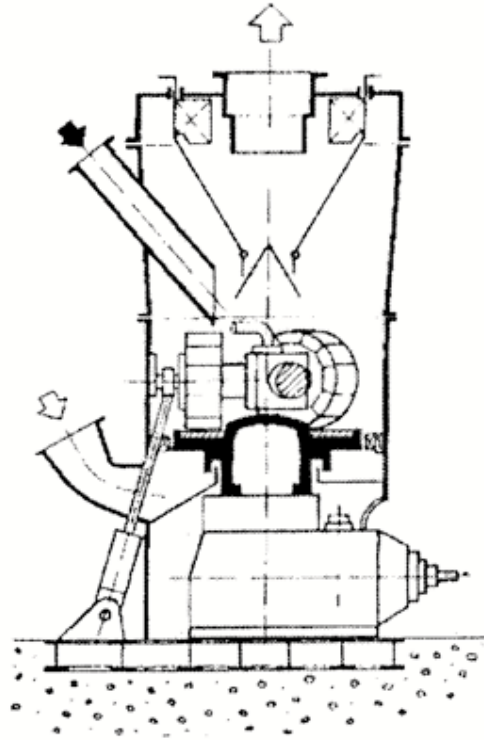


Figure 2.15 The Atox mill [22]

2.3.2. Current State of Vertical Roller Mill Technology

Various type of vertical roller mills was developed depending on the requirements until today. With the technologic development, manufacturers were focused on the design of vertical roller mills to meet the need of the industry in terms of capacity, energy consumption and grind size. Vertical roller mills in the market are basically differ from each other by grinding table and roller design.

In 1987, a new vertical roller mill which was called as the Chichibu-Kawasaki Pre-grinder (CKP) has introduced to the market by Kawasaki Heavy Industries in collaboration with the Chichibu Cement Company. It was designed with a mechanical material discharge system to overcome the inefficiency resulted from the high internal circulation [28]. The CKP mills have similar concept with grinding section of the conventional vertical roller mills. Material is fed onto the grinding table and centrifugal force arising from the rotation of the table distributes the product. Then, material is ground under the grinding rollers. The ground material passes through the periphery of table and discharged by the scrapers [29] (Figure 2.16).

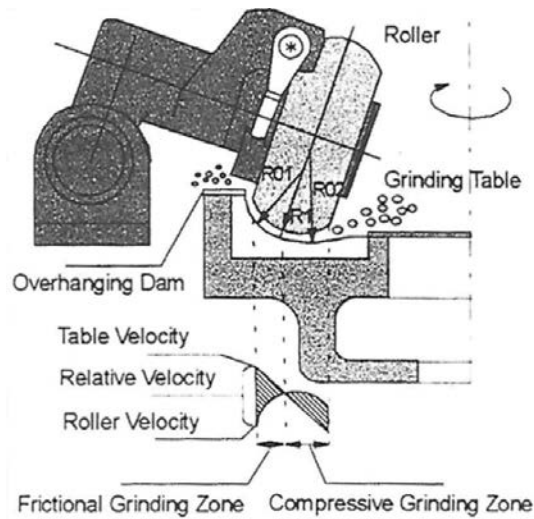


Figure 2.16 Operating principle of CKP mill [30]

It was reported that the energy consumption of the total grinding plant could be reduced by 20-30% for cement clinker and 30-40% for other raw materials by implementing the CKP mill to the conventional ball mill circuit [30]. Application examples of CKP system are presented in Figure 2.17 and Figure 2.18.

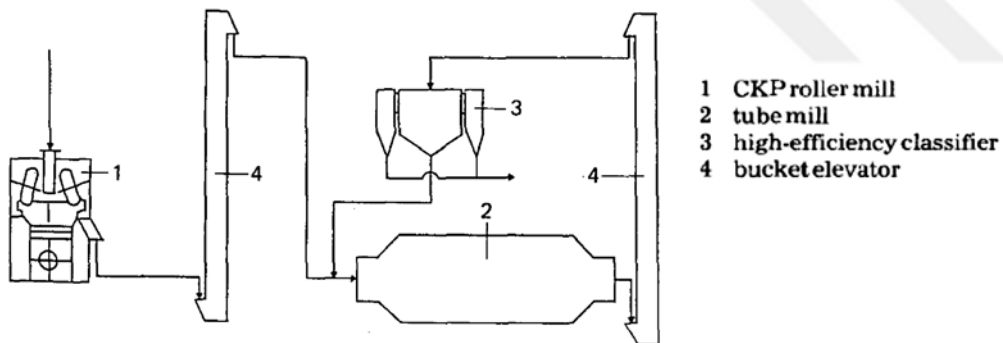


Figure 2.17 Open circuit application of CKP mill with a tube mill [28]

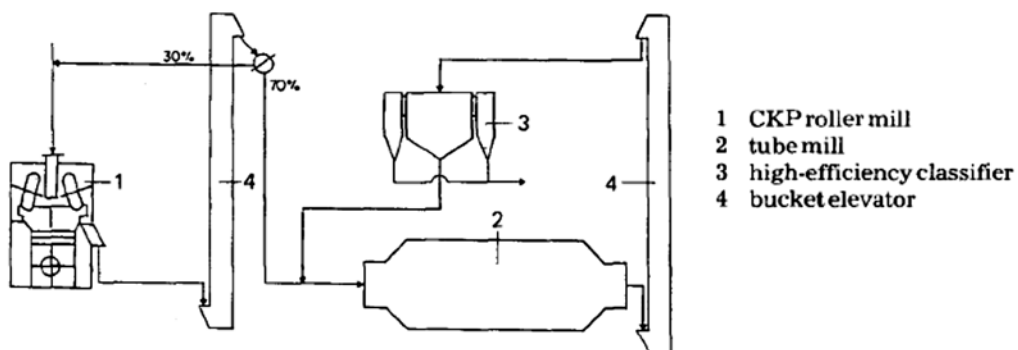


Figure 2.18 Recycled application of CKP mill with a tube mill [28]

In the mid 90's, Loesche GmbH introduced its vertical roller mills with the 2+2 technology for grinding of clinker and slag as well as for the production of cement with interground additives. In this system, two of four rollers were replaced by smaller rollers. Small rollers prepare the grinding bed and master rollers grind the material. By the end of the 20th century, 20 mills of that kind, with a total installed power of 54.9 MW and a production capacity of more than 2700 tph cement and ground slag have been marketed [31,32]. Loesche vertical roller mills have found applications in the mineral industry e.g. phosphate, iron ore, barite, colemanite, lead/zinc. Flowsheets of colemanite and pyroxenite applications of Loesche vertical roller mill are given in Figure 2.19 and Figure 2.20, respectively.

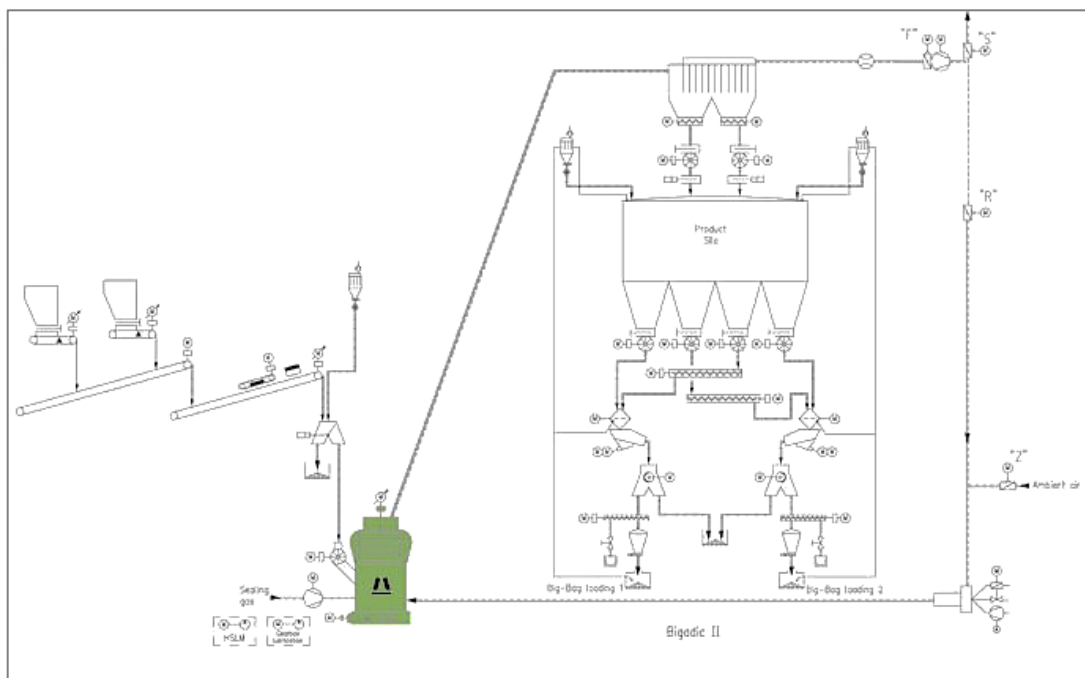


Figure 2.19 Colemanite application of vertical roller mill (Courtesy Loesche)

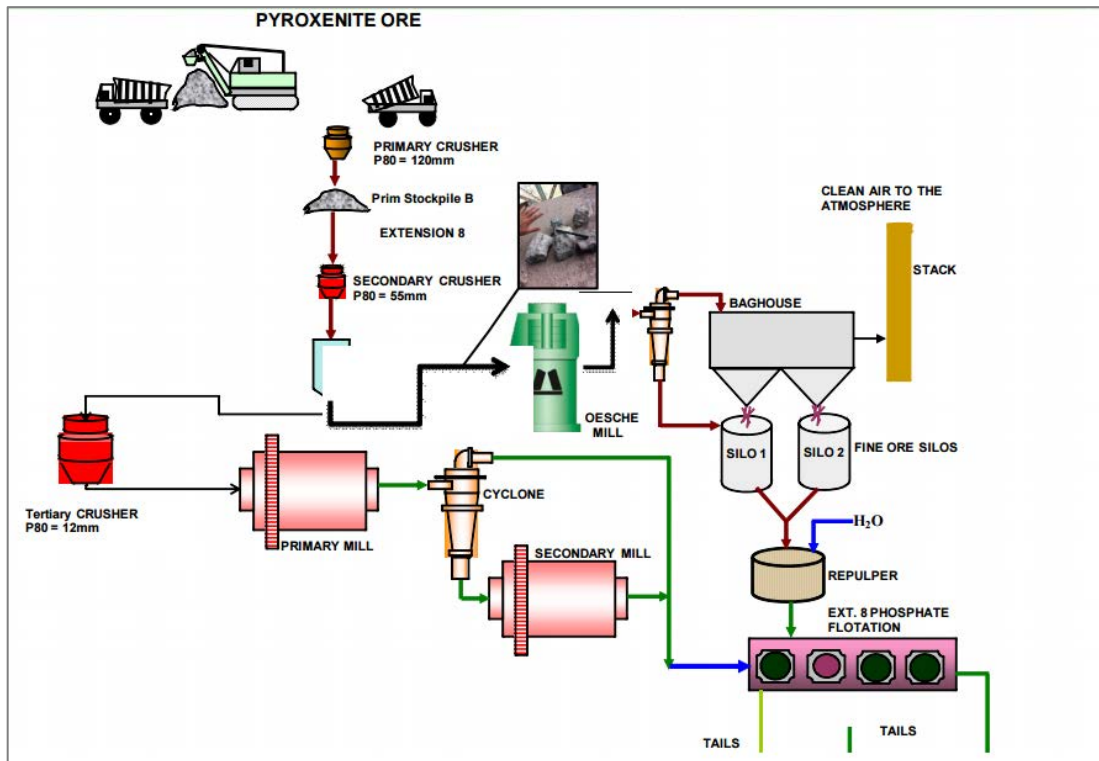


Figure 2.20 Pyroxenite application of vertical roller mill [30]

Loesche vertical roller mills (Figure 2.21) are characterized by a flat grinding table, 2 to 6 grinding rollers of conical shape, individual fixed rollers, modular design and hydro pneumatic spring system [34].



Figure 2.21 The Loesche mill

The largest Loesche mill developed for grinding of cement clinker is the LM 70.4 with a table diameter of 6.9 m and installed power of 8800 kW [35]. Nominal throughput of this mill is 1200 tph. Achievable throughput for grinding cement and granulated blast-furnace slag is about 350 tph with 7800 kW installed power [36].

MPS and MVR mills are produced by Gebr. Pfeiffer which has been a supplier to the cement industry for 140 years [37]. Pfeiffer MPS vertical roller mill (Figure 2.22) have been used for the grinding of cement raw material, cement, clinker, granulated blast-furnace slag, coal, limestone and gypsum [38]. The diversifying feature of the MPS vertical roller mills is 3 grinding rollers, which are pressed onto the grinding track by a pressure frame, external pull rods and the hydraulic system [39].

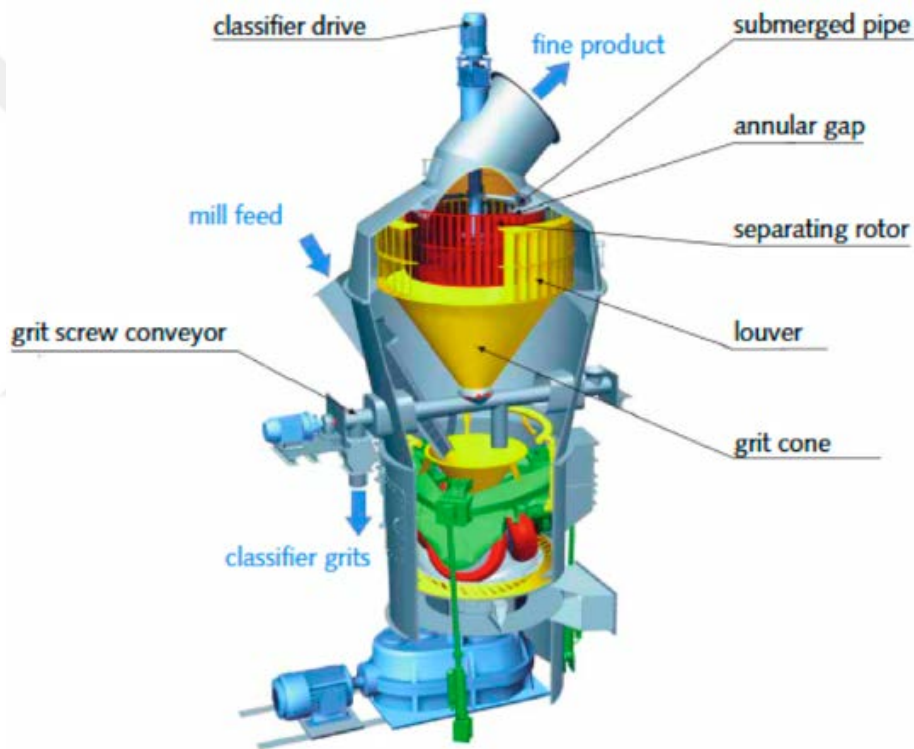


Figure 2.22 The Pfeiffer MPS mill [38]

The capacity and the size of the mill vary by material to be ground. Capacity of the MPS vertical roller mills can reach up to 650 tph with installed power of 6500 kW for cement raw materials. However, the largest MPS mill for grinding granulated blast furnace slag and cement has 5500 kW of installed with the capacity of 300 tph [40].

Gebr. Pfeiffer SE has developed another vertical roller mill called the MVR mill (Figure 2.23) to meet requirements of the market. The MVR vertical roller mill is

used for grinding of cement raw material, cement and granulated blast-furnace slag. Design of the mill commits sustainable operation even if one of the rollers fails [41].



Figure 2.23 The Pfeiffer MVR mill [42]

The MVR mill consists of four to six grinding rollers with cylindrical wear part geometry, flat grinding table, gas-guiding housing with nozzle ring, classifier and “MultiDrive®” drive unit or alternatively a conventional drive with planetary gears [42]. The MVR roller mill was designed for processing higher throughput rates. Maximum capacity of MVR roller mill for raw materials is 1400 tph with 12000 kW of installed power. Throughput rates decrease to 50 tph for blast furnace slag and cement with the same installed power [38].

Atox mill has a flat grinding table, three grinding rollers, adjustable nozzle ring and dam ring. These mills are generally used for grinding of raw materials and coal. Coal grinding circuits can be operated in non-inert and inert conditions. Circuit configurations for coal grinding of Atox mill are presented in Figure 2.24.

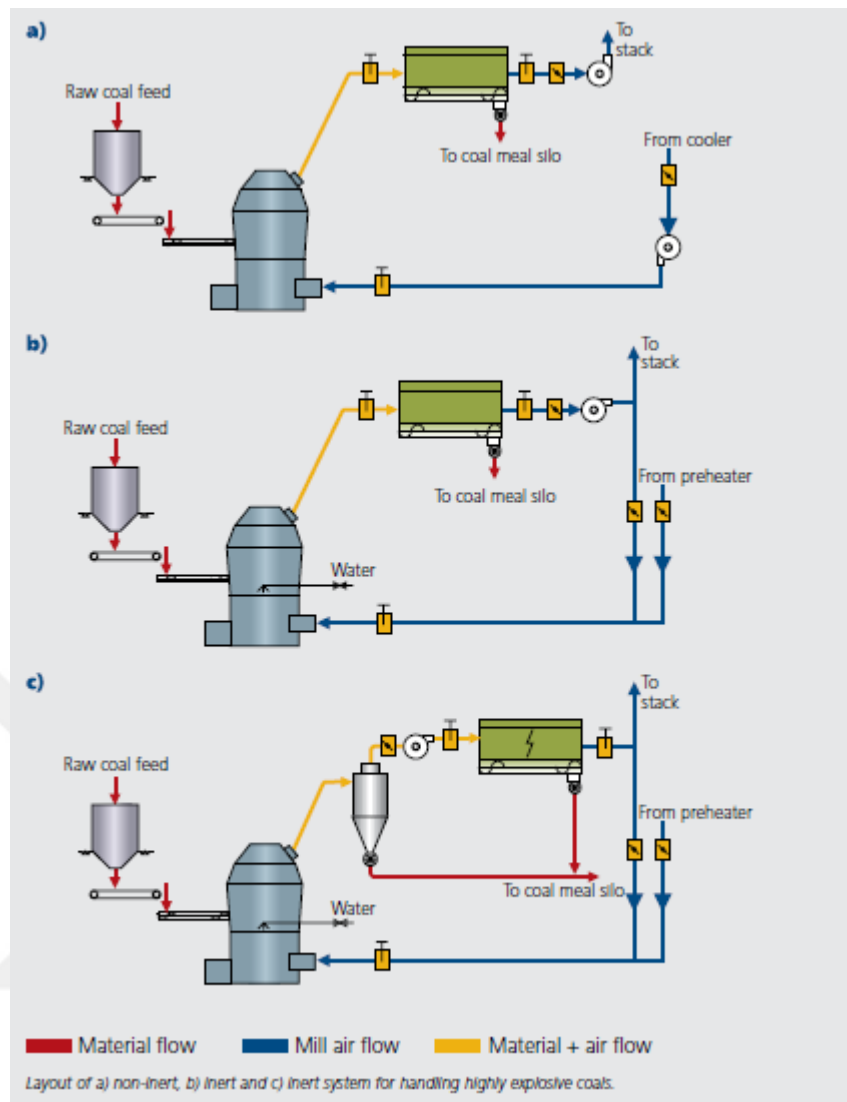


Figure 2.24 Coal grinding applications of Atox mill [43]

The OK mill is preferred for grinding of harder materials like slag and clinker. The OK mill was developed in Japan by Onoda Cement Co., Onoda Engineering and Consulting Co. and Kobe Steel in the 1980s. In 1993 FL Smidth-Fuller Engineering acquired a license to manufacture and market the OK mill [44]. The OK mill (Figure 2.25) is used for grinding of Portland cement, slag and blended cements.

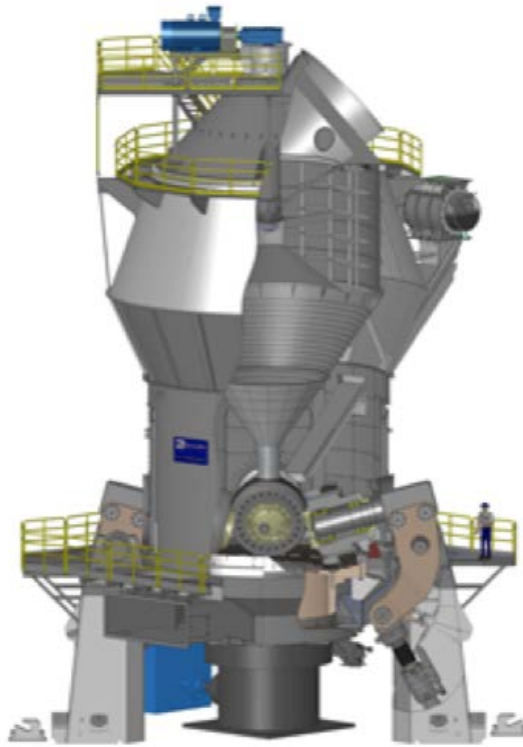


Figure 2.25 The FL Smidth OK mill [45]

The OK vertical roller mills have grooved profile roller and curved table. Grooved roller profile creates a high grinding pressure on the outer path and allowing air to escape in the middle. The roller tires and table track are composed of several pieces or segments that enable utilization of very hard anti-abrasive materials for the wear protection [46]. The profile between the rollers and the table is specially designed to eliminate vibration even in the case of grinding hard materials to high fineness [47]. Maximum capacity for cement grinding is 685 tph with 11000 kW motor power. Throughput rates reach up to 500 tph with 13200 kW installed power [48].

The Quadropol vertical roller mill (Figure 2.26) has been developed by the ThyssenKrupp AG to meet the requirements of market for high throughput rates and drive powers with smaller plant footprint. Generally, Quadropol vertical roller mills are utilized for cement raw material grinding. The maximum throughput rate is 990 tph with 7400 kW installed drive motor [49].

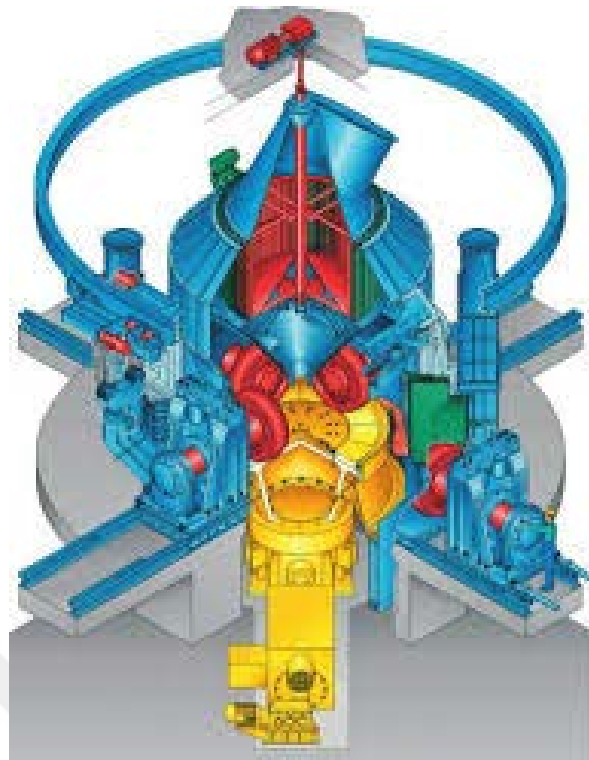


Figure 2.26 The Quadropol mill [50]

The Quadropol mill has four grinding rollers whose shaft-bearing arrangements are outside the mill. The standard crowned geometry of the grinding roller has been retained as a reliable design with wear resistance. The Quadropol mill has a more compact design than the Polysius mill, with a lower overall height and therefore a smaller enclosed volume.

Recently, ThyssenKrupp AG has introduced a new concept of the Quadropol QMC RD mill to the market. In this design, on the contrary to common vertical roller mills, roller drive is offered. This gives an opportunity to increase material pull in capability by higher roller speed [51]. Also, possibility of operating with two removed rollers for four roller mill and lower power requirement are other advantages of this new system. The throughput rate can be increased up to 550 tph with 8600 kW installed drive power for cement grinding [52].

2.3.3. The Significant Features of Vertical Roller Mills

The vertical roller mills are airswept grinding machines and operated in closed circuit. These mills offer a number of advantages over conventional milling systems. In this section, remarkable features of vertical roller mills are given.

2.3.3.1. Specific Energy Consumption

The most important feature of vertical roller mills is low specific energy consumption. Grinding energy has a critical position in mineral processing and cement grinding plants. As an example, electrical energy used in cement grinding is 60% of total energy used [53].

In the literature, there are many studies conducted at cement plants where an energy based comparison was performed between conventional grinding systems and vertical roller mills. In a study, it was noticed that the OK vertical roller mill consumed about 31% and 43% less energy in grinding, respectively, for ordinary and high early strength cement [46]. Total energy consumption for grinding circuit is also less in spite of higher fan power. Total energy saving was 28.6% less than the tube mill-classifier circuit for Portland cement [47]. Vertical roller mills can achieve up to 30% energy saving when used in cement grinding applications [54]. Low specific energy consumption of vertical roller mills for cement grinding was verified by other studies [44, 55, 56]. Comparison of variation of energy consumption with blaine of ball mill and Loesche vertical roller mills are illustrated in Figure 2.27.

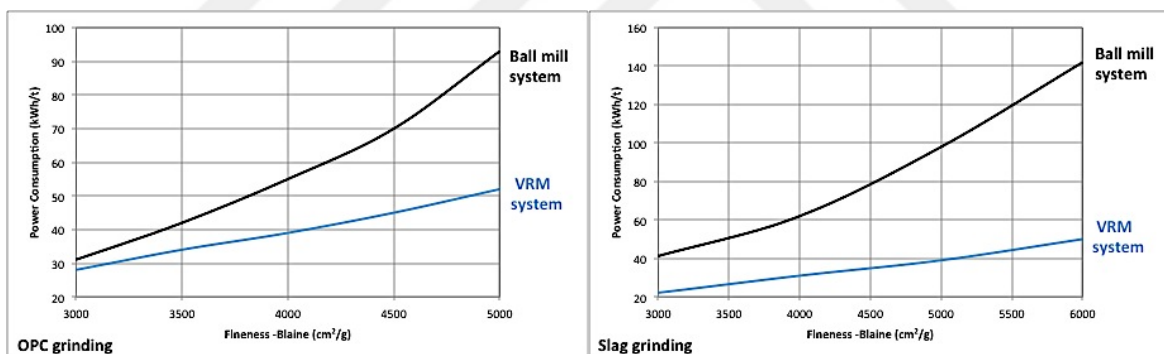


Figure 2.27 Specific power consumption of ball mill vs. vertical roller mill system for ordinary Portland cement (OPC) and slag grinding [57]

Energy benefit of vertical roller mill increases when used for grinding hard material such as blast furnace slag. It is due to the efficient compression grinding mechanism of vertical roller mills. Compared to other grinding systems, and in the case of slag grinding its saving potential is 45-54% or more depending on the product fineness [58-60].

Successful operations of VRM technology in cement grinding applications encouraged the studies on mineral grinding applications. In recent years, pilot plant tests with the Loesche OGP mobile were performed for minerals to prove their

benefits in this area as well. Pilot plant test results for mineral grinding showed that low energy consumption feature of vertical roller mills is applicable to mineral industry. Grinding test results for zinc ore showed that it is possible to decrease total energy consumption from 20.11 to 11.40 kWh/t by using vertical roller mill instead of AG/SAG-ball mill circuit [61]. In another test performed with the Loesche OGP mobile, 22.9% and 34.4% energy savings were obtained for copper slag grinding [62]. This situation was confirmed for chalcopyrite ore with 18% less energy consumption against to conventional ball milling circuit [63]. In another application for copper slag, 34.4% energy saving can be achieved by VRM operating in overflow mode [64].

2.3.3.2. Feed Particle Size and Moisture Content

The properties of fresh feed material, in terms of particle size distribution and moisture content play an important role on the performance of grinding operation. Particle size of feed material for vertical roller mills is generally larger than ball mills. Because of large diameter of rollers, feed size can be as large as 80 to 150 mm. This enables to eliminate the secondary/tertiary-crushing stages [65, 66].

Vertical roller mills are also drying machines and have higher drying capacity. So, they can handle highly moist feed material. In operation, the moisture content of feed can be higher than 20% [65]. Industrial scale studies were performed for grinding high moisture material by VRM. Product having 0.7% moisture content was obtained by grinding of feed material having 20% moisture content [67,68].

2.3.3.3. Floor Space

The vertical roller mills are compact machines. The classifier and the mill are combined in a single unit and the number of auxiliary equipment are less compared to other systems. Therefore, vertical roller mills have less floor space than a closed circuit ball mill circuit with a similar capacity. The required building volume for different grinding systems are given in Figure 2.28. The difference in required floor space between vertical roller mills and conventional systems increases with increasing circuit capacity.

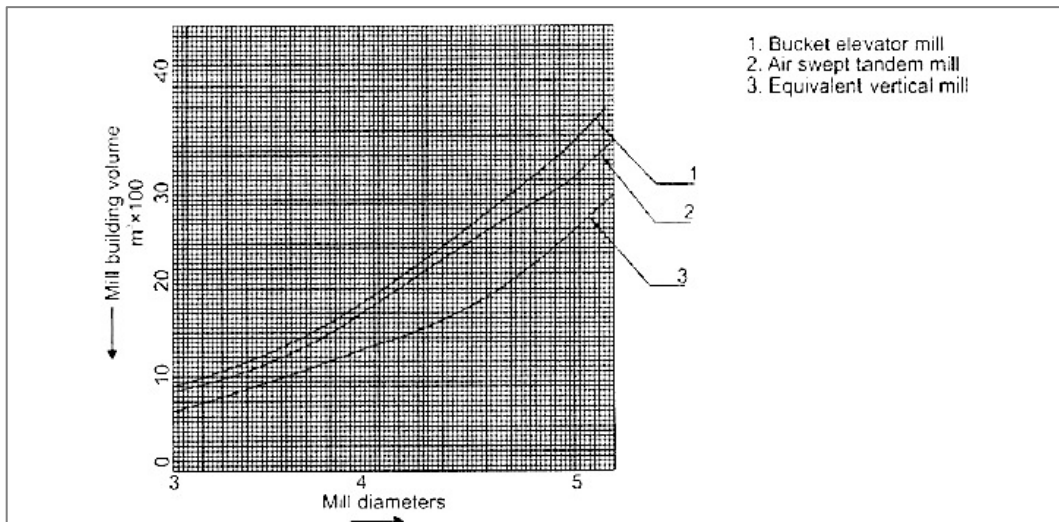


Figure 2.28 Building volume required for equivalent output for different mill systems [69]

2.3.3.4. Product Quality

Product quality is the major concern of all the grinding operations. The product size distribution has an effective control parameter for both cement and mineral industries. The particle size distribution of vertical roller mill product is steeper than the size distribution of ball mill product that is caused by different grinding mechanisms between these systems. The residence time of a material in ball mill is higher than vertical roller mill hence high proportion of fine material is produced. The steeper size distribution of vertical roller mill can generate some problems for cement quality like low early strength and higher water demand however with the introduction of special type of grinding chemicals it can be overcome. It is possible to achieve ideal size distribution using vertical roller mill by making adjustments to pressure, air flow, classifier rotor speed and dam ring height [57]. In some cases, steeper product size distributions become an advantage for downstream processes. As an example, when using VRM for iron ore grinding the amount of $-10\ \mu\text{m}$, which affects flotation performance adversely, was reduced by 30% compared to the grinding product of the ball mills [64]. The effects of interparticle comminution on flotation performance were investigated by pilot scale VRM tests. In a study performed by Viljoen et al. [70], flotation performance of VRM and conventional mill products were compared at similar fineness. Flotation recovery of copper and nickel ore was increased from 74% to 84% and from 79% to 86%, respectively [71]. Test studies showed that higher Zn recoveries could be obtained at efficient energy use

[61]. In another pilot scale VRM test study performed for copper sulfide, nickel sulfide, UG-2, PGM showed that grade-recovery relationships were improved by VRM. Also, metal deportment to narrower range of size classes has improved [71]. In a similar pilot scale tests carried out by Loesche LM4,5 for two different magnetite ores showed that liberation degree of VRM products is higher than conventional plant products [72]. Additionally, mass pull to flotation has been increased 4.5% for iron ore [64]. Comparably to flotation, VRM has a positive effect on leaching processes. In a study, performance of gold leaching has been improved by VRM system [73].

Cement production studies performed for different cement types indicated that vertical roller mills achieved similar cement strength when compared to ball mill circuits with lower specific energy consumption or higher throughput [44, 55, 56, 74-76].

The water demand is determinative on concrete quality. Water content is affected by particle size distribution and gypsum dehydration. Vertical roller mill product generally requires more water to achieve a standard concrete stiffness compared to conventional ball mills. This results from steeper size distribution of vertical roller mill. It is easy to obtain ideal particle size distribution to control water demand. In industrial tests performed by different types of vertical roller mills, similar water demand with ball mill circuit was obtained [44,56,57 and 76].

2.3.3.5. Wear

The wear of size reduction equipment is one of the major problems of the industry. The wear is related to the properties of material ground and the equipment used. Wear on the grinding parts affects the performance of the system directly. If vertical roller mills are considered, radius of the grinding parts gradually decreases due to the outer wear of roller and this leads to the increase of speed difference between the rollers.

A number of studies have been carried out on vertical roller mills to define the wear profile and to decrease the wear rates. In vertical roller mills, two wear mechanisms have been defined, which are; friction wear and jet wear. Friction wear is observed on rollers, grinding tracks and chutes, while jet wear occurs on the components exposed to the gas stream. Wear parts of vertical roller mill is shown in Figure 2.29.



Figure 2.29 Wear parts of VRM [77]

Vertical roller mills are equipped with wear parts of either high chrome cast alloys or welded wear facings. Mainly, wear-resistant alloyed cast iron has been used for a long time [77]. Besides, there are many wear protection materials available in the form of alloyed cast iron, hardfacing, alloyed steel plate, composite materials and ceramic linings with the developments of the metallurgy [78].

Magotteaux SA has developed a wear protection material called as Xwin. High-chromium base of a layer is reinforced with hard ceramic particles. It has been applied to rollers and grinding table of the MVR mill and 33% improvement in service life has been achieved [79].

Hard facing is very common application. Rollers and grinding table liners have to be hard faced for grinding of blast furnace slag. Hard faced grinding elements with high carbide content have a lower wear rate than that of cast metals with a high chromium content. Wear rate is under 5 g/t for hard faced grinding elements [51].

Pilot plant studies showed that low wear rates could be achieved by vertical roller mills. The studies on abrasive gold ore showed that, wear rate decreased from 2.73 to 0.8 kg/t by using vertical roller mill instead of rod mill [73]. Another test results showed the advantage of vertical roller mills over conventional milling systems. Vertical roller mill provided a 58.7% decrease in the expenditure of wear cost for chalcopyrite ore [73].

2.3.4. Working Principle of Vertical Roller Mills

The working principle of the vertical roller mills is based on the interparticle comminution, which is stated as the most efficient method for breakage by Schönert [6]. Interparticle comminution takes place in a gap between the rotating grinding table and the stationary grinding rollers [31]. Although there are numbers of different vertical roller mill designs, breakage principles of the systems are similar to each other (Figure 2.30).

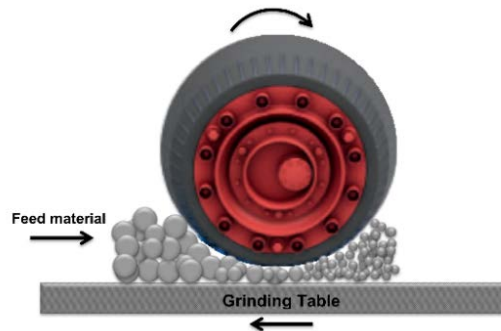


Figure 2.30 The grinding mechanism of vertical roller mills

During the operation of the mill, firstly, fresh feed is directed to the center of rotating table and moved to the edges under the influence of centrifugal forces. On the edges of table, the material is nipped by the rollers, on which pressure is exerted, and ground between the rollers and grinding table. After comminution, broken particles discharges from a dam ring, which is used to control the height of material layer, and is picked up by hot gas following from below the grinding table through a nozzle ring. The hot gas dries the material and the finer fraction is carried to the dynamic classifier mounted to the top of the mill. The finished or fine product leaves with the gas and is collected in a filter. The coarser particles are circulated back onto the grinding table for further grinding. Nowadays, most of the mills have external recirculation system to decrease the energy cost arising from pneumatic transportation. In external recirculation, coarse material that falls through the louvre ring and into the mill gas ducts is fed to the mill with the fresh feed by belts or bucket elevators. Literature reports that significant reduction in energy consumption is achievable [65].

2.3.5. Elements of Vertical Roller Mills

Main components of a vertical roller mill can be listed as,

- grinding elements (rollers and grinding table),
- nozzle ring and
- classifier.

Within the section, these elements will be explained in detail.

2.3.5.1. Grinding Elements

The geometric form of rollers and the grinding table differ for vertical roller mills on the market although the working principle is similar [9]. As an example, Loesche mills have conical rollers with flat grinding table while OK mill has spherical grooved roller with curved grinding table (Figure 2.31) [45].



Figure 2.31 The roller and grinding table profile [39,42]

In addition to the roller and grinding table designs, the number of grinding elements together with their arrangements in the mill shows variations. Pfeiffer MVR mill consists of four to six grinding rollers with cylindrical wear part geometry [42]. The Pfeiffer MPS mills have 3 grinding rollers, which are pressed onto the grinding track by a pressure frame, external pull rods and the hydraulic system [40]. The Polysius Quadropol mill has four rollers that can be independently controlled by hydraulic system [49]. This arrangement allows an improvement in the throughput during partial-load operation of the mill. The Loesche mills have different roller module system, which enables to be arranged a different number of grinding rollers with the same dimension around the grinding table depend on the capacity requirements (Figure 2.32).

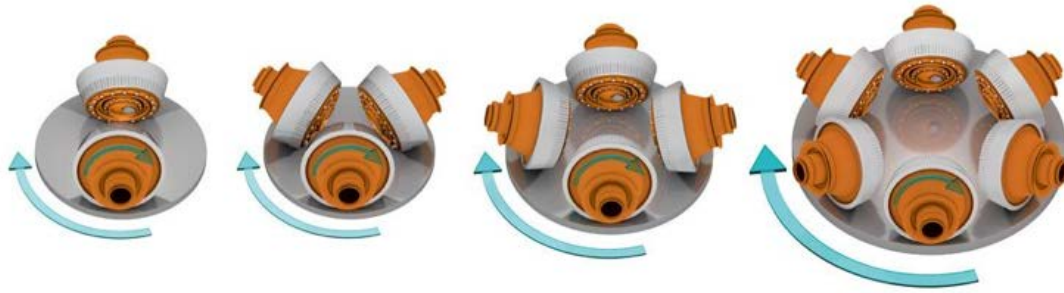


Figure 2.32 The Loesche roller module concept [80]

Comminution pressure is provided by hydro-pneumatic spring system, which enables adjusting the grinding operation depending on the changes in operational conditions [66].

Differently from other vertical roller mill manufacturers, Loesche uses a master (M) and support (S) roller mechanism. The master rollers transmit the grinding force for interparticle breakage and the support rollers are used for the material preparation and stabilizing the grinding bed [81]. This mechanism reduces the dynamic load on the individual component during operation and provides smooth mill running [82]. Working principle of the M and S rollers is illustrated in Figure 2.33.

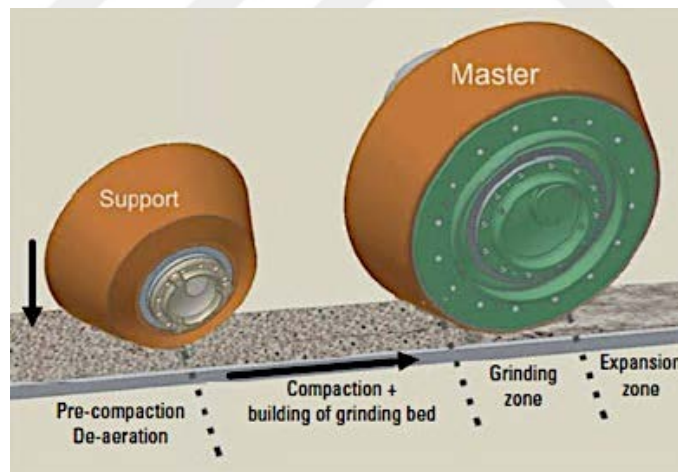


Figure 2.33 Working principle of the master and support rollers [83]

2.3.5.2. Nozzle Ring

The hot gas is supplied to the system for both drying and conveying operations. This hot gas is introduced through a duct into the chamber below the grinding table and nozzle ring (Figure 2.34).

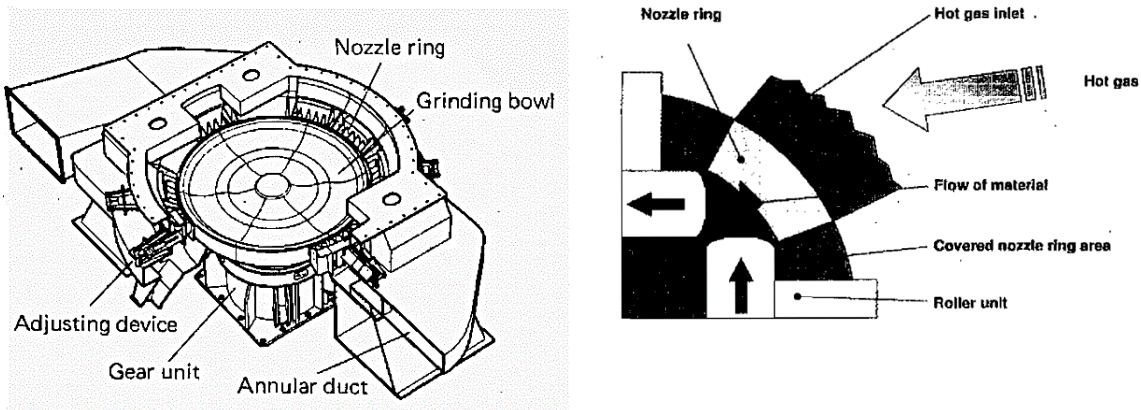


Figure 2.34 Nozzle ring section [84, 85]

The hot gas flows through the nozzle ring and conveys the ground material to the classification zone. Open area of each nozzle can be adjusted to regulate the velocity and distribution of the gas flow rate [85]. This regulation improves the conveying and grinding bed formation [84]. Also, energy consumption decreases depending on the reduction of the gas flow [84].

2.3.5.3. Classifier

Implementing classification operation to the vertical roller mill is a big step during the historical development of these mills. Air classification is a process employed to control or adjust the final product fineness of the circuit. Various types of air classifiers were developed up to now. Air classifiers are grouped as static and dynamic air classifiers according to mechanical properties. Static classifiers have no moving parts and the target size is adjusted by changing magnitude and direction of the air flow. V-separators [86] is the most common type of these classifiers. Typically, dynamic classifiers consist of a fan and rotor used for dispersing and separating [47]. Material is transferred and dispersed on to the rotating plate by centrifugal force. Particles are thrown towards the classifier wall and air is introduced in to the chamber. Classification is carried out in the separation chamber [87]. Dynamic air classifiers can be grouped as first, second and third generation (high efficiency).

With the introduction and evolution of the air classifiers, these equipment has been started to use in the vertical roller mill system to improve the efficiency of the process. Within the VRM technology, classification right after the grinding action prevents overgrinding of the material. Ground material is carried to the classifier

chamber by hot gas through the guide vane. Material/gas flows into the space between guide vane and rotor with blades. The particles thrown outward by the effect of the centrifugal force, and fall down by the effect of the gravity.

The first vertical roller mills on the market were provided with static classifiers or low efficiency dynamic classifiers. High efficiency dynamic classifiers are used in vertical roller mills because of their improved performance in cement grinding circuits. New generation classifiers enable to control the performance of classification by adjusting setting parameters. High efficiency dynamic classifiers are located at the top of the mill. A caged-rotor dynamic classifier is illustrated in Figure 2.35.

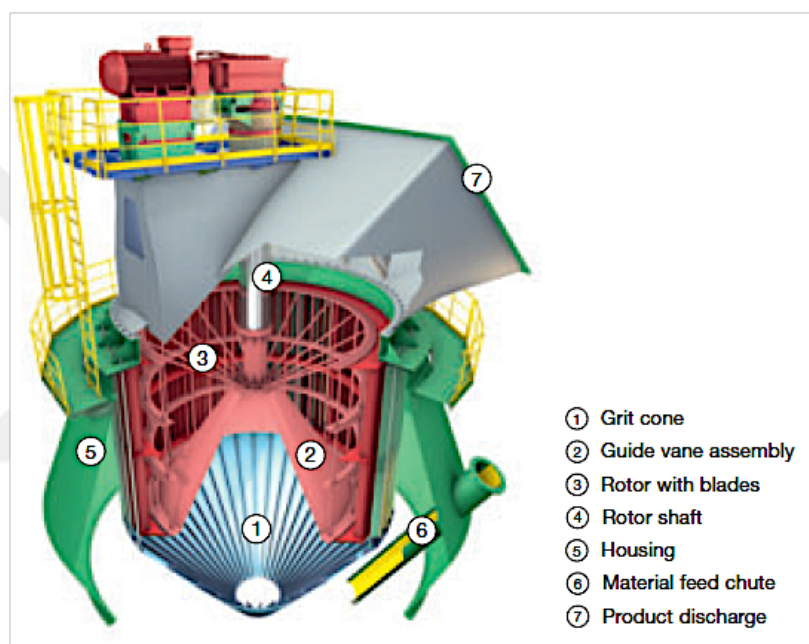


Figure 2.35 A high efficiency dynamic classifier in a Loesche vertical roller mill [35]

The classifier performance has a significant effect on the grinding efficiency. The classifier reject material creates coarser material bed on the table. The coarser bed increases the grinding performance, because finer material in bed cause cushion effect. An efficient classifier leads to decrease in grinding energy consumption and vibrations as well [88,89]. Reduced coarse particle residues improve the burning characteristics of raw mill [65].

2.3.6. Design and Operating Parameters Affecting the Vertical Roller Mill Performance

Studies on investigation of effects of design and operational parameters on vertical roller mill performance are limited in the literature. In this section, these parameters and their effects are discussed.

Dam ring height: Dam ring is a kind of barrier surrounding the grinding table (Figure 2.36). Dam ring is used to keep the material on the grinding table. Height of the dam ring is adjustable and control the thickness of the grinding bed on the table.



Figure 2.36 A photo of dam ring height

Relationships between dam ring height and bed height, product rate were investigated under controlled conditions by Demir [90]. Results are presented in Figure 2.37. Grinding bed height increases with the increasing dam ring height. Product fineness and dam ring height are inversely proportional to each other. Higher dam rings increase the retention time of the material on the grinding table so this results in finer product. In parallel to this, mass flow of the product stream increases.

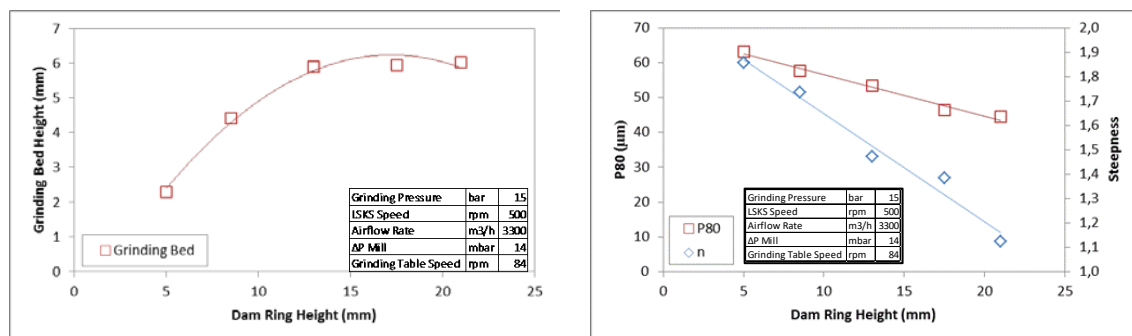


Figure 2.37 Effect of dam ring height on product size and grinding bed height [90]

Table speed: Speed of the grinding table has not a significant effect on vertical roller mill performance. Table speed is directly related to the residence time of the material in the grinding zone [4]. Higher table speed decreases the residence time of the material and this effects the amount of material on the grinding table. In operation, table speed is generally kept at optimum which minimum vibration occurs.

Working pressure: Grinding pressure is an effective parameter on product fineness. Similar results were obtained in studies related with the effect of grinding

pressure on vertical roller mill [72,90,91]. The effect of working pressure on product rate is given in Figure 2.38. Increasing working pressure, improve the energy applied to the material and more fines are offered to the classifier and leaving the circuit faster. Table product size decreases and reject material which cannot be transported to the classifier decreases. This result in higher production rates.

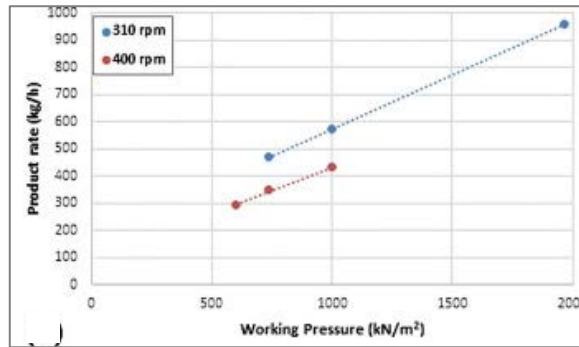


Figure 2.38 Effect of working pressure on product rate [91]

Air flowrate: Air flowrate through the mill is crucial control parameter for material transportation inside the mill and product fineness. A number of researches published showing the effect of airflow rate on production rate [47, 90]. Production rate of the circuit increases as the rate of volumetric air increases as a result of the high drag force (Figure 2.39). This leads to reduction in reject material, because amount of particles transported to the classifier increases with the increasing air flowrate. It was reported that the higher air flowrates increase the product fineness. Velocity of the coarse particles are increased by high volumetric air flowrate so coarse particles have a chance for classification.

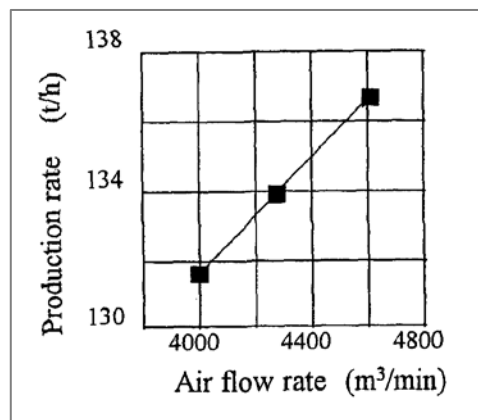


Figure 2.39 Effect of air flowrate on product rate [47]

Classifier rotor speed: Rotor speed of the classifier is the main parameter related with the product rate and product particle size. The cut size of classification can be controlled by adjusting the speed of the classifier rotor.

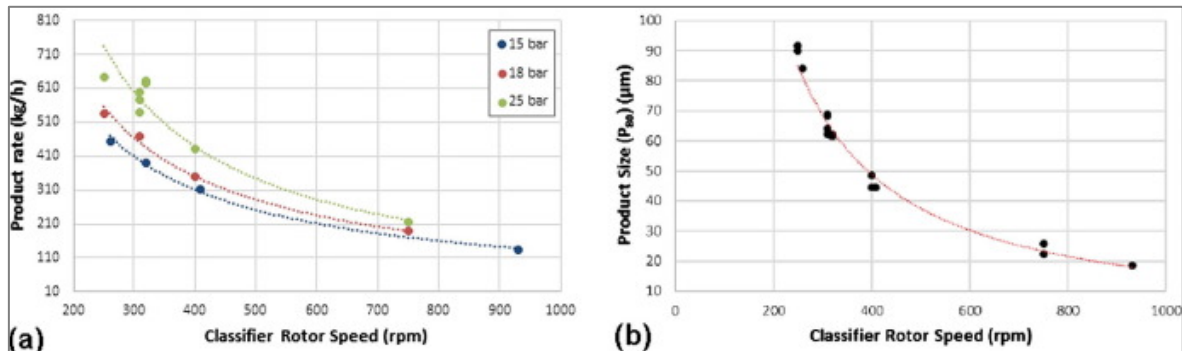


Figure 2.40 Relationship between classifier rotor speed & (a) product rate and (b) product size (P₈₀) [91]

Lower rotor speed decreases the internal circulation and this causes an improvement in product rate (Figure 2.40a). Rotor speed of the classifier and the product size is inversely proportional to each other. Higher classifier rotor speed increases the amount of coarse material in the reject stream and finer product is obtained (Figure 2.40b).

2.3.7. Modelling Approaches of Vertical Roller Mills

Modelling of the VRM operation has recently attracted the interest of the researchers. Different models have been developed in order to analyze and model the vertical roller mill system that may have improved benefits on grinding operations. A number of these models were based on theoretical and empirical approaches. Among them, empirical models have limited capabilities in simulating the non-tested conditions. Modelling studies that were supported by industrial scale data is limited in the literature. Generally, laboratory and pilot scale tests were carried out for modelling of vertical roller mills.

Musto and Dunn [4] published a paper on the effects of operational parameters to analyze the performance of vertical roller mill. Laboratory scale test results showed that having coarser product size distribution increases the maximum transmittable power to material. The relationships between product fineness, mill speed, capacity and power was also developed within this study.

A mathematical model for a ring-ball mill was developed by Austin et al. [92]. This model is based on mass-size balance model and includes internal and external classification (Figure 2.41).

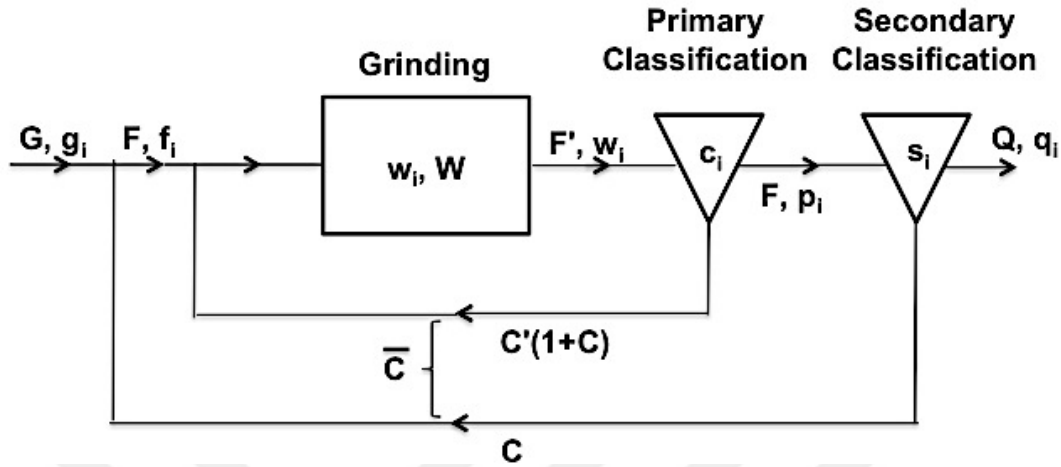


Figure 2.41 Complete circuit model with internal and external classification [92]

The model comprises several of the mathematical expressions. Base equations of grinding and classification zones are given. The mass balance at the grinding zone is expressed by Equation 2.1. Breakage parameters are determined from Hardgrove test results.

$$F'w_i = F'f_i' - S_iw_iW + \sum_{\substack{j=1 \\ i>1}}^{i-1} b_{i,j}S_jw_jW \quad (2.1.)$$

where,

F' : Flowrate at the grinding zone (kg/min)

W : Hold up in the mill (g)

w_i : Weight fraction of size i hold up

w_j : Weight fraction of size j hold up

f_i' : Weight fraction of size i in the feed to the grinding zone

S_i : Specific rate of breakage of size i (1/min)

S_j : Specific rate of breakage of size j (1/min)

$b_{i,j}$: Fraction of particles broken from the size interval j appearing in size interval i

Primary and secondary classification zones are calculated from Equation 2.2. and Equation 2.3., respectively.

$$1 + C' = \frac{1}{\sum_i w_i(1 - c_i)} \quad (2.2.)$$

$$1 + C = (1 + \bar{C}) \sum_i w_i(1 - c_i) \quad (2.3.)$$

where,

C' : Circulation ratio at primary classification zone

C : Circulation ratio at secondary classification zone

\bar{C} : Net circulation ratio

w_i : Weight fraction of size i hold up

c_i : Weight fraction of size i material in stream F' which is returned to the table

The model has no scale-up procedure although it predicts the capacities and particle size distributions for coals with different Hardgrove indices correctly.

Austin et al. [93] was developed a scale-up procedure. According to this study, capacity of an industrial mill can be calculated by using Equation 2.4.

$$Q = (1.33 \cdot 10^4) D^{2.5} Q_H \quad (2.4.)$$

where,

Q : Industrial mill capacity (t/h)

D : Industrial mill diameter (m)

Q_H : Mill capacity determined by model for Hardgrove mill (t/h)

Total power of an industrial mill (m_{pT}) is a function of industrial mill diameter (D) and motor efficiency (η_m) (Equation 2.5.).

$$m_{pT} = (1/\eta_m) 29.5 D^{2.5} \quad (2.5.)$$

Kersting [3] developed a mathematical model for vertical roller mill system that can be used for simulating both steady and unsteady state conditions. In this model,

vertical roller mill process is divided into three sub-systems, which are linked by mass and energy flows (Figure 2.42).

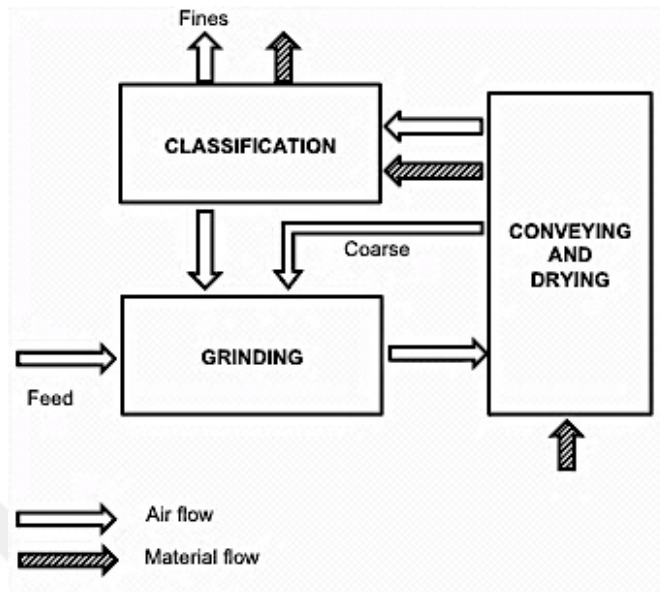


Figure 2.42. Sub - models of the vertical roller mill [3]

For the sub-model describing the conveying, the motion of material on the grinding table, the temperature and the moisture content of each particle size class are used as model parameters. The mass transfer coefficients and the comminution rate that is affected by material bed depth, grinding roller force, dimensions of particles are defined to model the grinding operation.

Jung [94] reported that specific energy consumption of a vertical roller mill was independent from the size of the machine but only dependent on the material being ground. Based on this principle, installed power of an industrial vertical roller mill can be calculated from the pilot scale grinding tests (Equation 2.6.).

$$P_B = W_T m_B \quad (2.6.)$$

where,

- P_B : Installed power of industrial scale mill (kW)
- W_T : Specific power consumption of test mill (kWh/t)
- m_B : Capacity of industrial scale mill (t/h)

Installed power is also a function of the material being ground, fineness of the product, speed of grinding table etc. [95]. Drive power of an industrial mill can be calculated by Equation 2.7.

$$P_B = f_T F_B Z_B V_B \quad (2.7.)$$

where,

- f_T : Material factor
- F_B : Grinding force (kN/roller)
- Z_B : Number of grinding rollers
- V_B : Grinding table speed (m/s)

Extended version of Equation 2.7. has been proposed by Jung [96]. In this version, classifier efficiency has been introduced (Equation 2.2.). In Equation 2.8. η_{Sn}/η_{Sa} defined as classifier efficiency new/old (%).

$$m_B = \frac{P_B}{W_T} = \frac{f_T F_B Z_B V_B \frac{\eta_{Sn}}{\eta_{Sa}}}{W_T} \quad (2.8.)$$

Sato et al. [97] constructed a mathematical model for batch ring roller mill to predict the steady state performance of an industrial scale mill. This model is based on model developed by Austin et al. [92]. Specific breakage rates and breakage distribution parameters were determined by experimental data. Classification sections in the model were defined by empirical equations. Also, scale up factors were developed depending on design and operational parameters like capacity, diameter and shaft speed. Then, this model was improved for unsteady-state conditions [98]. Mass transport was correlated to mill hold-up, mass flowrate through the mill and mill sizes to simulate the mill behavior during changes in load, feed and operational conditions.

In another study, a simple matrix model has been used for modelling the grinding process in a cement vertical roller mill (CKP) [5]. In this model, multiple grinding cycles have been taken into account to obtain the final product size distribution with real data. Grinding operation is expressed for first and second cycle grinding in Equation 2.9. and Equation 2.10., respectively.

$$P_1 = B.f \quad (2.9.)$$

$$P_2 = (B.S + I - S)P_1 \quad (2.10.)$$

where f and P are the particle size distributions of the feed and the product materials, B is a breakage distribution function, which is determined from experimental data and S is a selection function.

As stated in this section, vertical roller mill loom large in the cement and mineral industry. Improving the performance of these mills is possible by analyzing the mill operation properly. Necessity of making relationships between operational parameters and size reduction performance have been arose to keep the mill and circuit under control. With this aim, a detailed test program was carried out. In consideration of the indications in the literature, data obtained from the grinding tests results were evaluated for model development. Details of this study are presented in the next sections.

3. EXPERIMENTAL STUDIES

Within the context of this thesis, pilot and industrial scale grinding tests were performed to develop a mathematical model for vertical roller mill operation. Road map of the study is summarized in Figure 3.1. In the first step, pilot scale tests were performed under controlled conditions to define the relationships between design and operational parameters. Different ores were used for the grinding tests to reflect the material effect into the model. In the second step, industrial scale grinding tests were carried out to make a comparison with the pilot scale test results and investigate the applicability of the model developed for pilot scale tests.

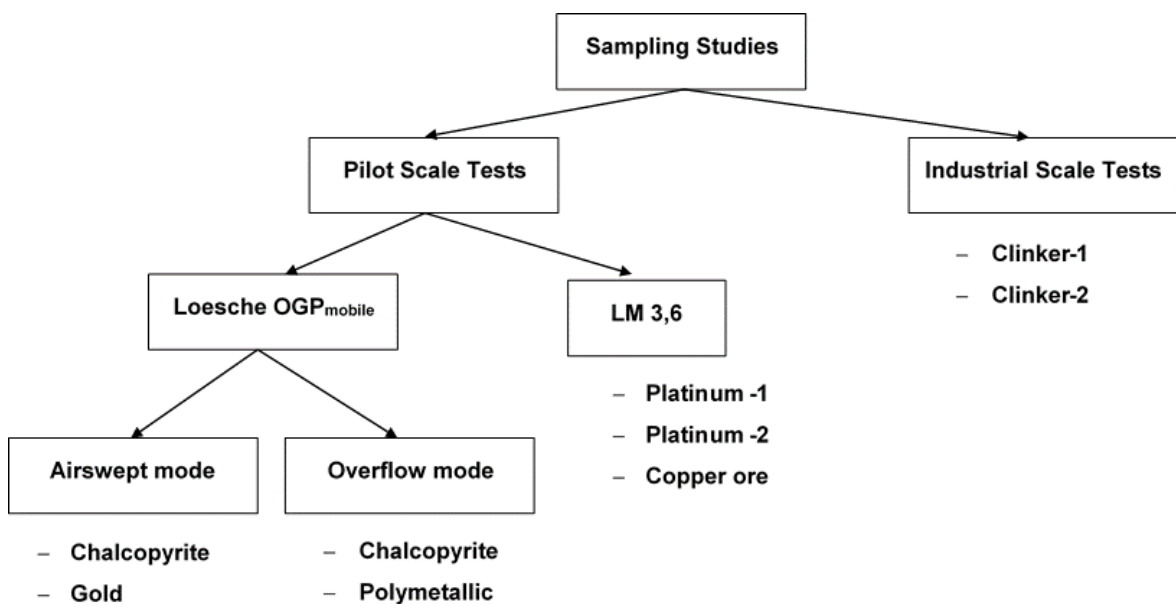


Figure 3.1 Summary to test program

After sampling studies, particle size distributions and densities of the collected samples were determined. Fresh feed samples were subjected to material characterization tests. In this context, confined compressed bed breakage tests were performed.

3.1. Pilot Scale Studies

As part of this study, grinding tests were carried out at different operating conditions for different ores to evaluate the relations between design and operational parameters and to create a first basis for a computational performance evaluation of a vertical roller mill model. Two different pilot scale vertical roller mills were used in this study. Certain parts of grinding tests were performed by conventional airswept

vertical mills LM 3,6. But, these mills are a black box, it is not possible to take accurate samples inside the mill because of the physical constraints. Process and performance of the vertical roller mill should be analyzed in detail for realistic model. A new pilot plant vertical roller mill concept was developed to define the process inside the system. Tests for model development were carried out in this new vertical roller mill concept.

3.1.1. Grinding Tests with OGP_{mobile}

Grinding tests were performed by using an LM 4,5 installed in the mobile ore grinding plant (OGP_{mobile}) constructed by Loesche for ore grinding. The installation of the OGP is illustrated in Figure 3.2.



Figure 3.2. Pictures of the OGP_{mobile}

The OGP_{mobile} consists of three containers. Two containers contain grinding, classifying, product separation and transportation units. Process control system and control room are located in the third container. Design and operational parameters of the plant are summarized in Table 3.1.

Table 3.1. Technical specifications of the mobile VRM plant

Throughput rate (t/h)	0.5-3
No of rollers	4
Table Diameter (mm)	450
Installed Power (kW)	420
· Mill Power (kW)	37
· Heater Power (kW)	300
Separator Air Flow (m ³ /h)	1500-5000

Loesche OGP_{mobile} is a fully automated system. Measured parameters during operation can be followed from the control room. Screenshot of the control system is given in Figure 3.3.

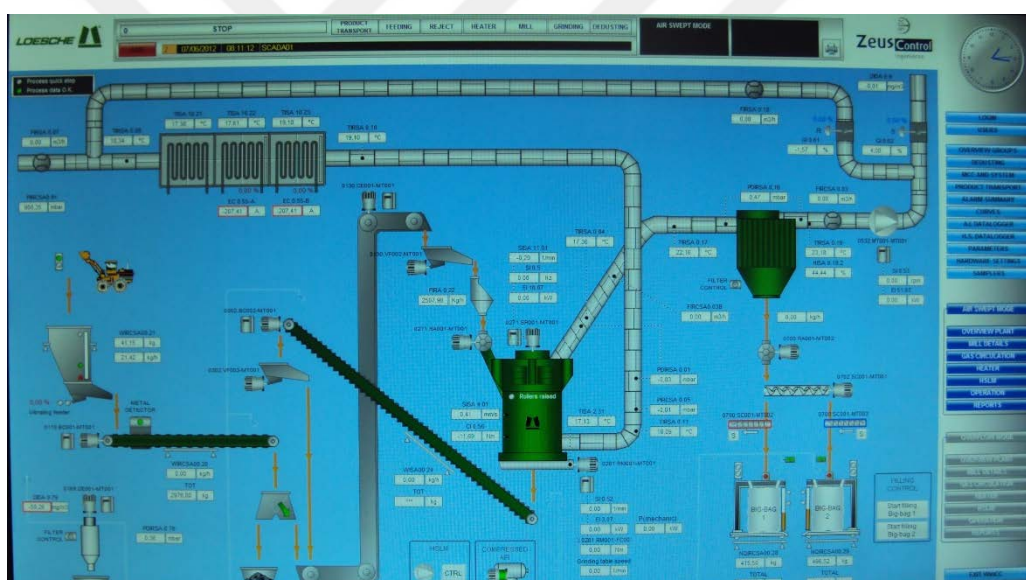


Figure 3.3 Loesche OGP_{mobile} control system

Loesche OGP_{mobile} can be operated in two grinding modes characterized by location of the classification systems as airswept and overflow mode. In the airswept mode, the vertical roller mill and a high efficiency dynamic classifier are suited above each other as a single unit (Figure 3.4). Material is fed to the grinding chamber and transported by table rotation to the grinding gap between the fixed grinding rollers and the mill table. Crushing and grinding take place by compressive grinding. Ground material is transported over the edge of grinding table and lifted pneumatically to the dynamic classifier. After classifying, coarse material is sent

back to the grinding table and combined with the fresh feed. Classifier fine product is collected as final product in a following bag filter.

In the overflow mode, there is a two-stage air classification system consisting of static and dynamic types and separate from the mill body (Figure 3.5). This system was developed in order to reduce specific energy consumption of the whole system since the material transportation is carried out mechanically. Overflow mode is important for model development because it enables to collect samples inside the system so it is possible to evaluate the performance of each operation in the mill. During the operation, fresh feed is fed to the static classifier initially and fine product is directed to the dynamic classifier before being ground. The coarse streams of static and dynamic classifiers are sent to the mill to be ground then ground particles mixing with fresh feed is conveyed mechanically e.g., belt conveyor, bucket elevator, to the static classifier again.

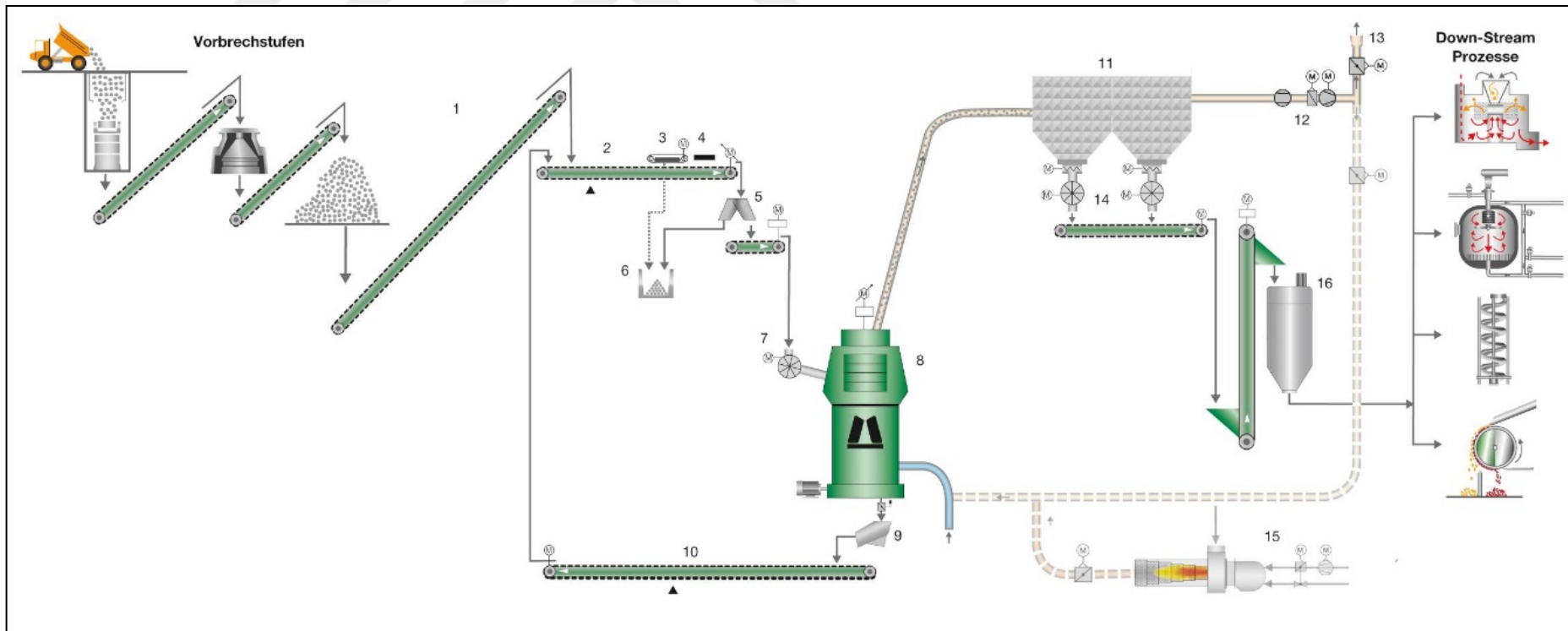


Figure 3.4. Flowsheet of Loesche OGP_{mobile} in air-swept mode

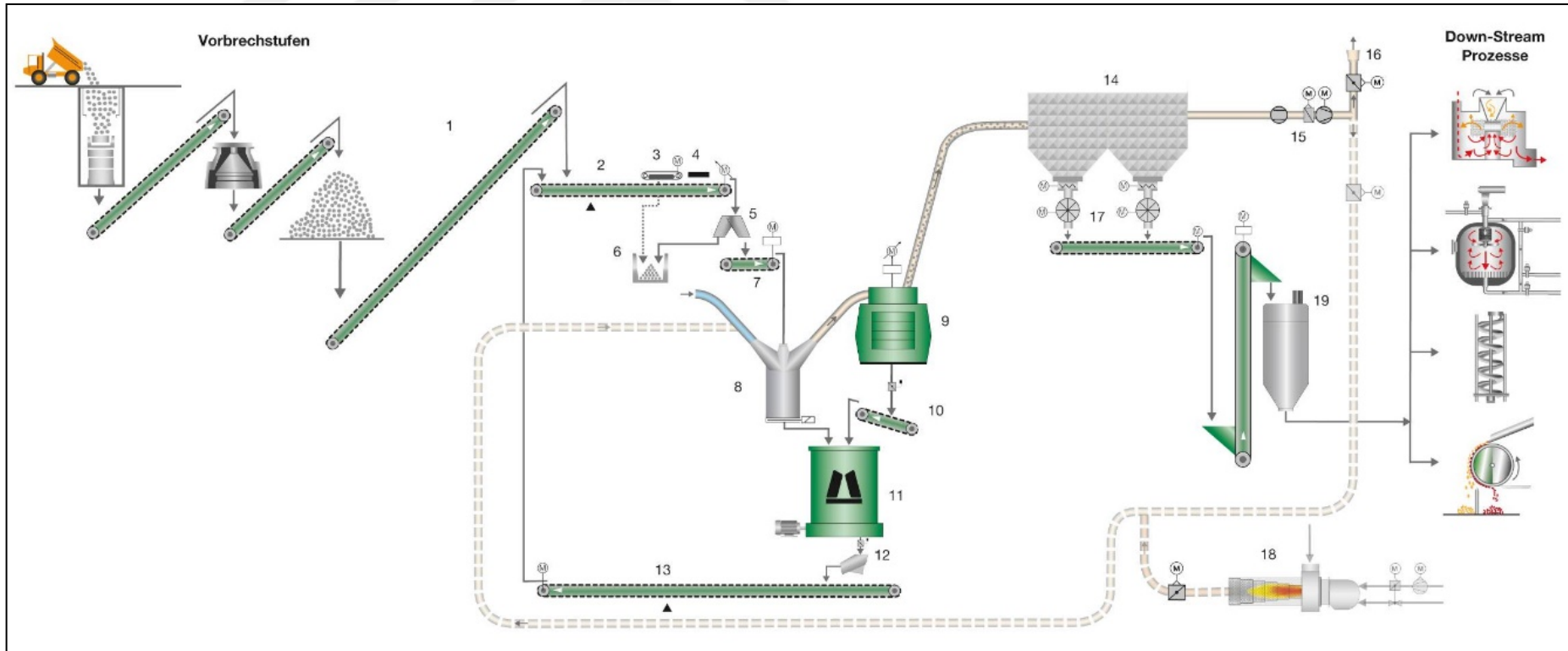


Figure 3.5. Flowsheet of Loesche OGP_{mobile} in overflow mode

Grinding tests were performed for polymetallic, chalcopyrite and gold ores which is the epithermal gold associated in quartz vein. Polymetallic ore contains gold, silver, copper, lead, and zinc within the minerals chalcopyrite, galena, sphalerite and gahnite. Physical properties of the tested materials are given in Table 3.2.

Table 3.2 Specifications of the ores tested

	Polymetallic ore	Chalcopyrite ore	Gold ore
Bond Work Index (kWh/t)	18.7	11.2	18.1
Specific Gravity (g/cm ³)	2.8	4.1	2.8

Sampling studies were conducted during the steady-state condition of the vertical roller mill circuit. For the airswept mode, pressure difference is the main parameter that indicates the system is at steady state. Therefore, the variation of this parameter together with the flow rate of the product are followed for a given operating condition then it is decided to commence the sampling of the product stream. Followed trends curves from control room at steady state condition are given in Figure 3.6.

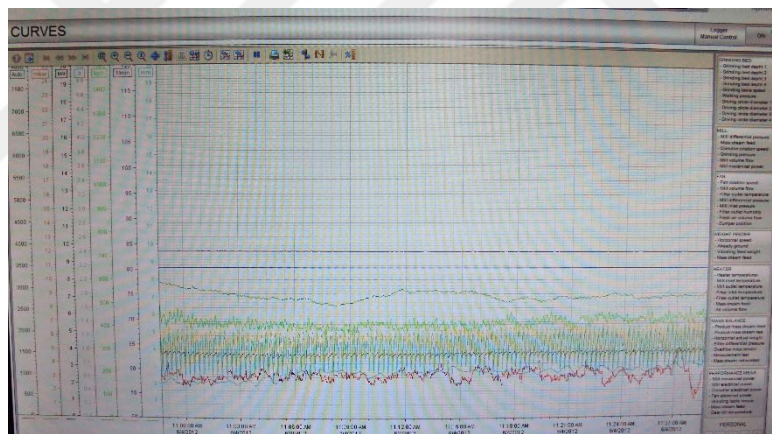


Figure 3.6 Trend curves at steady state conditions

For the overflow mode, since the classification system is set up at the outside of the mill body, the flow rate of mill discharge stream conveyed to the static classifier and product stream are followed. Once the steady state condition was established, the final product stream was sampled for the airswept mode. Simplified flowsheet and sampling points of airswept mode are illustrated in Figure 3.7.

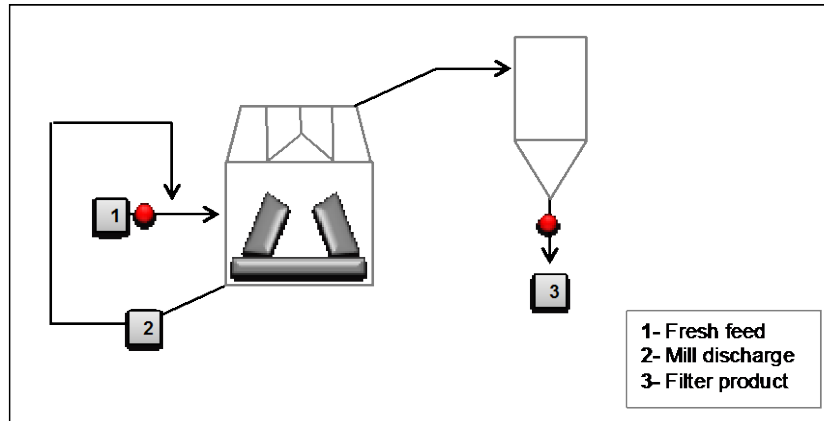


Figure 3.7. Flowsheet and sampling points of Loesche OGP_{mobile} in airswep mode
Operational parameters recorded during the tests were presented in Table 3.3 and Table 3.4 for airswep mode.

Table 3.3 Test conditions for chalcopyrite ore (airswep mode)

	Product rate (kg/h)	Working pressure (kN/m ²)	Classifier rotor speed (rpm)	Volumetric air flowrate (m ³ /h)	Grinding bed average (mm)	Specific Energy Consumption (VRM-grinding) (kWh/t)
T1	189.3	600	900	2500	5.53	28.6
T2	480.5	600	328	2500	11.25	18.1
T3	765.4	1000	305	2500	10.03	15.3
T4	682.4	800	315	2500	11.00	15.6
T5	921.3	800	219	2500	11.43	11.7

Table 3.4 Test conditions for gold ore (airswep mode)

	Product rate (kg/h)	Working pressure (kN/m ²)	Classifier rotor speed (rpm)	Volumetric air flowrate (m ³ /h)	Grinding bed average (mm)	Specific Energy Consumption (VRM-grinding) (kWh/t)
T1	315.0	700	409	2800	9.13	21.4
T2	392.6	700	320	2800	9.45	18.2
T3	453.5	700	260	2800	9.33	15.8
T4	137.0	700	930	2800	5.55	32.2
T5	349.0	850	400	2800	9.03	22.0
T6	468.2	850	310	2800	8.78	17.2
T7	188.0	850	750	2800	5.80	30.1
T8	431.6	1200	400	2800	7.73	22.6
T9	540.5	1200	310	2800	8.05	19.1
T10	213.8	1200	750	2800	4.53	30.9

For the overflow mode, samples were collected from the fresh feed, mill discharge, dynamic classifier underflow and product streams. Flowrates of mill discharge and dynamic classifier streams were measured by determining the weights of samples in a definite time. Flowsheet and sampling points of over flow mode is represented in Figure 3.8.

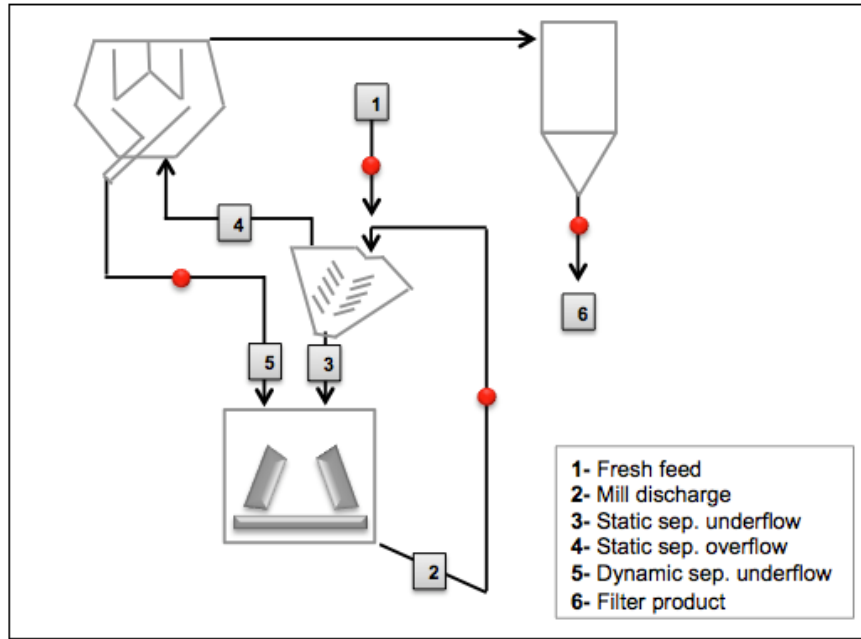


Figure 3.8. Flowsheet and sampling points of Loesche OGP_{mobile} in overflow mode
Recorded operational parameters for overflow mode test are given in Table 3.5 and Table 3.6.

Table 3.5 Test conditions for polymetallic ore (overflow mode)

		T1	T2	T3	T4	T5
Flowrates (kg/h)	Product	86.5	121.9	85.6	106.2	196.1
	Mill discharge	2220.1	2850.0	2225.8	3325.1	3734.3
	Dynamic classifier underflow	210.0	145.4	120.7	110.5	292.7
	Working pressure (kN/m ²)	600	600	600	600	600
	Classifier rotor speed (rpm)	320	370	230	120	120
	Volumetric air flowrate (m ³ /h)	2400	2400	1250	1250	1250
	Grinding bed average (mm)	2.00	2.00	1.70	1.60	2.60
	Specific Energy Consumption (VRM-grinding) (kWh/t)	20.7	18.6	22.3	18.3	14.2

Table 3.6 Test conditions for chalcopyrite ore (overflow mode)

	T1	T2	T3	T4	T5	T6	T7	
Flowrates	Product (kg/h)	198.0	204.1	475.6	160.1	373.1	312.3	382.1
	Mill discharge (kg/h)	2807.9	3234.9	4584.0	2218.0	3825.6	3687.6	3500.1
	Dynamic classifier underflow (kg/h)	465.3	524.3	408.0	236.1	460.3	575.1	176.3
	Working pressure (kN/m ²)	600	600	600	1000	1000	800	1000
	Classifier rotor speed (rpm)	900	800	100	900	340	360	90
	Volumetric air flowrate (m ³ /h)	2500	2500	2500	1500	2500	2500	2500
	Grinding bed average (mm)	4.13	4.33	6.35	2.23	4.00	4.13	3.98
	Specific Energy Consumption (VRM-grinding) (kWh/t)	19.0	18.9	10.8	30.8	16.0	15.5	13.1

The size distributions of the samples were determined by combining two different measurement techniques. Initially, dry sieving technique was applied from top size to 150 μm , after that the measurement was completed via laser scattering method that enabled to determine the distribution down to 0.5 μm . Measured particle size distributions around the vertical roller mill circuit for airswept and overflow mode are presented in Section 6.1 and Appendices 1-2, respectively.

3.1.2. Grinding Tests with LM 3,6

In this part of the study, grinding tests were performed by using a pilot scale vertical roller mill in the Loesche Test Center. LM 3,6 type mill (Figure 3.9) has 2 rollers with the 707 kg/h nominal capacity. LM 3,6 has an automation system similarly to mobile unit. Set data and measured data during the grinding tests are controlled instantaneously by this system.



Figure 3.9. Picture of the LM 3,6

LM 3,6 is a airswept mill which combines grinding and classifying in one single machine, with the classifier installed above the grinding table. Simplified flowsheet of the pilot plant configuration is given in Figure 3.10. Material is fed into the vertical roller mill chamber for grinding under the rollers. After rollers, ground material is lifted to the high efficiency dynamic classifier and fine material is separated from the coarse material. Rejected material from the classifier is back to the grinding table and recombined with the fresh feed.

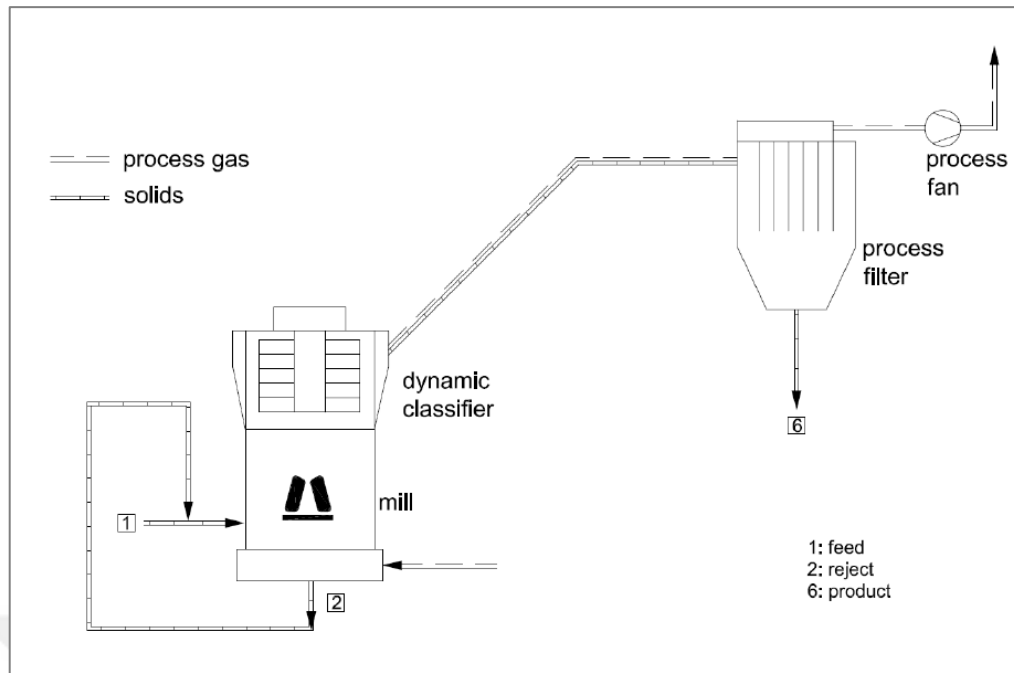


Figure 3.10. Flowsheet of the vertical roller mill plant configuration

Grinding tests were performed for two different platinum ores from Bushveld Complex and copper ore. The copper mineral consists of mainly of enargite and in minor amounts of chalcocite, chalcopyrite, tennantite, luzonite, colusite and bismuthinite. Specifications of the materials are given in Table 3.7.

Table 3.7 Specifications of ores used in tests

	Platinum-1 ore	Platinum-2 ore	Copper ore
Bond Work Index (kWh/t)	23.0	21.2	12.5
Specific Gravity (g/cm ³)	3.8	3.8	4.0

Averagely, 4 tonnes of material were ground for each ore. During the tests, steady state conditions were established initially. After recording operational parameters, representative samples were collected from the product. Table 3.8 - 3.10 presents the operating conditions of the mill at steady state conditions.

Table 3.8 Test conditions for platinum ore-1

	T1	T2	T3	T4	T5
Product rate (kg/h)	181.0	231.0	263.0	319.0	423.0
Working pressure (kN/m ²)	600	600	600	600	600
Classifier rotor speed (rpm)	449	380	355	301	247
Volumetric air flowrate (m ³ /h)	1774	1774	1775	1774	1774
Grinding bed average (mm)	5.15	6.00	6.30	6.70	6.75
Specific Energy Consumption (VRM-grinding) (kWh/t)	16.9	14.0	12.8	11.6	8.9

Table 3.9 Test conditions for platinum ore -2

	T1	T2	T3	T4	T5
Product rate (kg/h)	305.0	319.0	329.0	187.0	414.9
Working pressure (kN/m ²)	600	600	600	600	600
Classifier rotor speed (rpm)	310	294	280	384	220
Volumetric air flowrate (m ³ /h)	1625	1624	1625	1625	1621
Grinding bed average (mm)	6.15	5.65	5.8	3.65	7.20
Specific Energy Consumption (VRM-grinding) (kWh/t)	11.4	10.8	10.6	15.0	8.9

Table 3.10 Test conditions for copper ore

	T1	T2	T3
Product rate (kg/h)	166.0	222.0	262.0
Working pressure (kN/m ²)	600	600	600
Classifier rotor speed (rpm)	450	330	270
Volumetric air flowrate (m ³ /h)	1748	1747	1750
Grinding bed average (mm)	5.90	7.40	8.25
Specific Energy Consumption (VRM-grinding) (kWh/t)	18.5	15.4	14.0

The size distributions of the samples were determined by laser scattering method. Measured feed and product size distributions of pilot scale grinding tests are presented in Section 6.2.

3.2. Industrial Scale Tests

Industrial scale tests were performed using a Loesche vertical roller mill in a cement plant to evaluate the performance of the vertical roller mill and to obtain data for model development. In this context two sampling surveys were performed. In this study, a new sampling method developed by Aydogan [99] was used to obtain data. The methodology is based on collection of samples from both mill inside and around the system in order to evaluate the overall performance and additionally the grinding and separation mechanisms individually. Schematic view of a typical vertical roller mill with the streams is illustrated in Figure 3.11 and Table 3.11 gives the names of the streams. Broadly, the vertical mill operation is separated into three stages that are; feeding, static classification (transportation of the material from the table to the dynamic classifier) and dynamic classification.

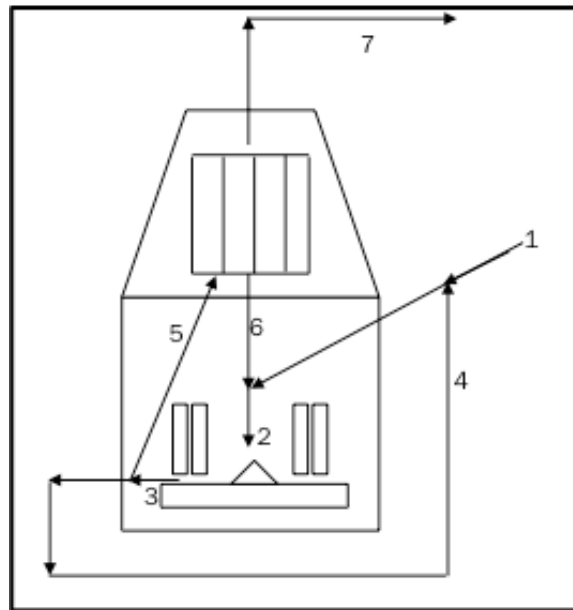


Figure 3.11 Schematic view of vertical roller mill and streams

Table 3.11 Name of the streams

Stream	Stream name
1	Fresh Feed
2	Table Feed
3	Table Product
4	Static Class. Reject
5	Static Class. Fine (Dynamic Class. Feed)
6	Dynamic Class. Reject
7	Dynamic Class. Fine (Product)

Prior to performing sampling campaign, operating conditions should be followed from the control system to determine whether the system is at steady state condition. In this context, the trends of mill, fan and elevator powers, differential pressure of the mill and feed tonnage are followed. The sampling campaign is commenced when the steady state condition is established. Sampling points are illustrated in Figure 3.12. Fresh feed (1) and product (7) streams are outer streams and could be sampled easily. Initially, final product stream is sampled while VRM is running. Afterwards, the mill is crash stopped to collect samples from fresh feed conveyor belt, mill discharge and mill inside. For the fresh feed, the whole material is collected from certain length of the belt and then weighed to calculate the flow rate by considering the belt speed. Static classification stage reject (4), was not sampled because the buckets of the elevator were empty. This results from the material transportation mechanisms of the mill. All material is transported by air

because of the high air flowrate inside the mill. As a final step of survey, sampling studies are performed inside the mill. The materials just before and after the rollers were assumed as total table feed (2) and product (3), respectively.

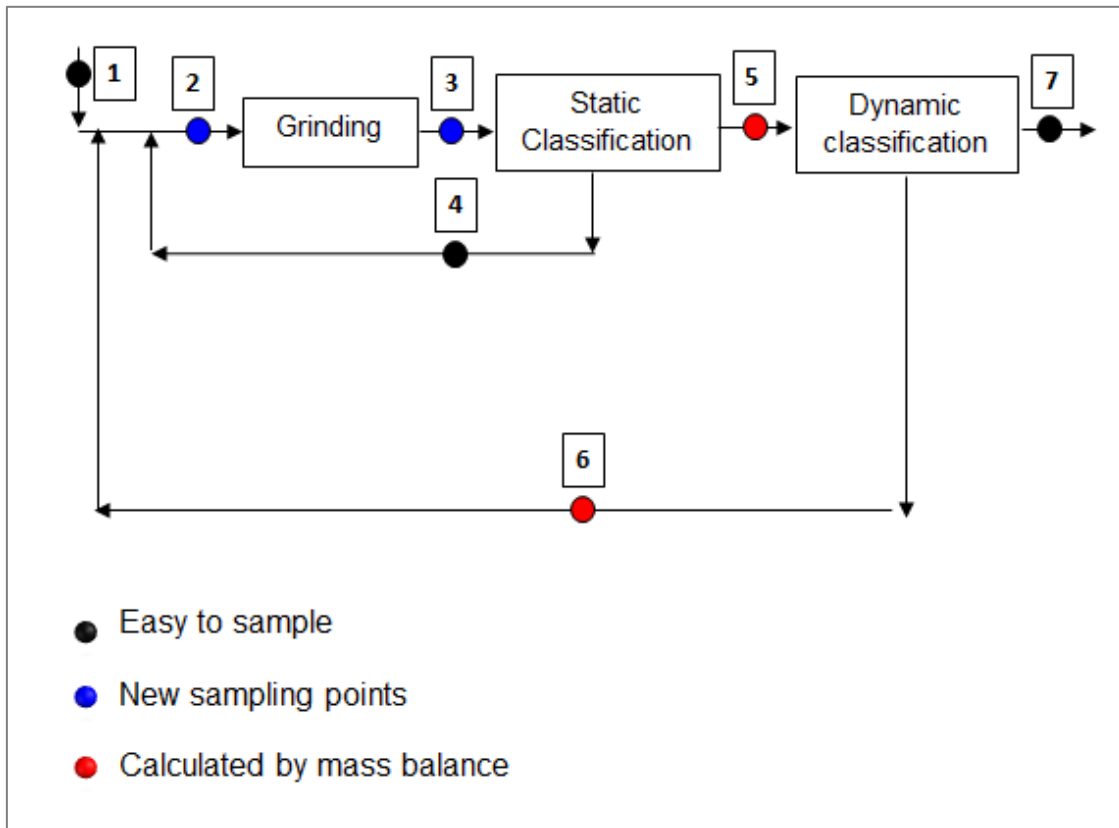


Figure 3.12 Industrial scale vertical roller mill sampling points

Design parameters of the vertical roller mill are summarized in Table 3.12.

Table 3.12 Design parameters of vertical roller mill

Table diameter (m)	4.6
Table speed (rpm)	24.21
Number of master and slave rollers	2 M+ 2 S
Max. working press [bar] (M-roller)	100
Min. working press [bar] (M-roller)	55
Maximum throughput (t/h) 4000 cm ² /g (GBFS)	120
Maximum throughput (t/h) 4000 cm ² /g (CEM I)	110
Classifier diameter (mm)	4300
Classifier max. rotor speed (rpm)	150
Max. fan capacity (kW)	1750
Min. fan capacity (kW)	416

During the sampling surveys, operational parameters measured were recorded at the control room. Control room data are given in Table 3.13.

Table 3.13 Operating conditions of the surveys

	Survey 1	Survey 2
Name of feed composition	CEM I	CEM I
Clinker (t/h)	113.01	116.3
Limestone (t/h)	2.65	2.72
Gypsum (t/h)	4.83	4.74
Limestone-2 (t/h)	3.38	3.46
Clinker (%-H ₂ O)	0.1	0.28
Limestone (%-H ₂ O)	4.76	4.69
Gypsum (%-H ₂ O)	2.7	4.96
Mill differential pressure (mbar)	52.07	54.45
Air flow filter outlet (m ³ /h)	322000	354365
Working press. M-roller (bar)	94	94
Classifier rotor speed (1/min)	108	111
Spec. power total (kwh/t)	28.74	29.85

Bond work indices were determined for two clinker samples. Calculated Bond work indices of clinkers from survey 1 and survey 2 is 14.2 kWh/t and 13.45 kWh/t, respectively. Then, all samples taken from the circuit were screened from 75 mm to 500 μ m. The particle size distributions of the minus 500 μ m materials were determined by laser sizing method. The particle size distributions of collected samples are shown in Figure 3.13 and Figure 3.14 for survey 1 and 2, respectively.

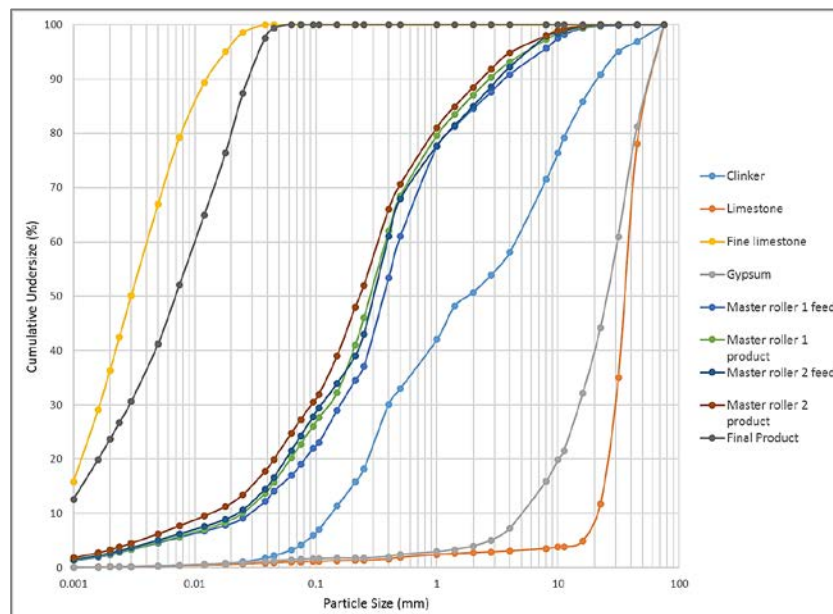


Figure 3.13 Particle size distributions of collected samples (Survey 1)

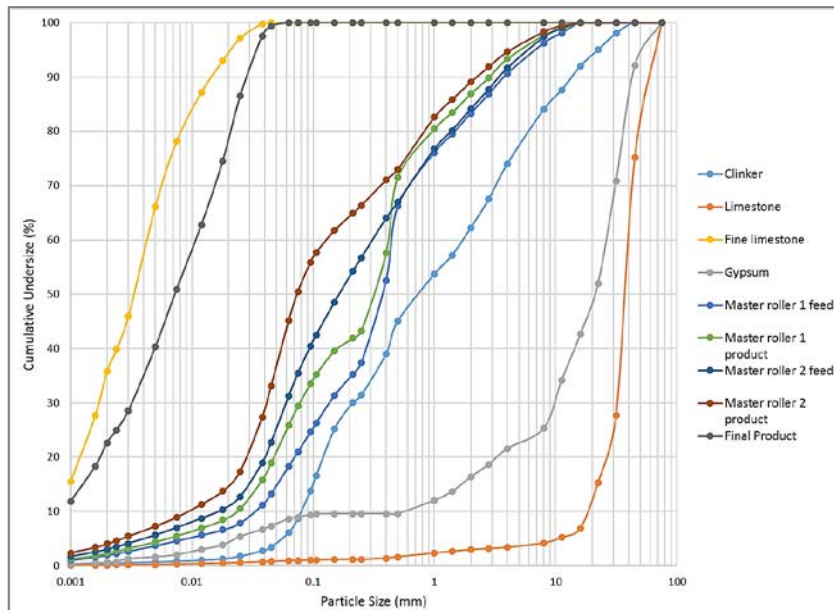


Figure 3.14 Particle size distributions of collected samples (Survey 2)

3.3. Material Characterization Studies

Breakage characteristics of materials are introduced into the model structure of comminution machines. Therefore, it has a significant importance to have a reliable model. Many different laboratory methods are suggested in the literature for ore characterization. For this study, piston-die bed breakage test was preferred to simulate the material breakage under pressure.

Material characterization studies were performed by using piston-die test equipment in the rock mechanics laboratory of Mining Engineering Department of Hacettepe University (Figure 3.15). Hydraulic press capacity of the equipment is 2000 kN. There is a unit deformation meter connected to computer to measure displacement in the material bed. Technical specifications of piston-die test equipment are given in Table 3.14.



Figure 3.15 Piston-die test equipment

Table 3.14 Technical specifications of piston-die equipment

Max. loading capacity	2000 kN
Max. loading rate	2.5 kN/sec
Precision of the LVDT gauge	10 μ m
Diameter of the cylindrical die	100 and 170 mm
Length of the cylindrical dies	200 mm

Throughout the studies the narrow size fractions were prepared for all fresh feed samples collected from pilot and industrial tests. Prepared samples were subjected to compression breakage under 3 different force levels. Piston-die test conditions for pilot and industrial test samples are given in Table 3.15 and Table 3.16, respectively.

Table 3.15 Piston-die test conditions for pilot scale test samples

Size Fraction (mm)	Force (kN)		
	100	500	1200
-9.5+8.0	✓	✓	✓
-5.6+4.75	✓	✓	✓
-2.8+2.0	✓	✓	✓

Table 3.16 Piston-die test conditions for industrial scale test samples

Size Fraction (mm)	Force (kN)		
	100	500	1200
-9.5+8.0	✓	✓	✓
-6.7+5.6	✓	✓	✓
-2.36+1.7	✓	✓	✓

During the piston die tests, the applied force and the displacement of material bed were recorded. Figure 3.16 shows the schematic view of the test. The particle bed is compressed from the bed height of h_1 to h_2 . The work done which is a function of the displacement is expressed with Equation 3.1.

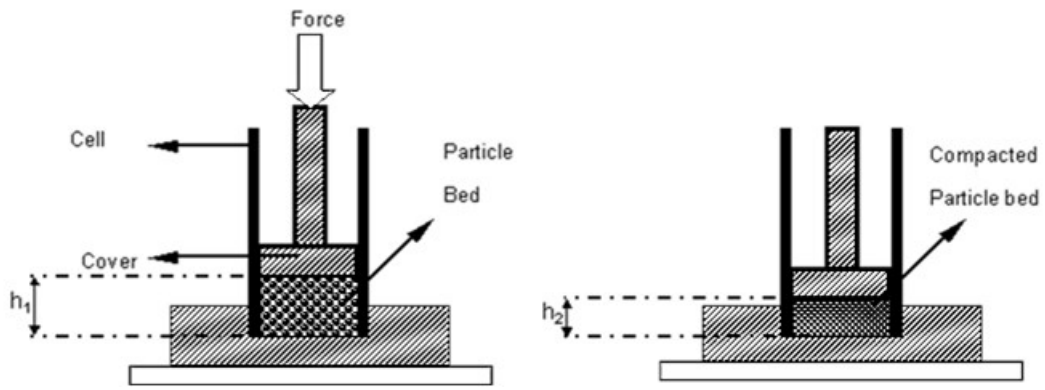


Figure 3.16 Representation of the particle bed compression

$$W = \int_{h_1}^{h_2} f(h) dh \quad (3.1.)$$

Where,

dh : Differential displacement,

f(h) : Force as a function of displacement.

Then, work done during compressed bed breakage test was calculated by drawing force-displacement curve initially. The area under the curve was calculated and noted as the energy of the breakage test. Typical force-displacement force graph is given in Figure 3.17.

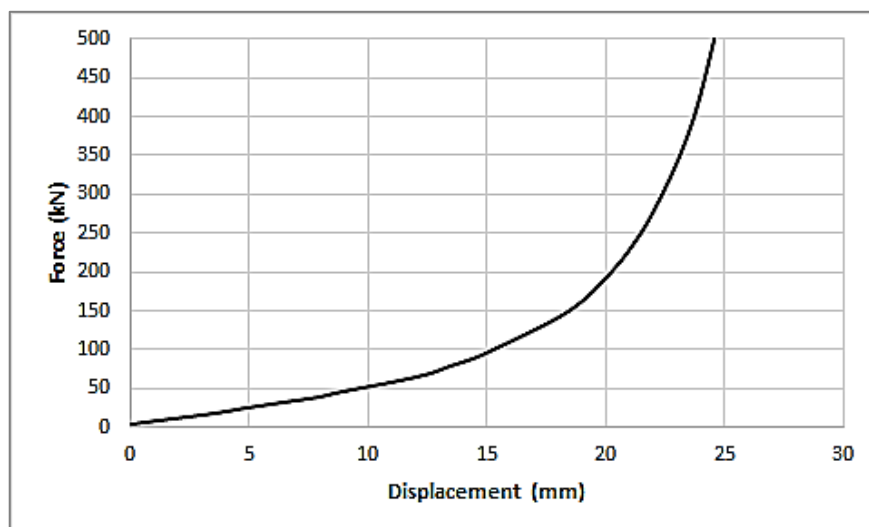


Figure 3.17 Typical force-displacement curve

After calculating the specific comminution energy (E_{CS}) for each test, particle size distributions of broken products were determined by sieve analysis. From the particle size distributions of the samples t_4 , t_{10} and t_{25} values were determined. t_{10} parameter is the fineness index that is defined as the percent passing of one tenth of the original mean particle size and t_4 , t_{25} is the percent passing 1/4, 1/25 of the original mean particle size.

E_{CS} - t_n ($n=4, 10$ and 25) data were fitted to size dependent breakage model (Equation 3.2.) developed by Eksi, et.al. [100]. Figure 3.18 - Figure 3.25 shows the t_n values as a function of specific comminution energy level (E_{CS}) and particle size. The markers represent the experimental results where the solid line represents the fitted data.

$$t_n = A * (1 - e^{-b.E_{CS}.X}) \quad (3.2.)$$

- A and b : Model parameters
- X : Particle size (mm)
- n : 4, 10 and 25

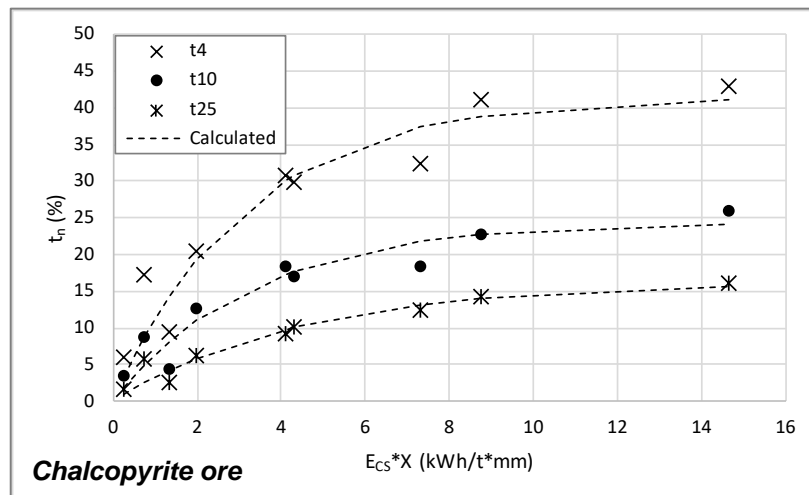


Figure 3.18 $E_{CS} \cdot X$ - t_n relationships of the chalcopyrite ore

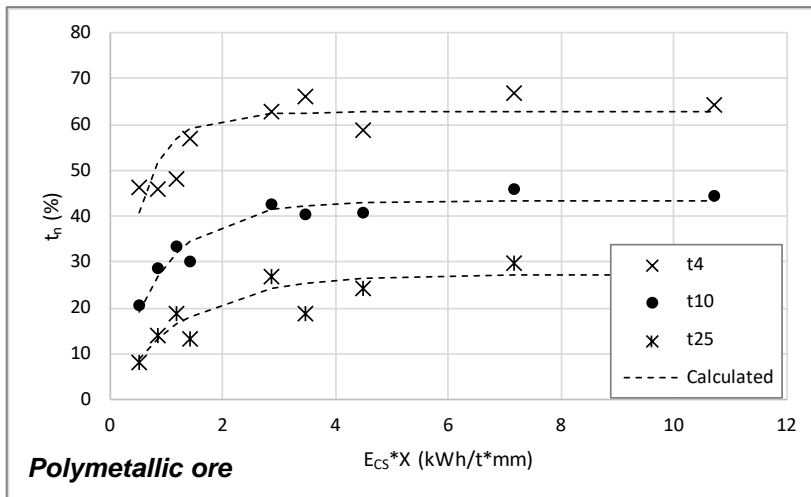


Figure 3.19 $E_{cs} \cdot X$ - t_n relationships of the polymetallic ore

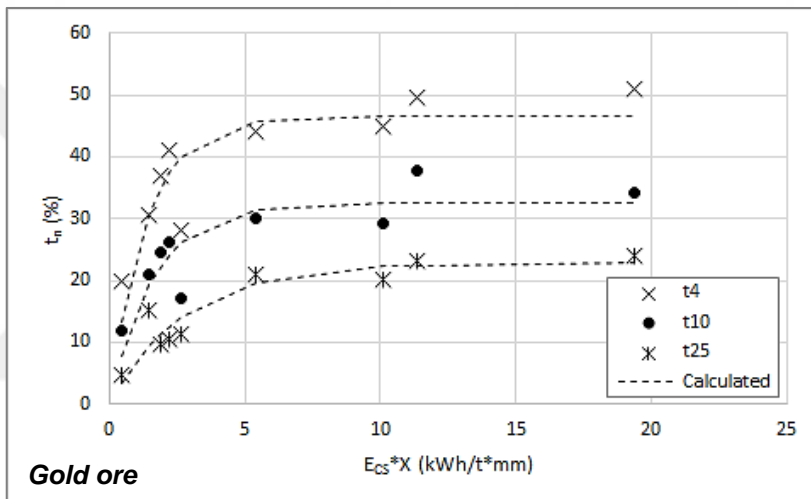


Figure 3.20 $E_{cs} \cdot X$ - t_n relationships of the gold ore

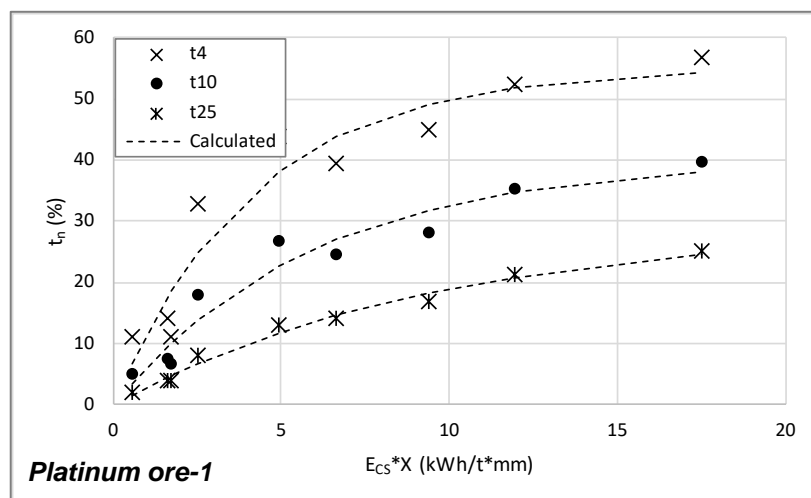


Figure 3.21 $E_{cs} \cdot X$ - t_n relationships of the platinum ore-1

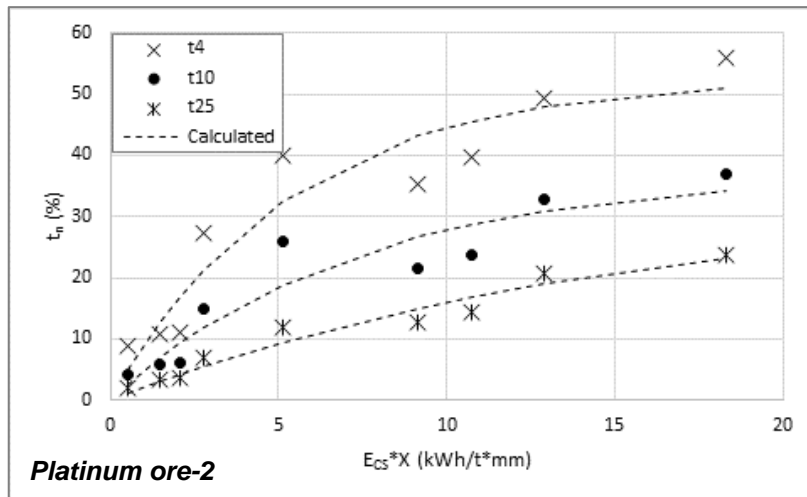


Figure 3.22 $E_{CS} \cdot X$ - t_n relationships of the platinum ore-2

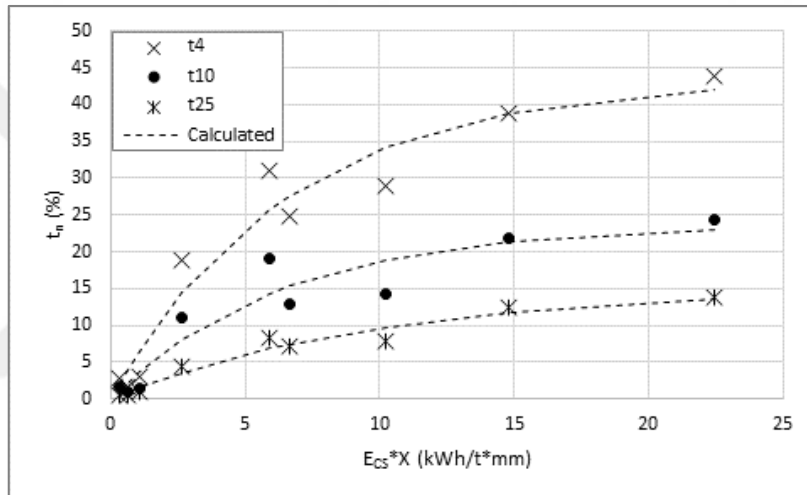


Figure 3.23 $E_{CS} \cdot X$ - t_n relationships of the copper ore

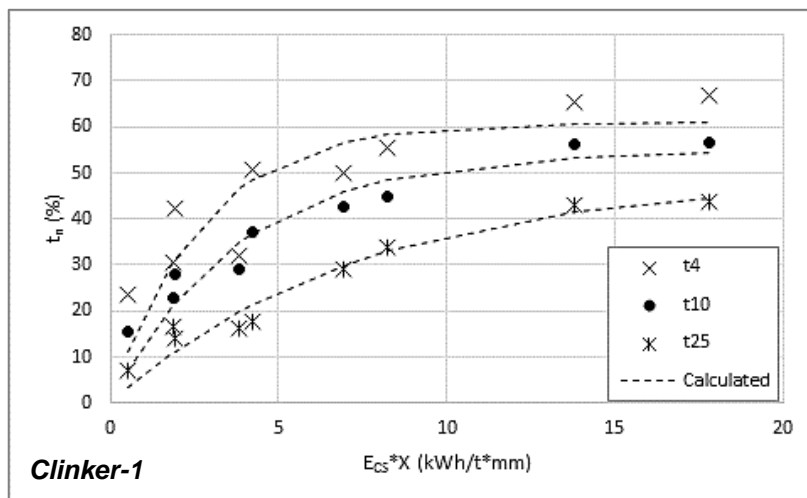


Figure 3.24 $E_{CS} \cdot X$ - t_n relationships of the clinker-1

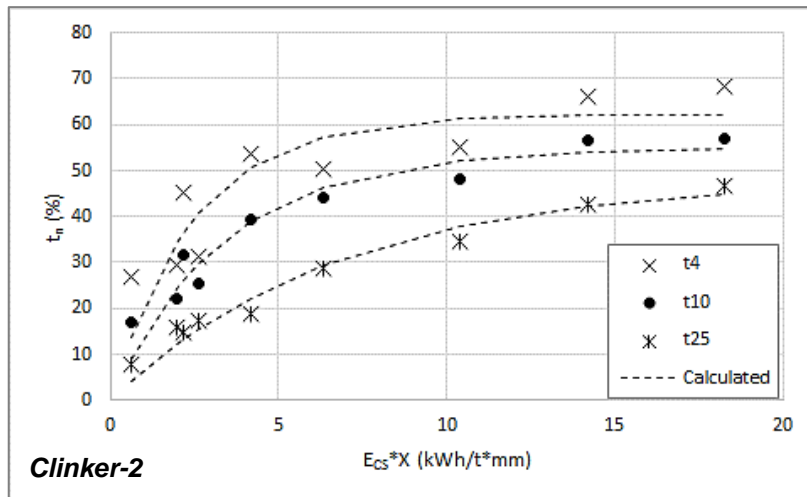


Figure 3.25 $E_{cs} \cdot X$ - t_n relationships of the clinker-2

Back calculated breakage model parameters of the samples are given in Table 3.17.

Table 3.17 Calculated breakage model parameters

		A	b
Polymetallic ore	t ₄	27.20	0.79
	t ₁₀	43.06	1.26
	t ₂₅	62.68	2.04
Chalcopyrite ore	t ₄	16.35	0.22
	t ₁₀	24.49	0.30
	t ₂₅	41.49	0.32
Gold ore	t ₄	22.86	0.36
	t ₁₀	32.67	0.61
	t ₂₅	46.63	0.74
Platinum ore-1	t ₄	29.76	0.10
	t ₁₀	40.39	0.17
	t ₂₅	55.06	0.24
Platinum ore-2	t ₄	33.97	0.06
	t ₁₀	37.11	0.14
	t ₂₅	52.65	0.19
Copper ore	t ₄	15.02	0.10
	t ₁₀	23.57	0.16
	t ₂₅	43.29	0.15
Clinker-1	t ₄	47.98	0.15
	t ₁₀	54.92	0.29
	t ₂₅	62.13	0.40
Clinker-2	t ₄	48.74	0.14
	t ₁₀	54.78	0.26
	t ₂₅	61.07	0.38

Particle size distributions for 2 kWh/t of each particle size fractions were estimated by using back calculated breakage model parameters. Then, breakage distribution functions of different size fractions are calculated and size dependent breakage matrix are created for each sample to use in the vertical roller mill modelling studies.

In addition to breakage distribution function, a material index should be defined to represent the effects arisen from the material properties to the model. In this context, disappearing rate concept was investigated developed by Dundar [101]. In this concept, the disappearance rate ($W_{broken}/W_{initial}$) of the fractions which is the ratio of mass fraction of that size fraction after breakage to before breakage. Then, E_{cs} - disappearing rate relationship is fitted to equation below (Equation 3.3). Multiplication of “c” and “d” model parameters are defined as material softness.

$$\frac{W_{broken}}{W_{initial}} = c * (1 - \exp(-d * E_{cs})) \quad (3.3)$$

In this study, disappearing rate was correlated with specific comminution energy (E_{cs}) and particle size (X) (Equation 3.4). Variations of disappearing rate with energy and particle size are presented in Figure 3.25 - Figure 3.33 for tested ores. Markers represents the experimental data and line represents the calculated data.

$$\frac{W_{broken}}{W_{initial}} = C * (1 - \exp(-d * E_{cs} * X)) \quad (3.4)$$

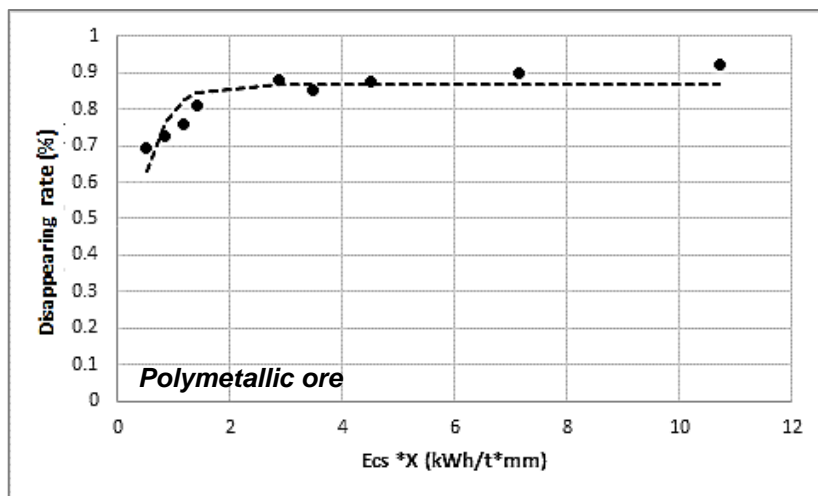


Figure 3.26 $E_{cs} * X$ -disappearing rate relationships of the polymetallic ore

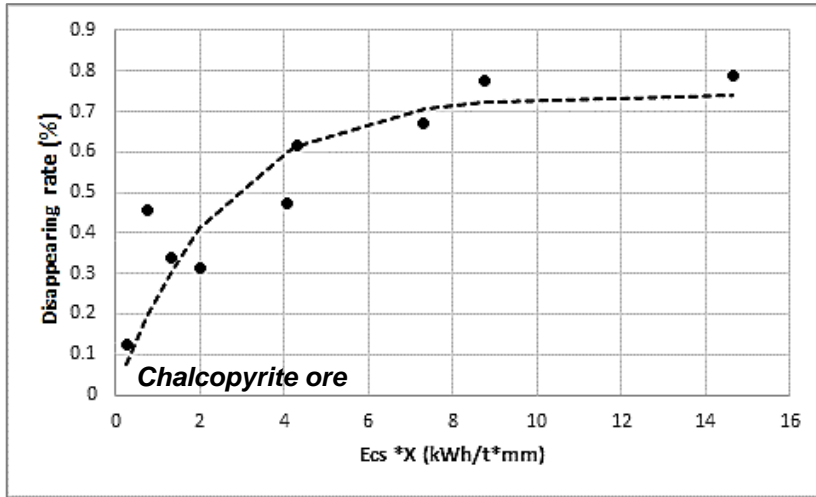


Figure 3.27 Ecs*X-disappearing rate relationships of the chalcopyrite ore

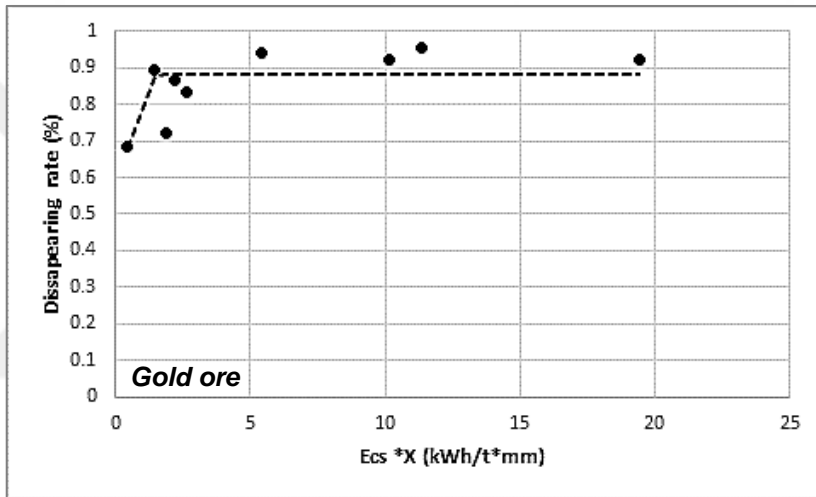


Figure 3.28 Ecs*X-disappearing rate relationships of the gold ore

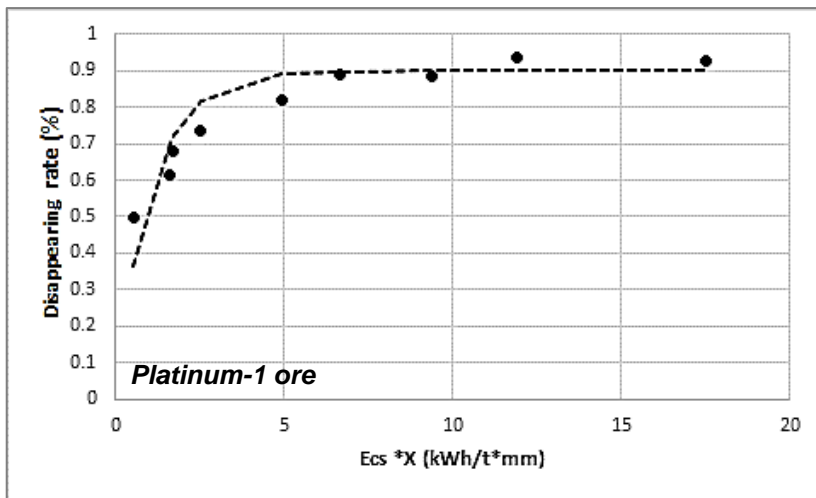


Figure 3.29 Ecs*X-disappearing rate relationships of the Platinum ore-1

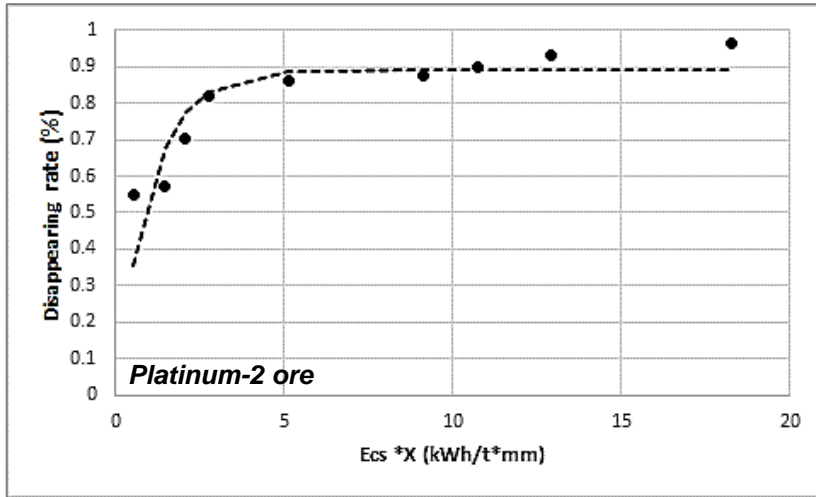


Figure 3.30 Ecs*X-disappearing rate relationships of the Platinum ore-2

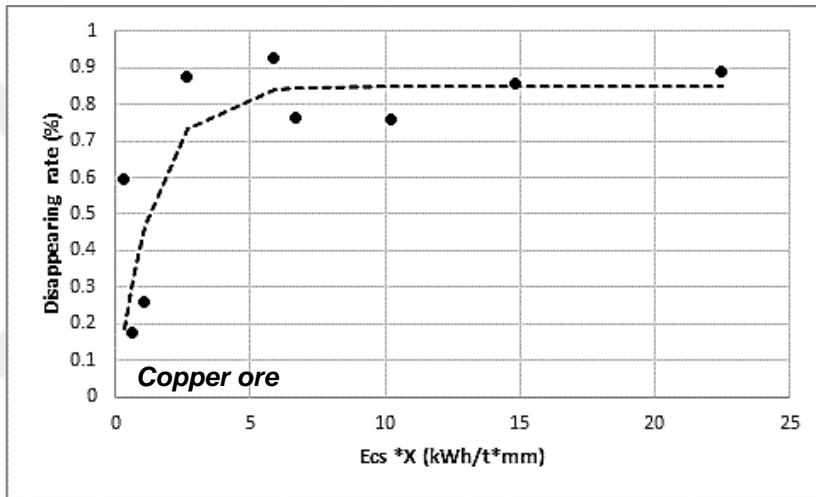


Figure 3.31 Ecs*X-disappearing rate relationships of the copper ore

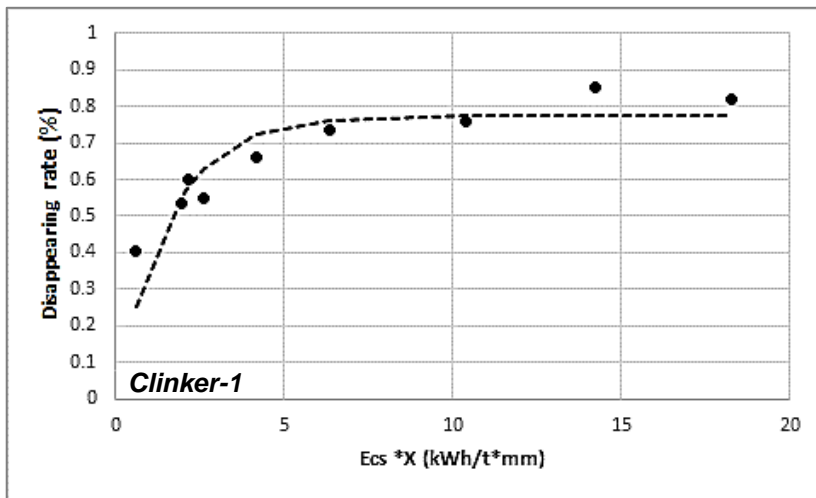


Figure 3.32 Ecs*X-disappearing rate relationships of the Clinker-1

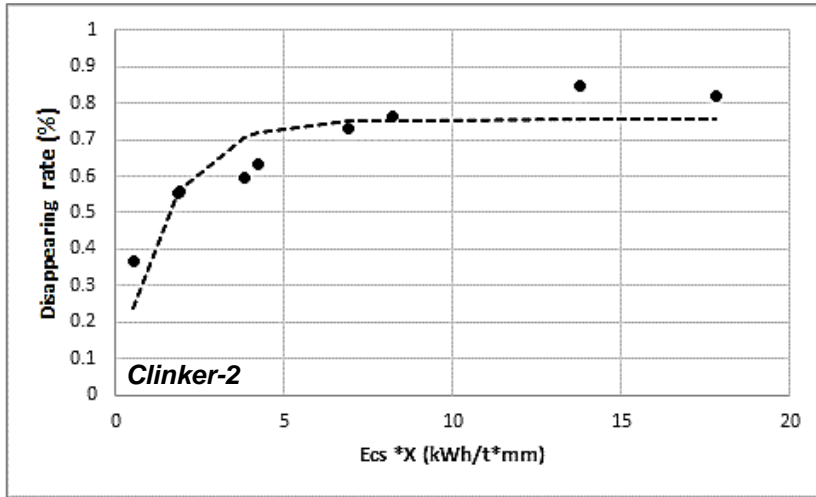


Figure 3.33 Ecs*X-disappearing rate relationships of the Clinker-2

Multiplication of “C” and “d” parameters is defined as material index. Material indices are given in Table 3.18 with calculated model parameters.

Table 3.18 Calculated disappearing rate model parameters

	C	d	Material Index (C*d)
Polymetallic ore	0.87	2.50	2.17
Chalcopyrite ore	0.74	0.40	0.30
Gold ore	0.88	3.26	2.88
Platinum ore-1	0.83	5.84	4.84
Platinum ore-2	0.89	0.97	0.86
Copper ore	0.85	0.75	0.64
Clinker-1	0.78	0.64	0.50
Clinker-2	0.76	0.71	0.53

4. MASS BALANCE STUDIES

Mass balancing is required to estimate the flowrates and the particle size distributions of unknown streams. Thus, performance evaluation of a circuit or an equipment is possible. During the sampling studies, some errors arise from the dynamic nature of the system, physical conditions, measurement and human. Mass balancing involves statistical adjustment of raw data to obtain best fit estimates of flowrates and particle size distributions. During the mass balance calculations, error for each stream is defined with the standard deviation values. Solution of the mass balance problem is obtained at the point of minimum sum of squared of errors (Equation 4.1).

$$SSQ = \sum_{j=1}^N \sum_{i=1}^L \left(\frac{X_{ij} - x_{ij}}{\sigma_{ij}} \right)^2 + \sum_{i=1}^L \left(\frac{A_i - a_i}{\sigma_i} \right)^2 \quad (4.1)$$

where,

SSQ : Sum of squares

N : Number of measurements

L : Number of streams

X : Measured value (size, grade, etc.)

x : Corrected value

A : Measured stream value

a : Corrected stream value

σ_{ij} : Standard deviation of measured values

σ_i : Standard deviation of measured stream values

In this part of the study, by using the particle size distributions and the control room data, mass balancing studies were performed for grinding tests in overflow mode of mobile unit and industrial scale tests.

4.1. Pilot Scale Mass Balancing

Mass balance studies were performed for overflow mode of mobile unit. Sampling studies were carried out and obtained data were used to evaluate the performance of grinding and classification sections individually. Calculated flowrates and particle size distributions of polymetallic and chalcopyrite ore grinding tests are given in Figure 4.1 - Figure 4.24.

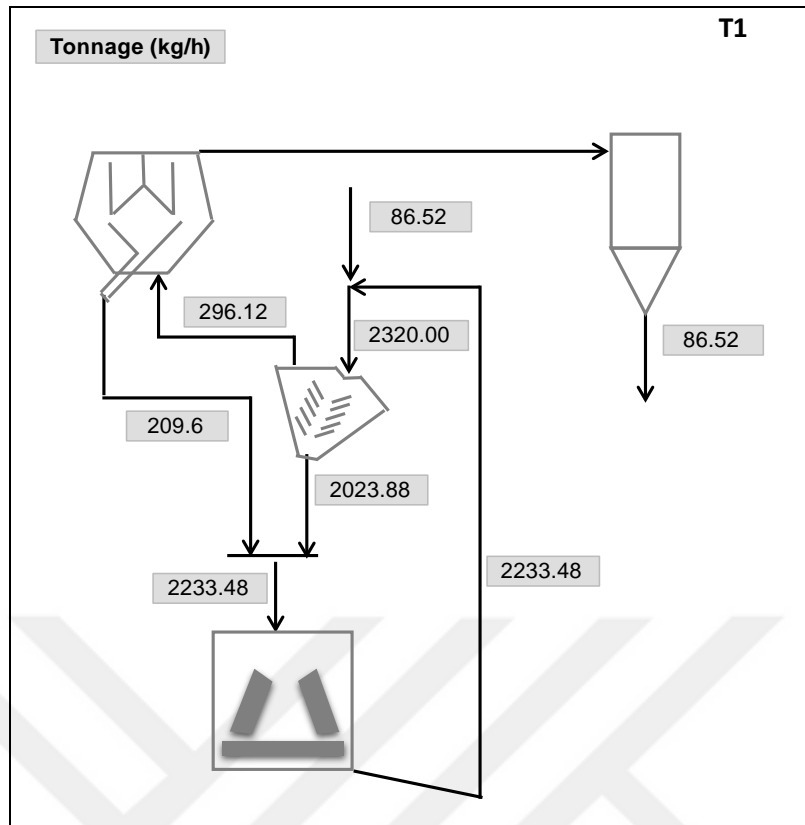


Figure 4.1 Mass balanced flowrates around the circuit for polymetallic ore-Test 1

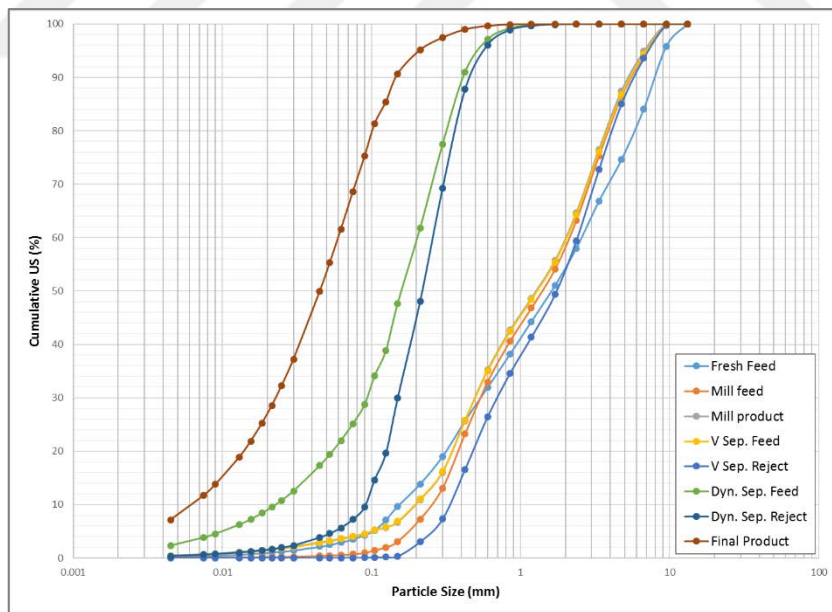


Figure 4.2 Mass balanced particle size distributions around the circuit for polymetallic ore-Test 1

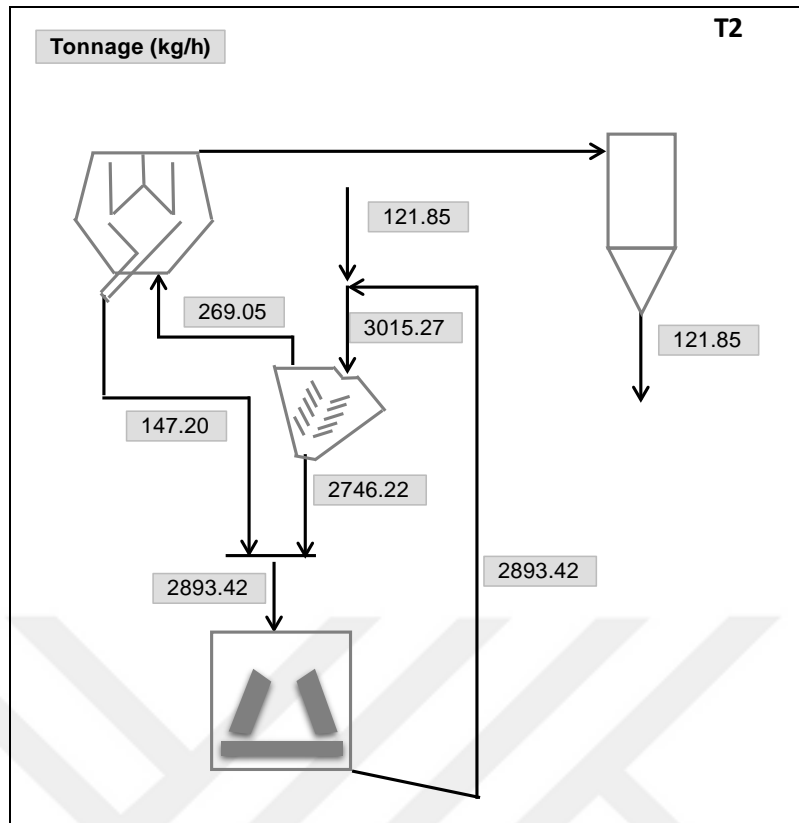


Figure 4.3 Mass balanced flowrates around the circuit for polymetallic ore-Test 2

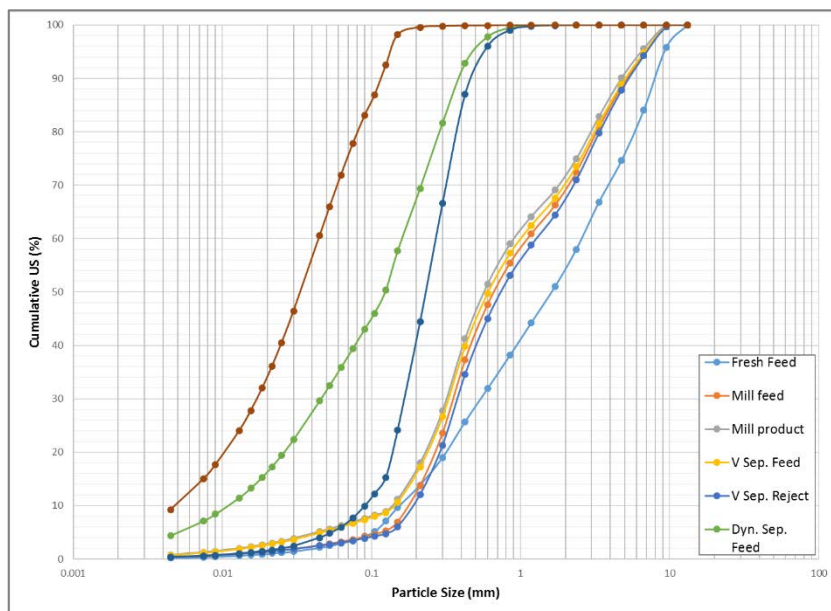


Figure 4.4 Mass balanced particle size distributions around the circuit for polymetallic ore-Test 2

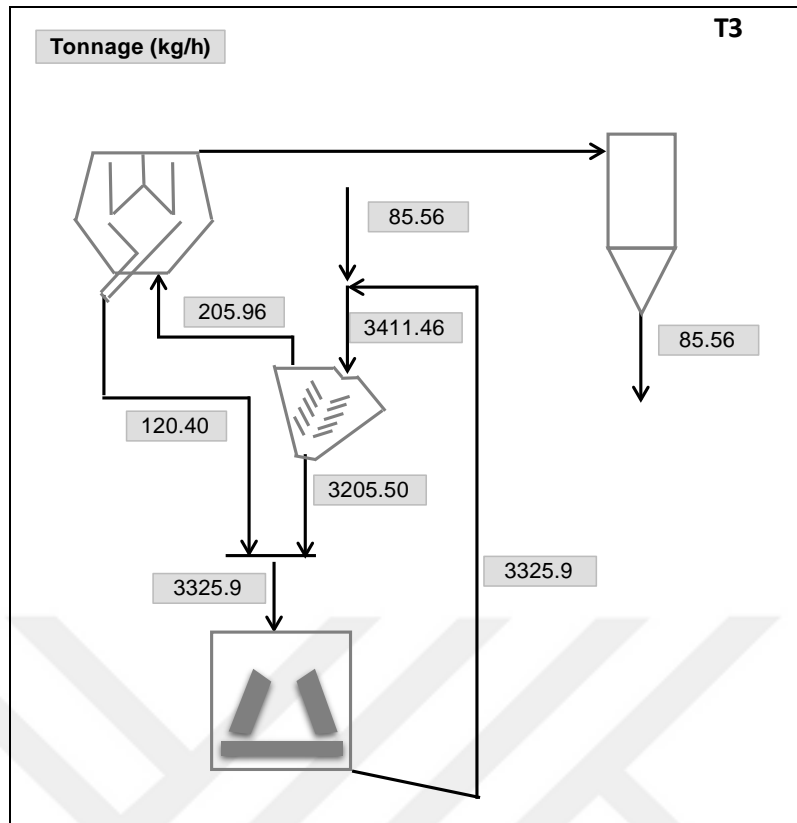


Figure 4.5 Mass balanced flowrates around the circuit for polymetallic ore-Test 3

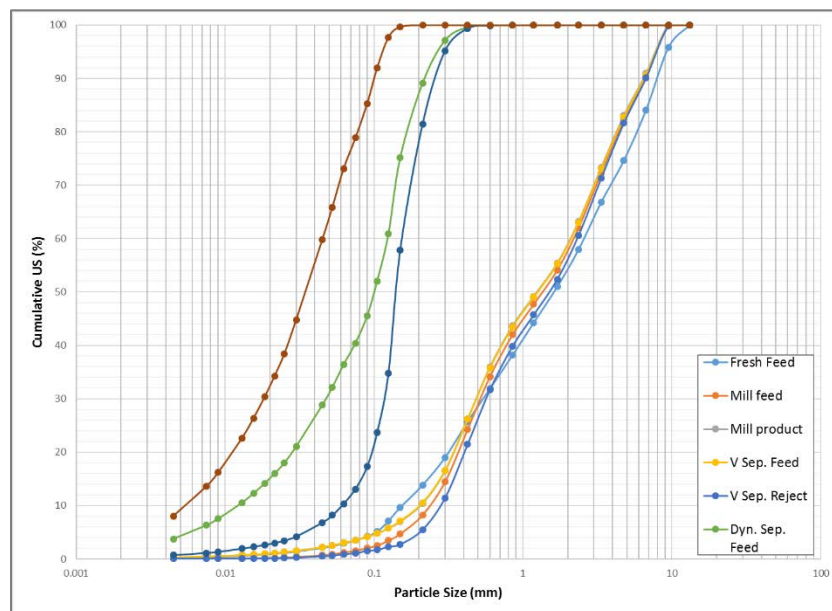


Figure 4.6 Mass balanced particle size distributions around the circuit for polymetallic ore-Test 3

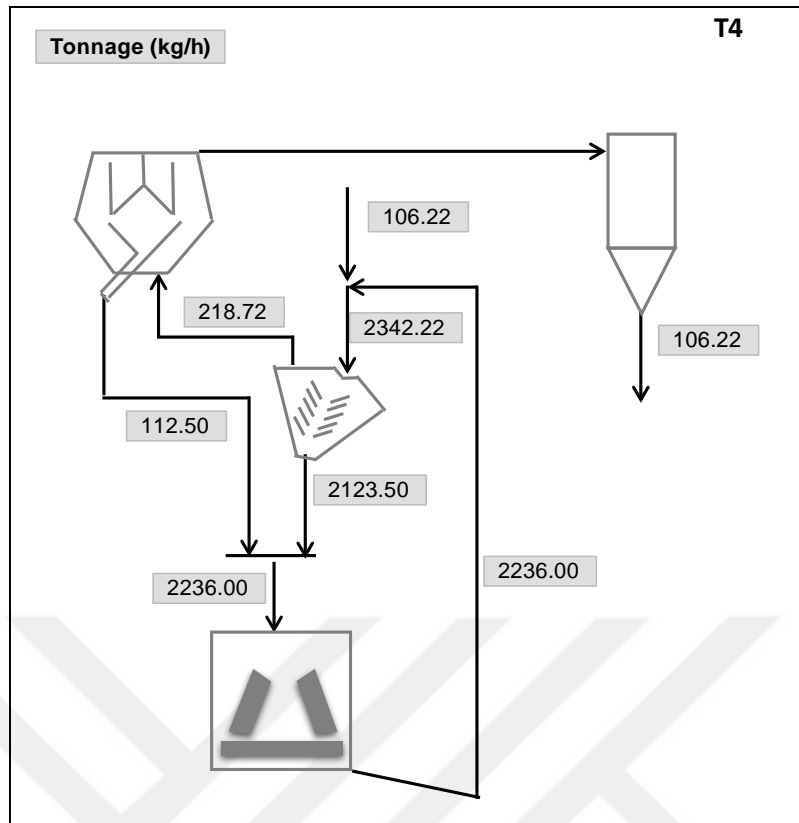


Figure 4.7 Mass balanced flowrates around the circuit for polymetallic ore-Test 4

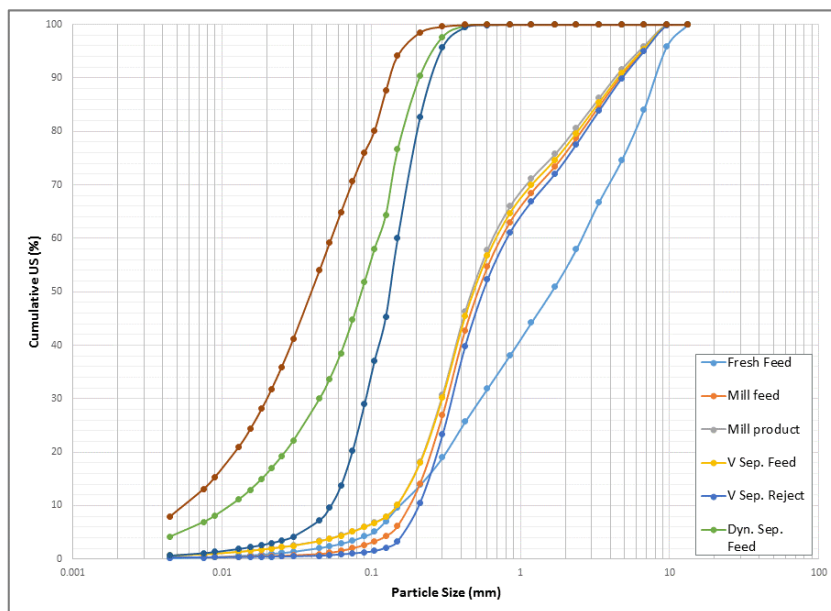


Figure 4.8 Mass balanced particle size distributions around the circuit for polymetallic ore-Test 4

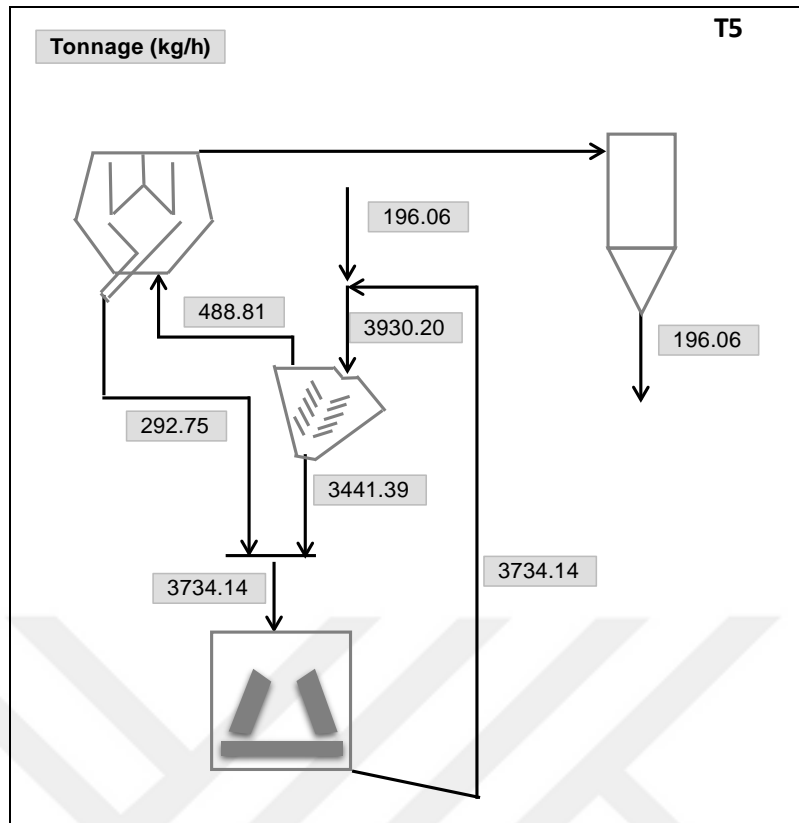


Figure 4.9 Mass balanced flowrates around the circuit for polymetallic ore-Test 5

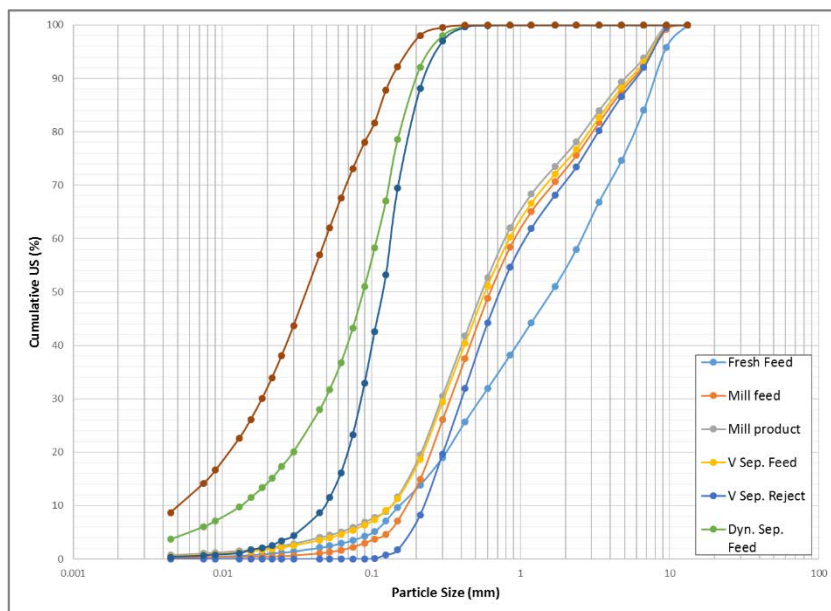


Figure 4.10 Mass balanced particle size distributions around the circuit for polymetallic ore-Test 5

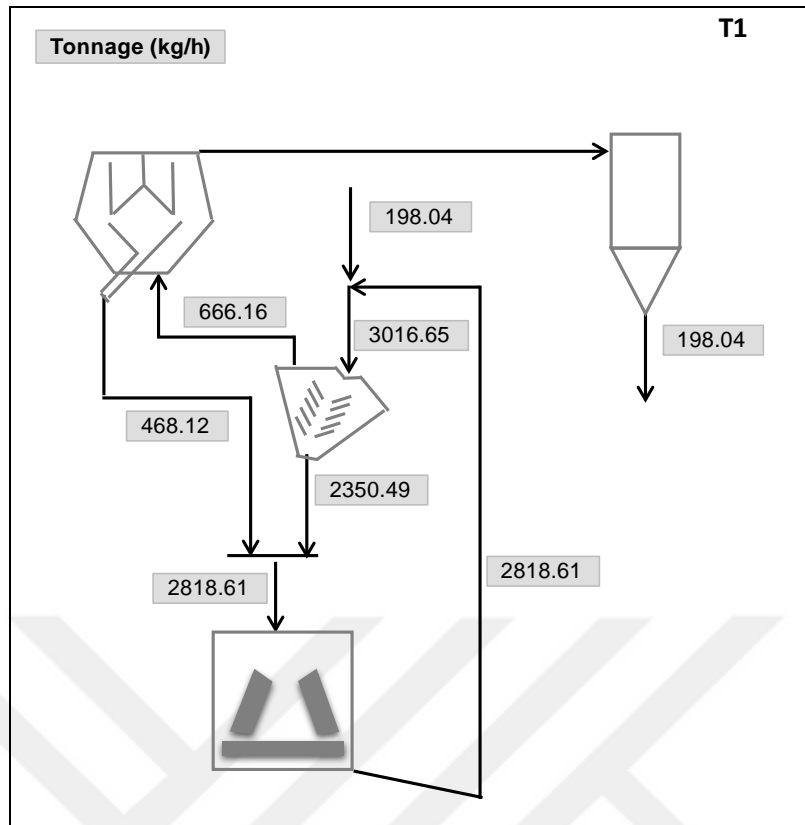


Figure 4.11 Mass balanced flowrates around the circuit for chalcopyrite ore-
Test 1

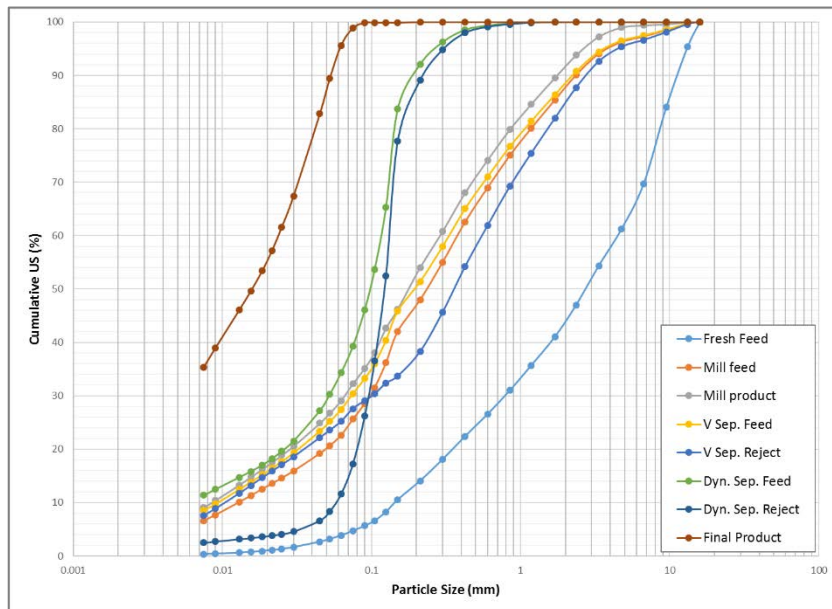


Figure 4.12 Mass balanced particle size distributions around the circuit for
chalcopyrite ore-Test 1

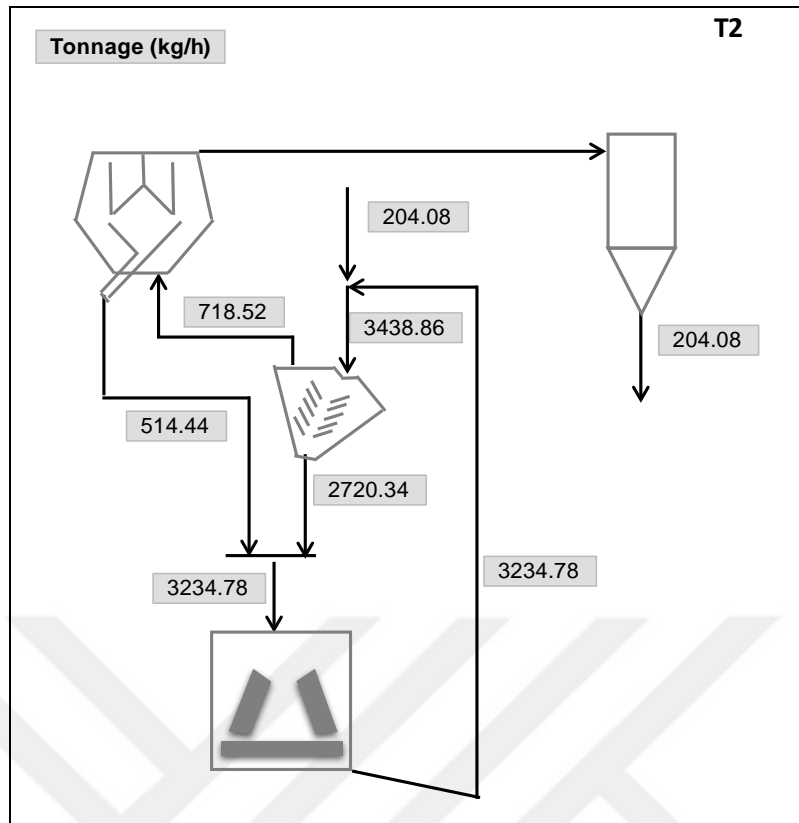


Figure 4.13 Mass balanced flowrates around the circuit for chalcopyrite ore-Test 2

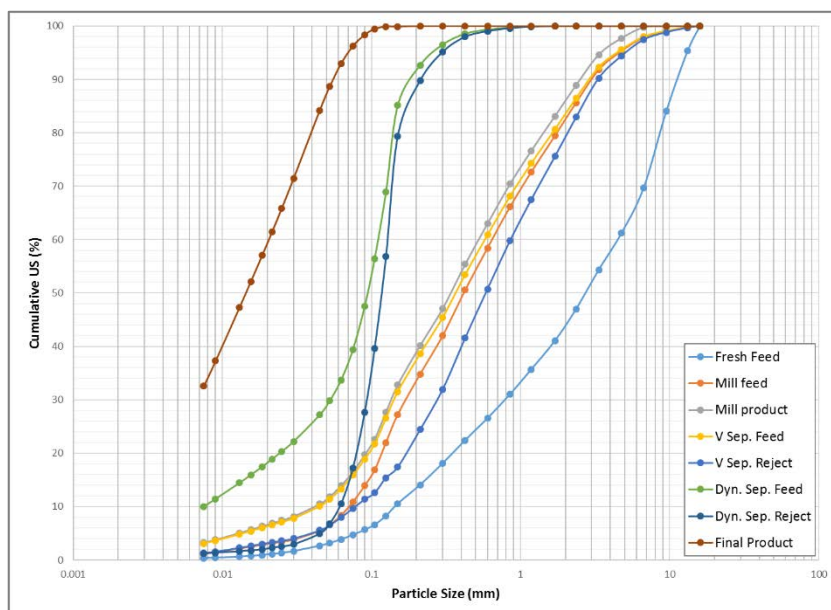


Figure 4.14 Mass balanced particle size distributions around the circuit for chalcopyrite ore-Test 2

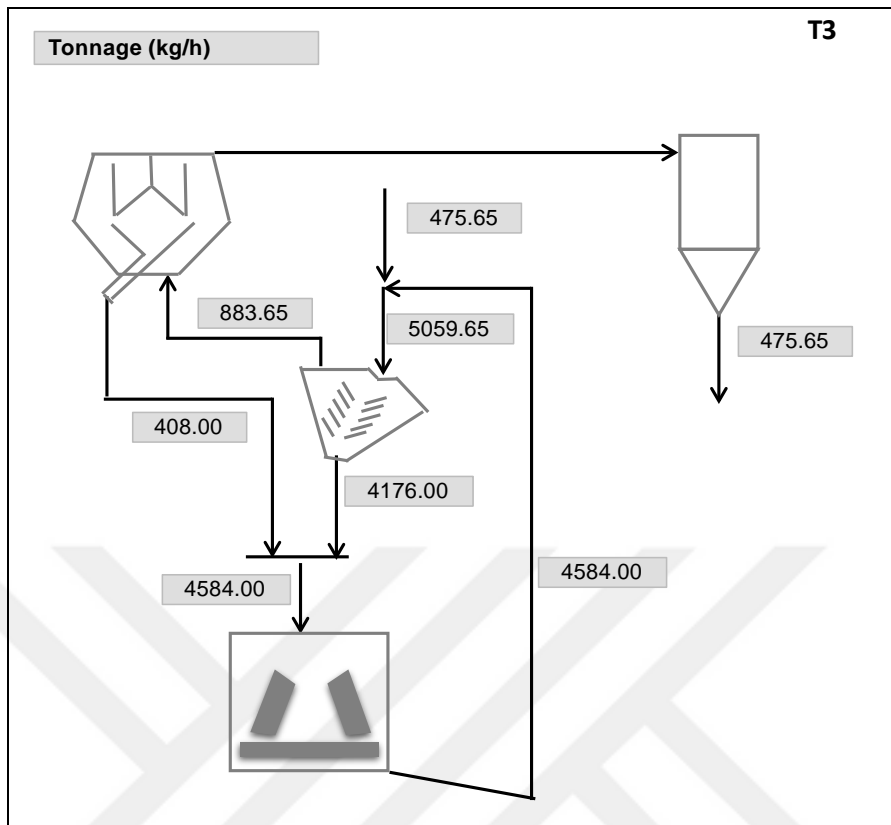


Figure 4.15 Mass balanced flowrates around the circuit for chalcopyrite ore-Test 3

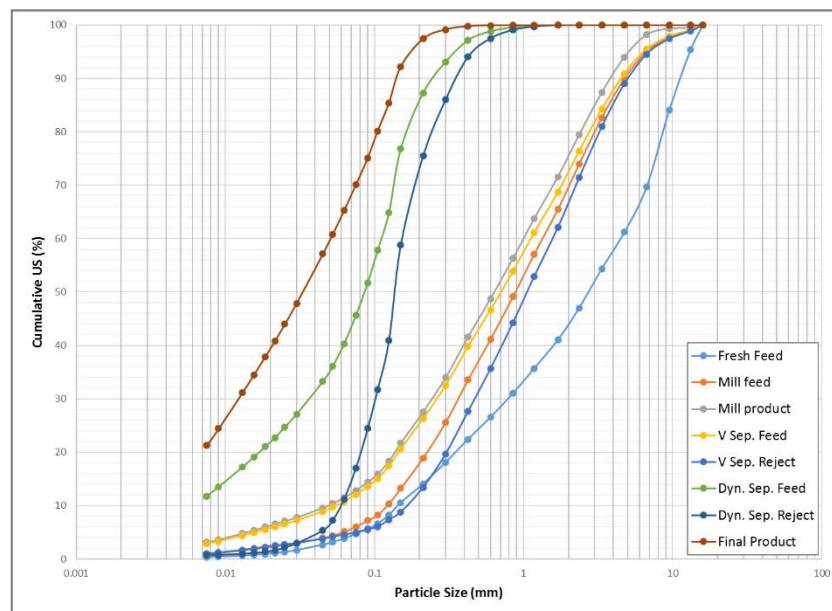


Figure 4.16 Mass balanced particle size distributions around the circuit for chalcopyrite ore-Test 3

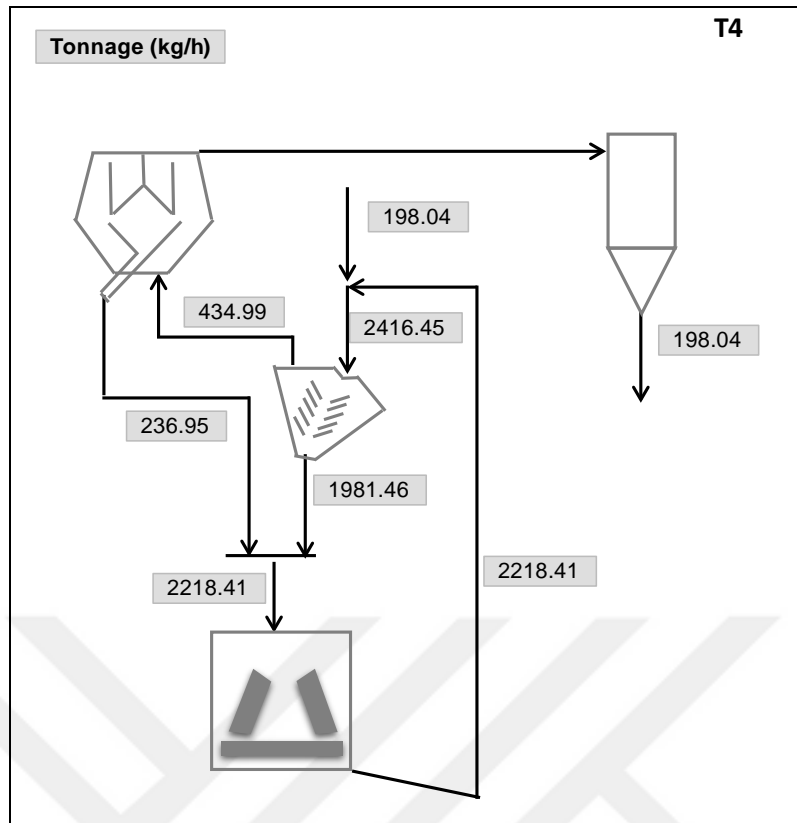


Figure 4.17 Mass balanced flowrates around the circuit for chalcopyrite ore-Test 4

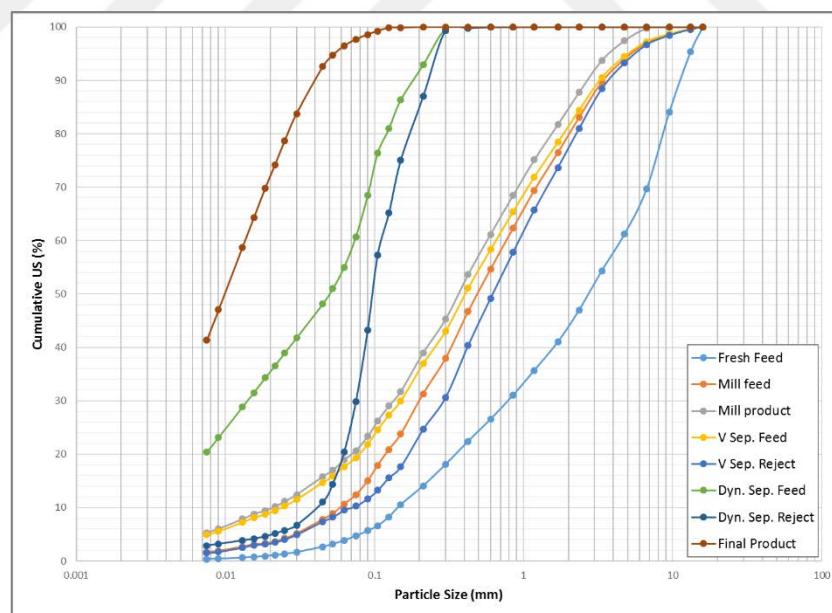


Figure 4.18 Mass balanced particle size distributions around the circuit for chalcopyrite ore-Test 4

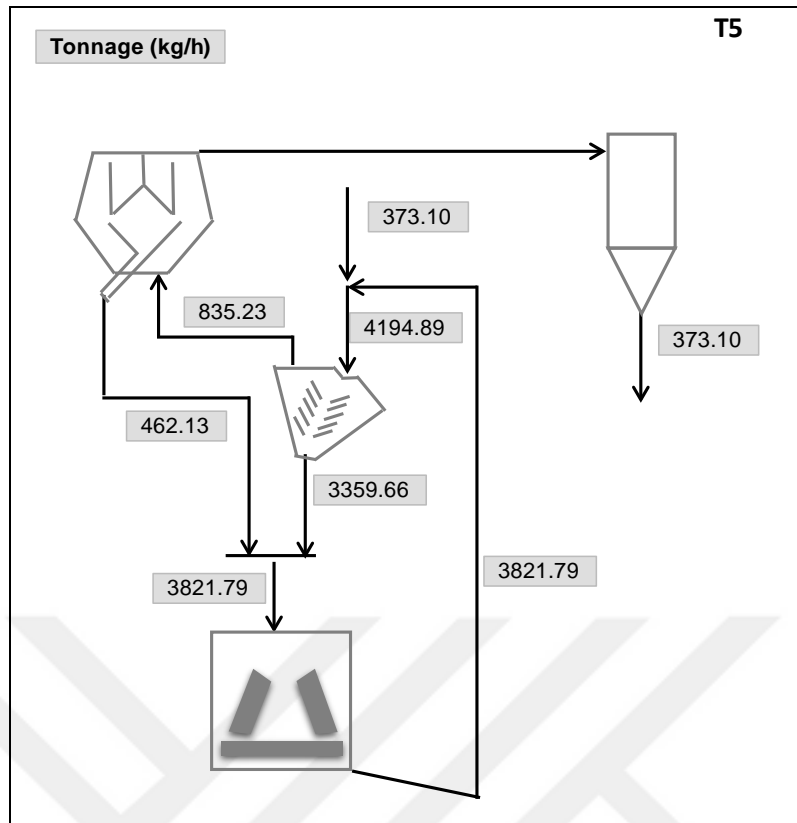


Figure 4.19 Mass balanced flowrates around the circuit for chalcopyrite ore-Test 5

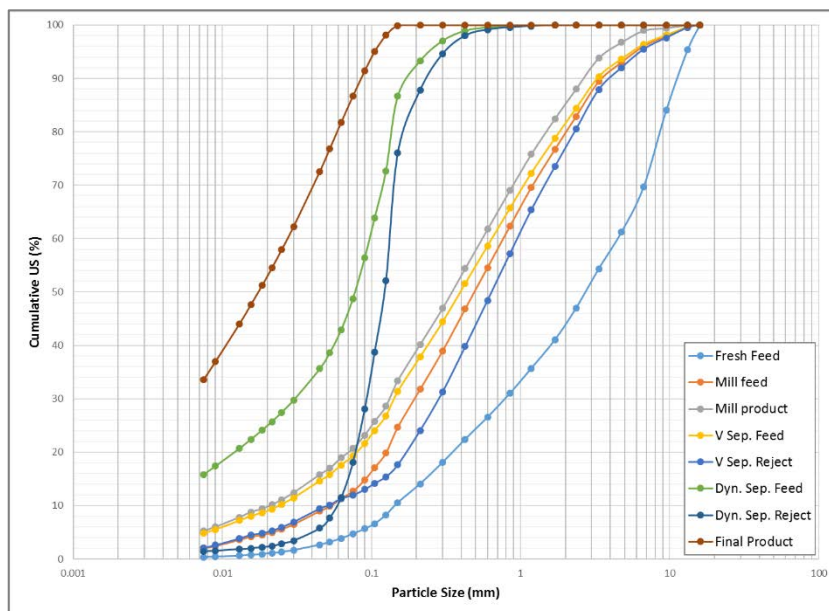


Figure 4.20 Mass balanced particle size distributions around the circuit for chalcopyrite ore-Test 5

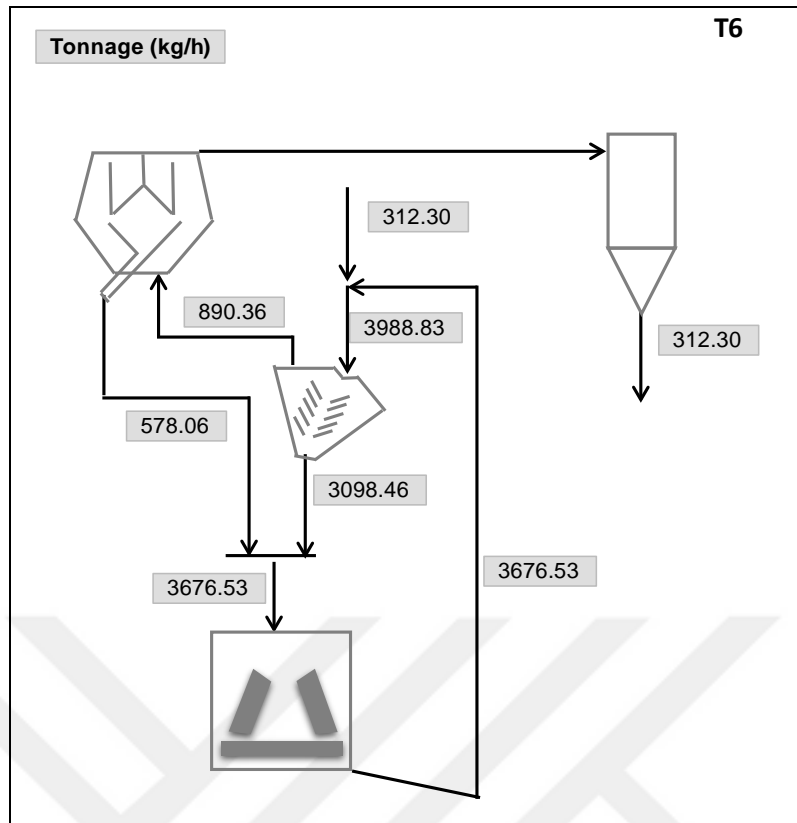


Figure 4.21 Mass balanced flowrates around the circuit for chalcopyrite ore-Test 6

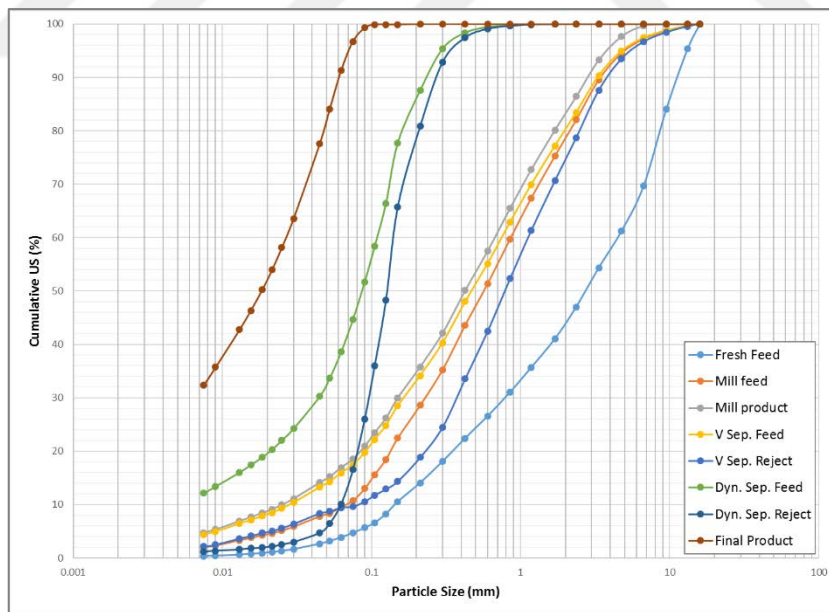


Figure 4.22 Mass balanced particle size distributions around the circuit for chalcopyrite ore-Test 6

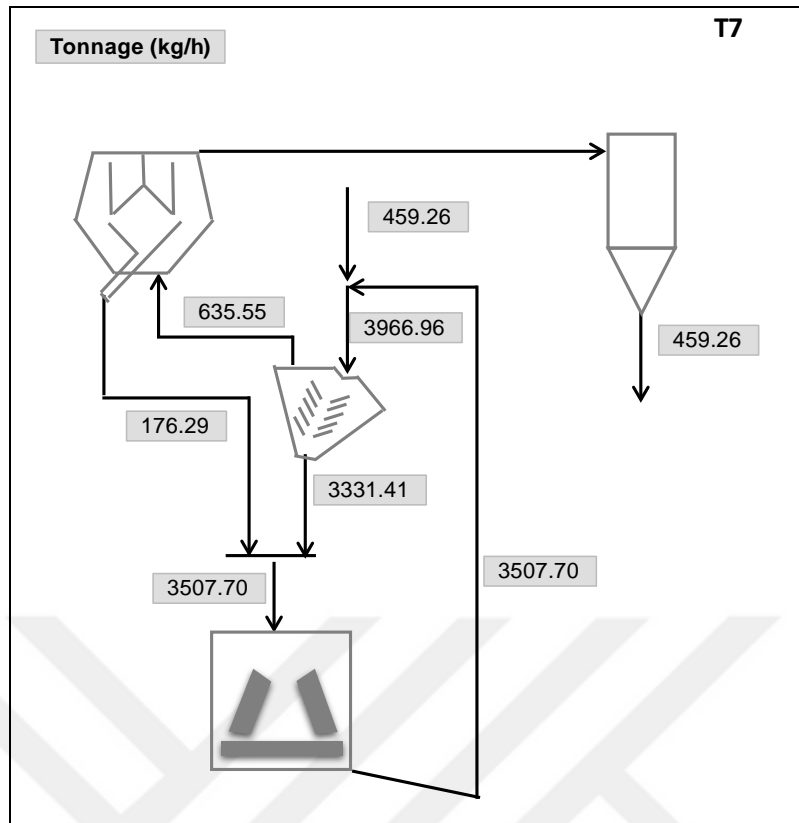


Figure 4.23 Mass balanced flowrates around the circuit for chalcopyrite ore-Test 7

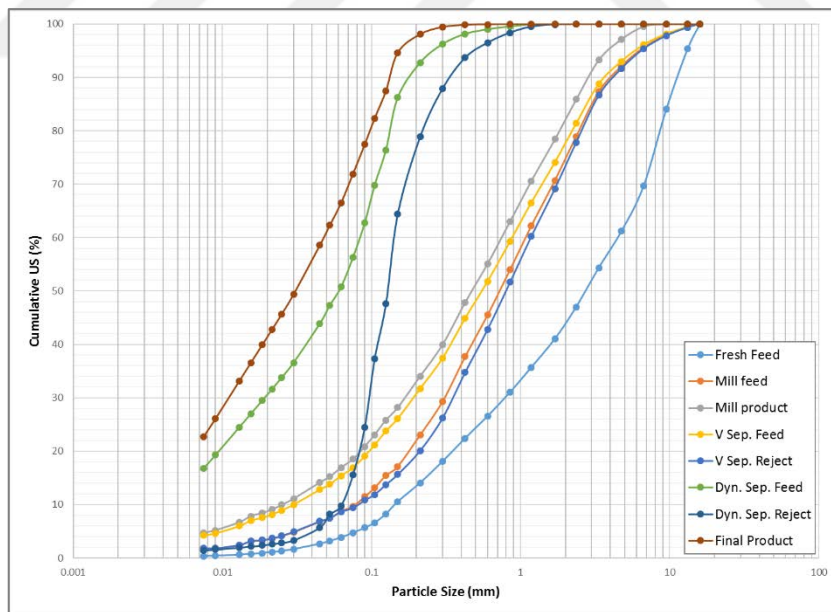


Figure 4.24 Mass balanced particle size distributions around the circuit for chalcopyrite ore-Test 7

The success of the mass balance studies was checked out by plotting the experimental and mass balanced particle size distributions (Figure 4.25). The

agreement between the measured and mass balanced data in a good fit and data could be used in modelling studies.

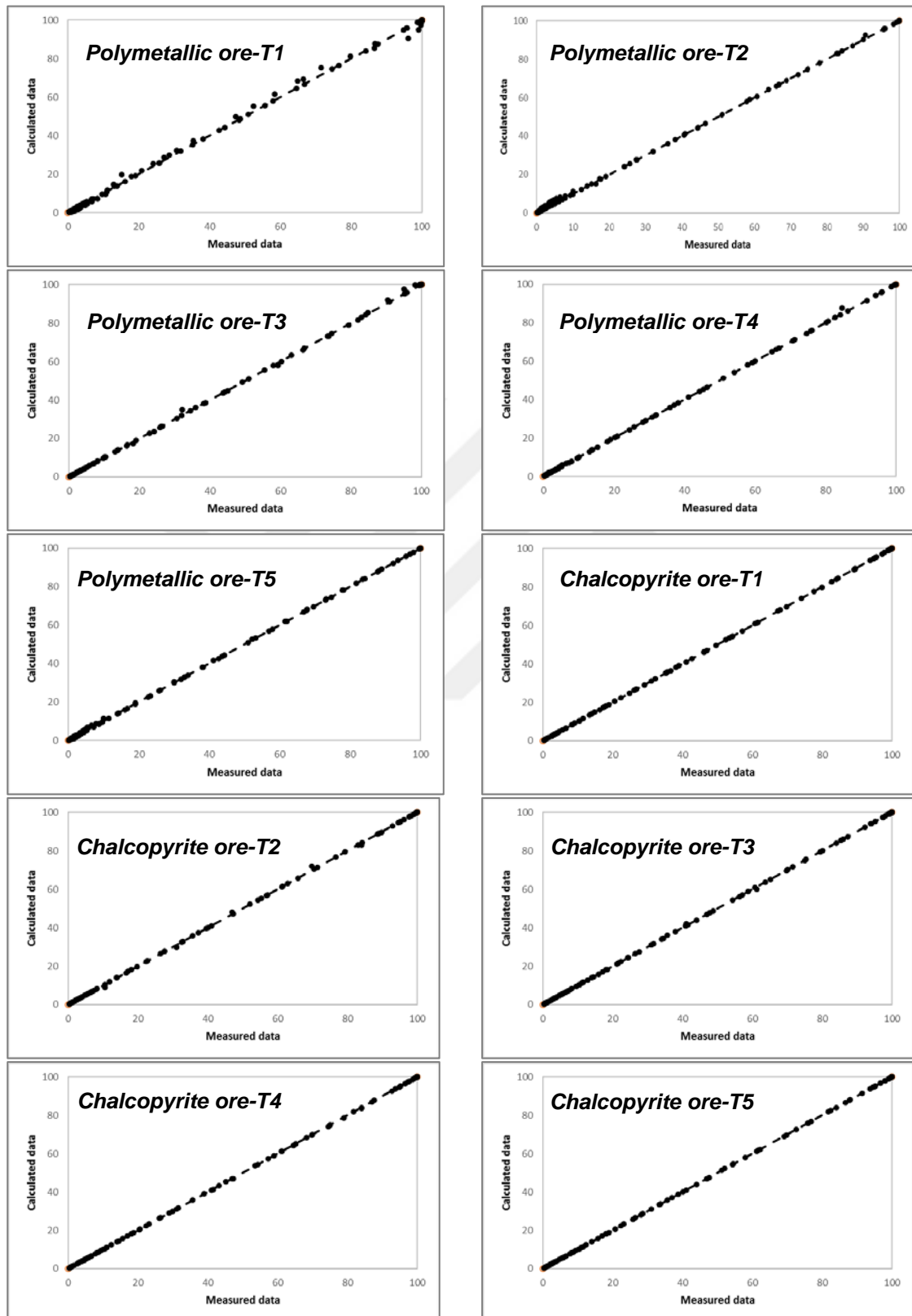


Figure 4.25 Comparison of measured and calculated data for polymetallic and chalcopyrite ore

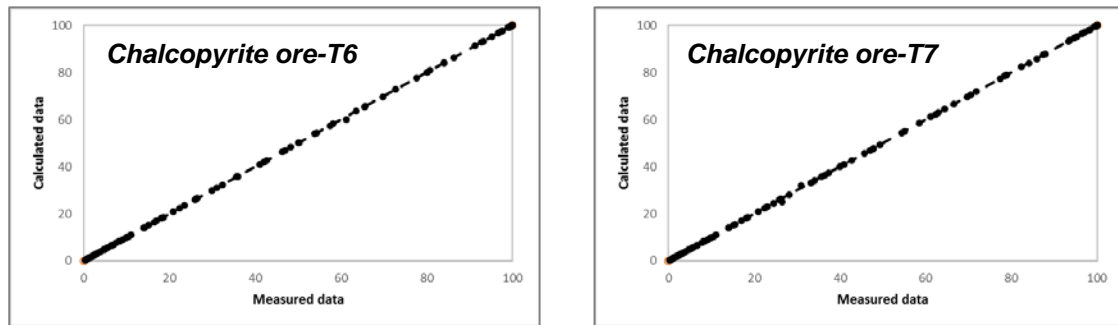


Figure 4.25 (continued)

4.2. Industrial Scale Mass Balancing

Mass balance studies were performed for industrial scale vertical roller mill circuit. Data obtained from two surveys was used to calculate the particle size distributions and flowrates of each stream. Statistical adjustment of the raw data was made by reconciliation procedure presented for vertical roller mills [99]. Lagrange multiplier method are used in this procedure. According to Lagrange multiplier method, general form of the function is given in Equation 4.3, when problem is defined as in Equation 4.2.

$$\begin{cases} \min f(X) \\ X \\ \text{subject to} \\ \Omega(X) = 0 \end{cases} \quad (4.2.)$$

$$\mathcal{L}(X) = f(X) + \sum_i \lambda_i \Omega_i(X) \quad \mathcal{L}(X) = f(X) + \sum_i \lambda_i \Omega_i(X) \quad (4.3.)$$

where,

\mathcal{L} :Lagrangian (new function)

Ω :Constaint function

λ :Lagrange multiplier

f :Criterion function

After reconciliation procedure, flowrates around the vertical roller mill system and particle size distributions for survey 1 and survey 2 were calculated. Balanced data are presented in Figure 4.26 - Figure 4.29.

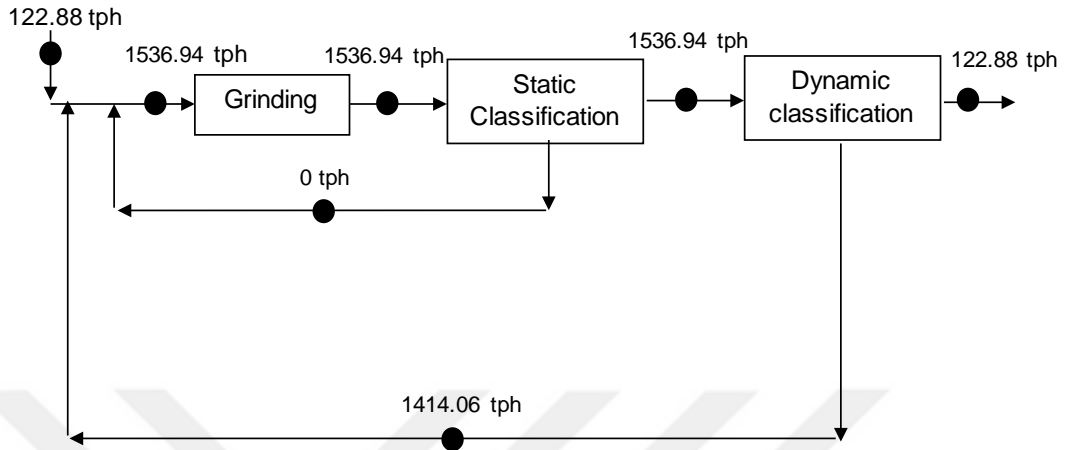


Figure 4.26 Mass balanced flowrates around the circuit for Survey 1

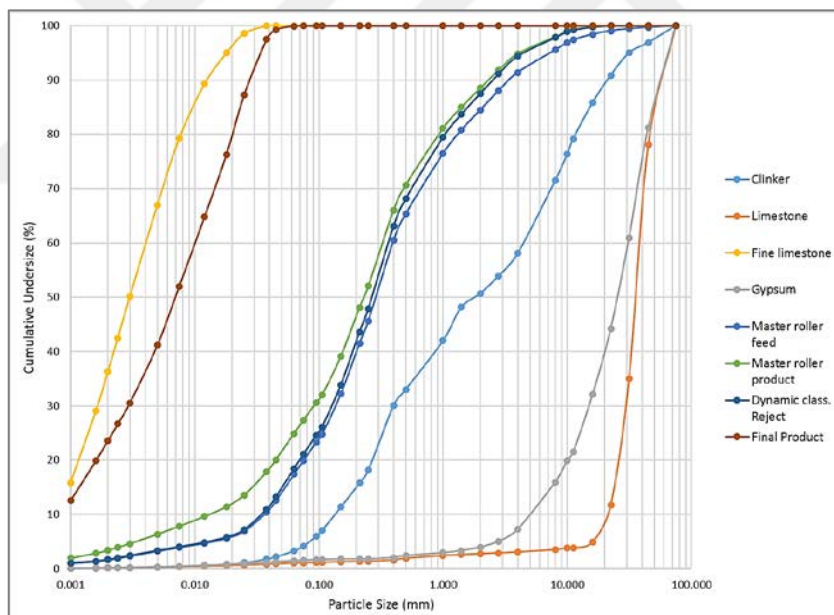


Figure 4.27 Mass balanced particle size distributions around the circuit for Survey

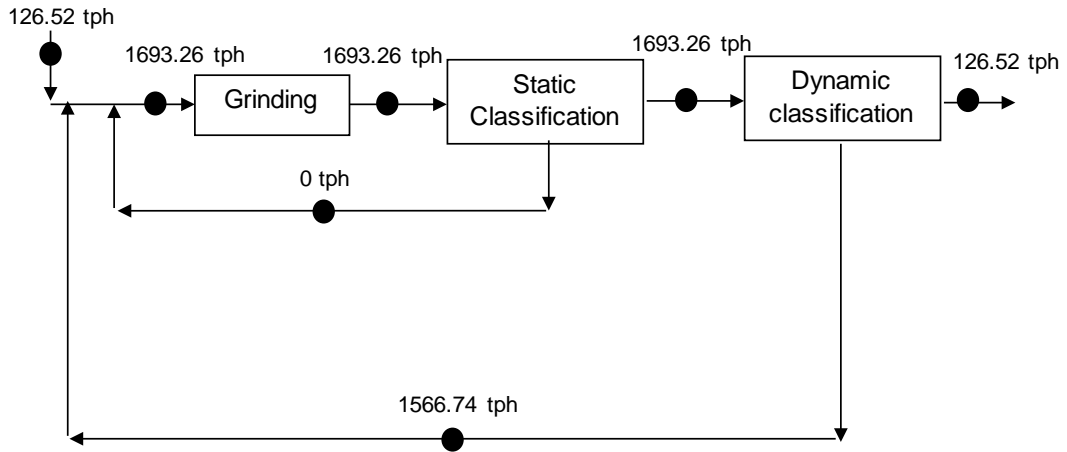


Figure 4.28 Mass balanced flowrates around the circuit for Survey 2

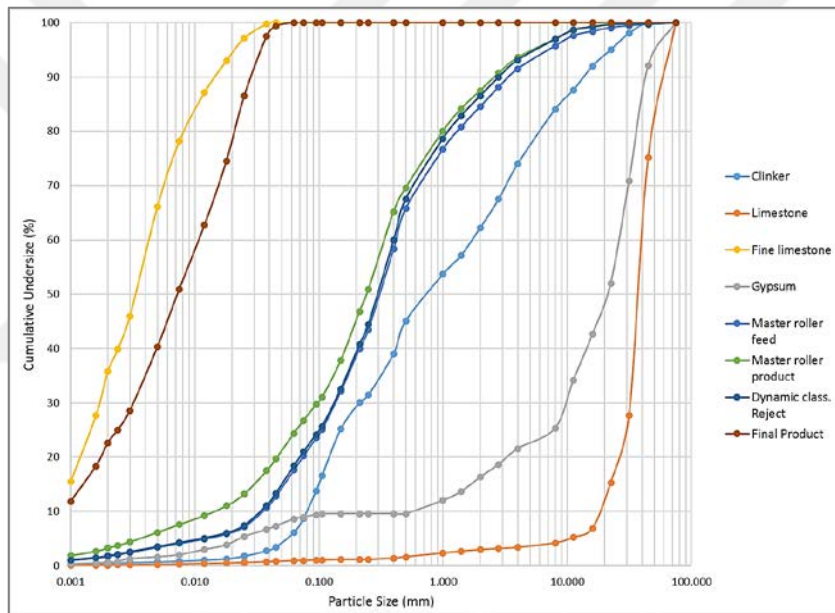


Figure 4.29 Mass balanced particle size distributions around the circuit for Survey 2

Accuracy of the results was assessed by plotting the experimental and mass balanced cumulative passing percentages on a graph (Figure 4.30). Experimental and calculated data set are good in agreement. This situation corresponds to an accurate sampling.

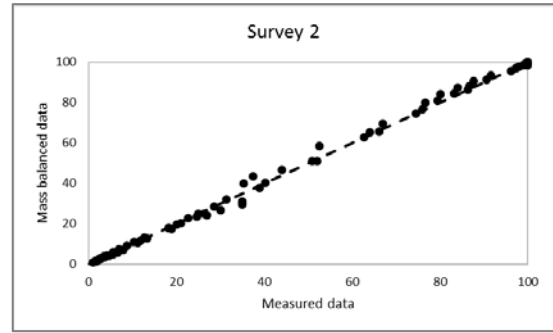
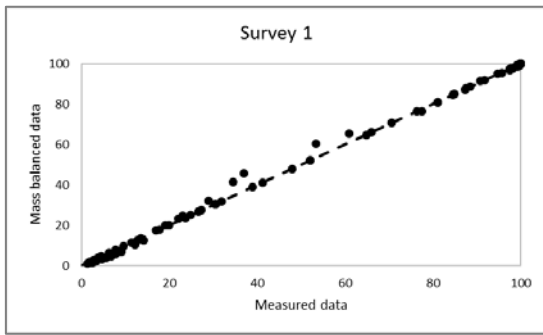


Figure 4.30 Comparison of measured and calculated data for Survey-1 and Survey

2



5. MODELLING STUDIES

Various theoretical and empirical approaches were developed to analyze and model the vertical roller mill systems. Most part of these studies were based on the effect of the relationships between operational parameters. Mostly, developed models is not supported by industrial scale data and not reliable for simulation of non-tested conditions. On the basis of this gap, it was aimed to developed a model for vertical roller mills supported with controlled data set. At the data collection stage, mobile unit enabled to evaluate each operation in the system, individually. For the industrial scale tests, grinding and separation operations were analyzed by sampling method developed by Aydogan [99]. By means of this opportunities, vertical roller mill system was divided into two sections as grinding and classification like models developed by Austin et al. [92] and Kersting [3]. In this section, model development studies were presented for grinding and separation operations. Full circuit model fit results are summarized in Appendix 2.

5.1. Modelling of Grinding Section

In this section, grinding operation was investigated to predict the flowrate and the particle size distribution of the grinding table product. With this aim, the population balance model was applied to vertical roller mill grinding operation. The population balance model which is referred as a simple mass balance for the size reduction was considered as a starting point. The population balance model was developed by Epstein [102]. In this model, size reduction process was described by two mechanisms: breakage rate and breakage distribution. Breakage mechanism of the model is presented in Figure 5.1.

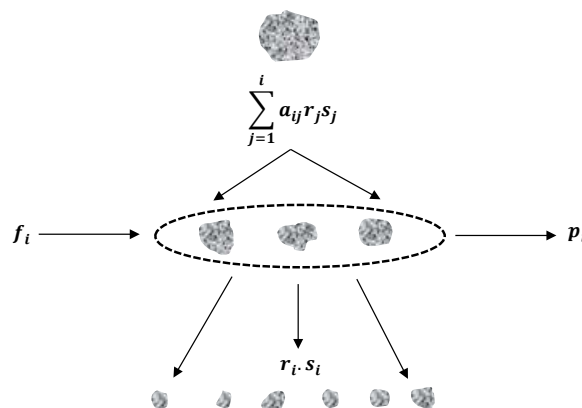


Figure 5.1 Breakage mechanism in population balance model [103]

A mass balance for size fraction of i in product can be calculated as follows;

- particles coarser than i size are broken into i size fraction,
- particles in i size fraction are broken into smaller sizes,
- feed in size i .

The mass balance equation can be written as follows;

$$p_i = f_i + \sum_{j=1}^i a_{ij}r_js_j - r_i s_i \quad (5.1.)$$

where,

p_i : Product size i

f_i : Feed size i

a_{ij} : Size dependent breakage function (appearance of size i material produced by breakage of size j material)

r_j : Breakage rate of size j

s_j : Amount of size j material within the mill

r_i : Breakage rate of size i

s_i : Amount of size i material within the mill

As a second step of the modelling of grinding operation in the vertical roller mill, breakage rate was defined by function developed by Austin et al. [92]. Breakage rate formula is given in Equation 5.2.

$$r_i = ax_i^\theta \quad (5.2.)$$

where,

r : Breakage rate

a and θ : Model parameters

x : Particle size

During the modelling studies, mill product size distributions were estimated by back calculating the model parameters “ a ” and “ θ ”. For this estimation; mill throughput, feed and product size distributions of grinding table which are defined as mill feed and mill product, size dependent breakage distribution functions (a) determined from bed breakage tests under pressure were used. Amount of material inside the mill

(s) was represented as material under the grinding rollers. Particle size distributions of the material under the rollers were assumed as similar as mill feed. For this purpose, initially the volume under the rollers between 1° and 10° by using grinding bed height and roller dimensions was calculated geometrically. Bulk densities under the roller are assumed as 75% percent of the solid densities because the material gets compressed under the roller and densities reaches up to 75-80 % of the solid densities.

Estimated product size distributions of each test for chalcopyrite and polymetallic ore are given in Figure 5.2. and Figure 5.3., respectively. Calculated product size distributions are in quite good agreement with the measured size distributions. It was decided that calculated parameters is reliable for model development studies.

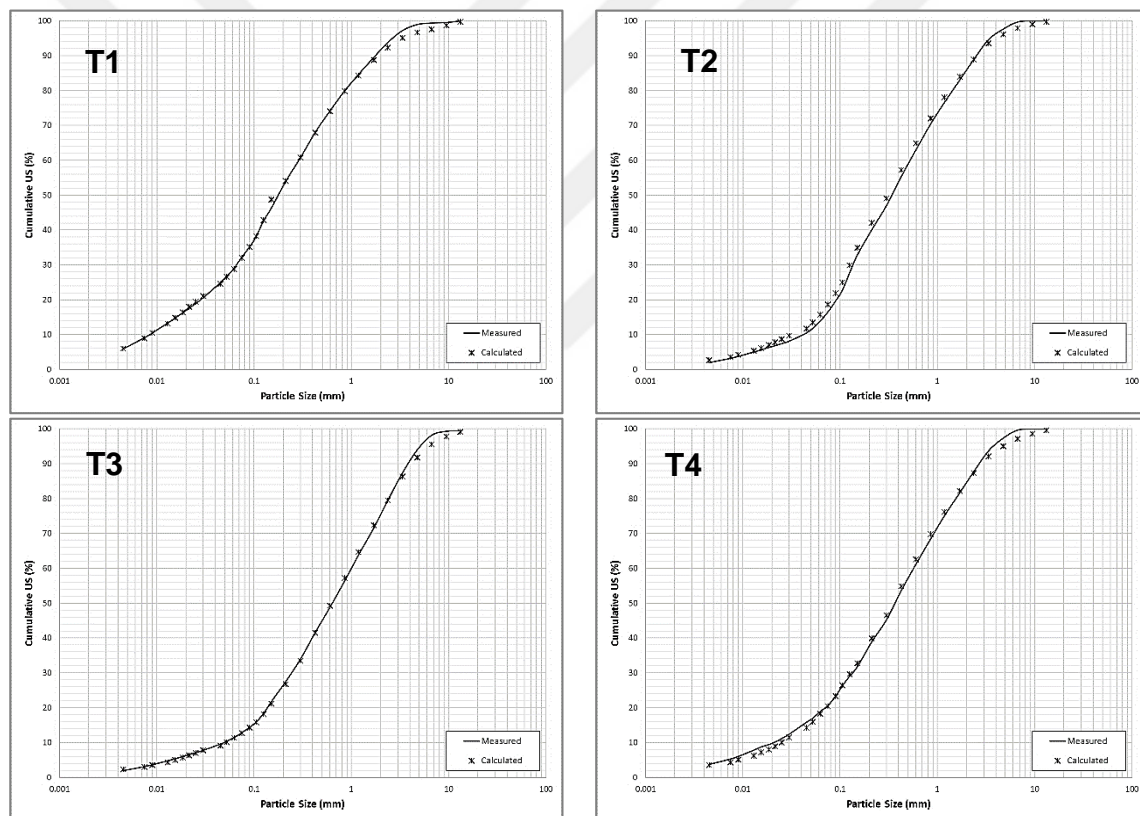


Figure 5.2 Measured and estimated product size distributions for chalcopyrite ore

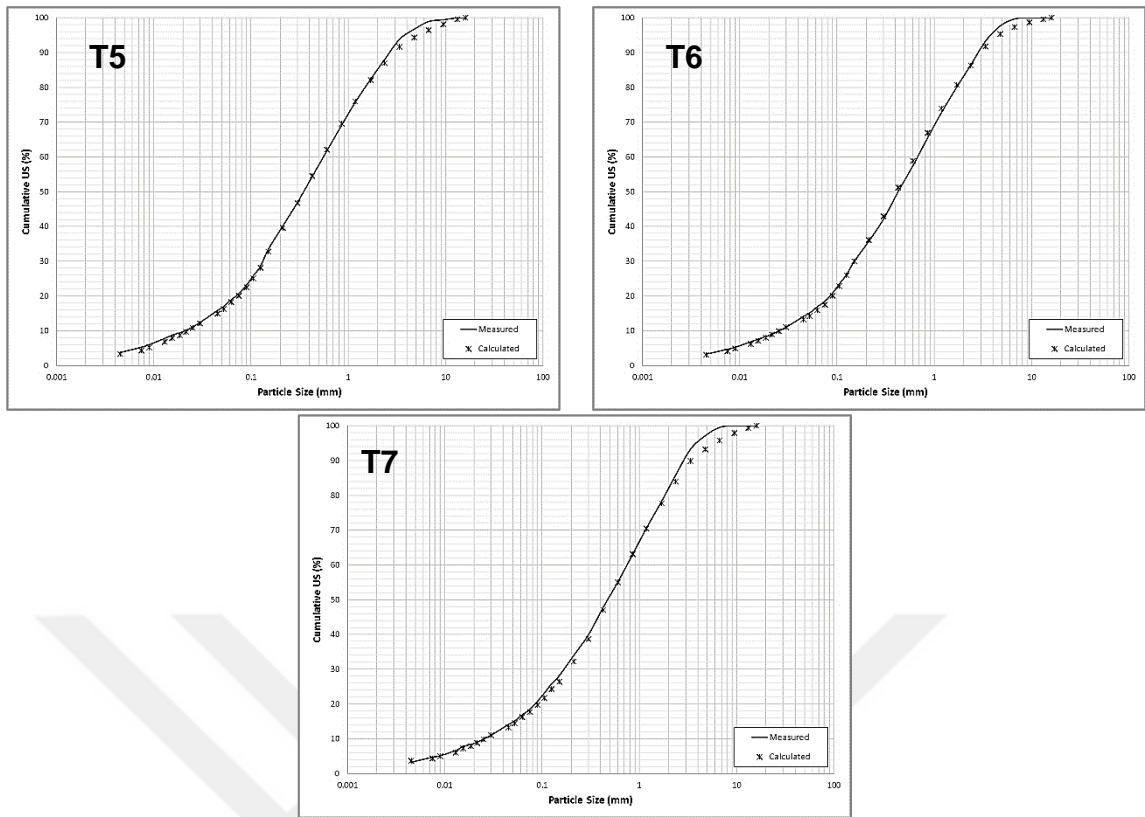


Figure 5.2 (continued)

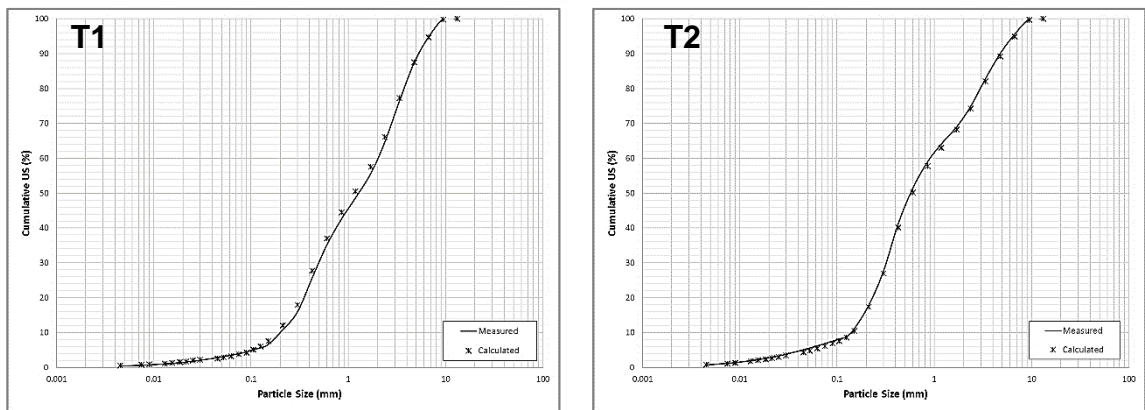


Figure 5.3 Measured and estimated product size distributions for polymetallic ore

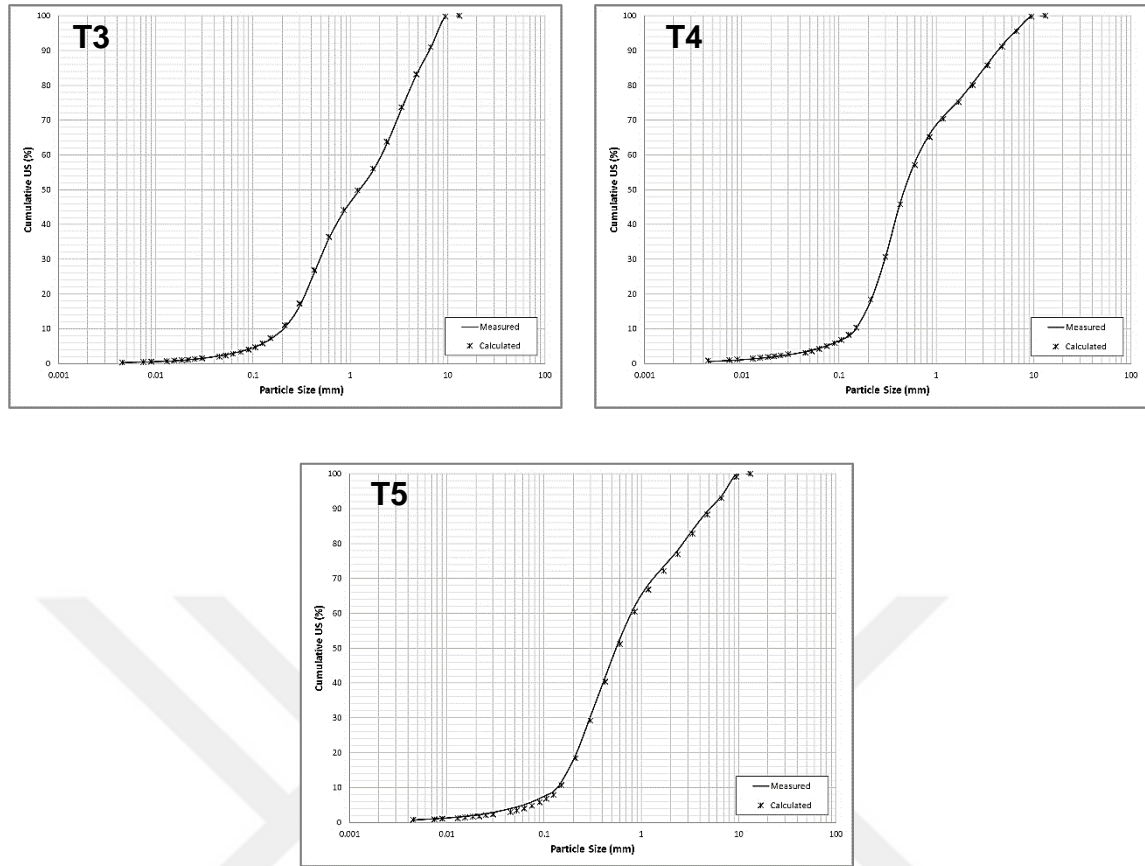


Figure 5.3 (continued)

After estimation of the product size distributions, back calculated model parameters were investigated. Calculated model parameters for chalcopyrite and polymetallic ore are given in Table 5.1.

Table 5.1 Calculated model parameters

		a	θ
Chalcopyrite ore	T1	11527.15	0.239
	T2	11680.09	0.138
	T3	11597.84	0.094
	T4	19401.23	0.136
	T5	19410.46	0.179
	T6	15073.74	0.145
	T7	19410.46	0.120
Polymetallic ore	T1	7591.42	0.010
	T2	7685.01	0.098
	T3	7695.37	0.019
	T4	7781.90	0.072
	T5	7723.08	0.062

It is observed that “a” parameters are similar for each polymetallic ore grinding tests. Common characteristic of these tests is having similar specific grinding force, which is a function of the applied pressure and roller dimensions. On the basis of this, relationship between specific grinding force and “a” parameter was investigated for these two tested ores (Figure 5.4.). Specific grinding force has an influence on breakage rate. Breakage rate increases with the increasing specific grinding force. “a” parameter has the same effect on breakage rate as specific grinding force. There is a directly proportional relationship between “a” parameter and specific grinding force.

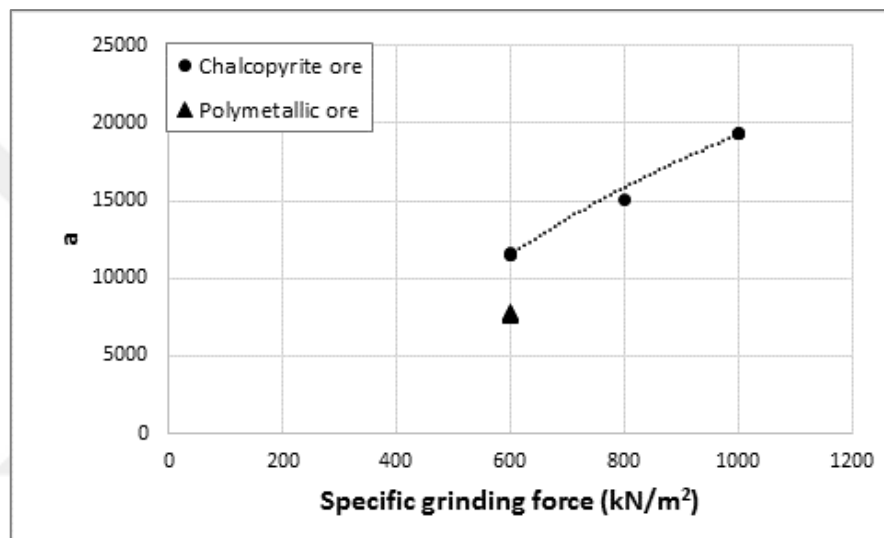


Figure 5.4 Relationship between specific grinding force and “a” parameter

Variation of the calculate “a” parameter at the same specific grinding force was investigated, individually. Average of “a” parameter at the same specific grinding force is take into consideration for further calculations because difference in data is acceptable. The data presented in Figure 5.5 were for the polymetallic and chalcopyrite ore.

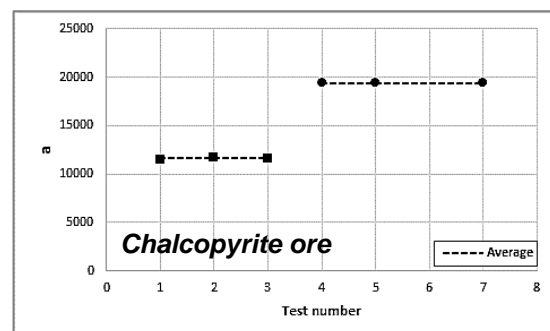
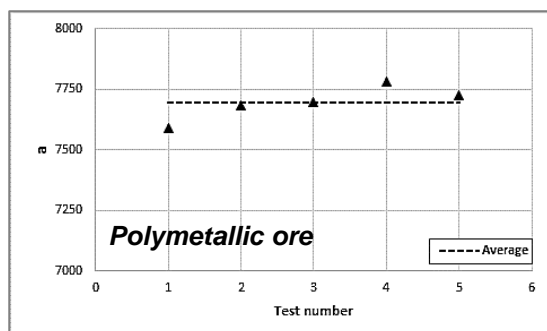


Figure 5.5 Variation of “a” parameter

On the other hand, different “a” parameters were calculated for different materials at the same specific grinding force. This difference results from the material characteristics. A material constant should be defined into the rate model to reflect the material effect on “a” parameter. This constant was determined by evaluating the bed breakage test results. Multiplication of C and d parameters obtained from $E_{cs} \cdot X$ -disappearing rate relationship was defined as material index which was explained in Section 3.3 in detail. Specific grinding force was normalized with the material index and it was able to calculate “a” parameter for various specific grinding force and material. Normalized data are presented in Figure 5.6.

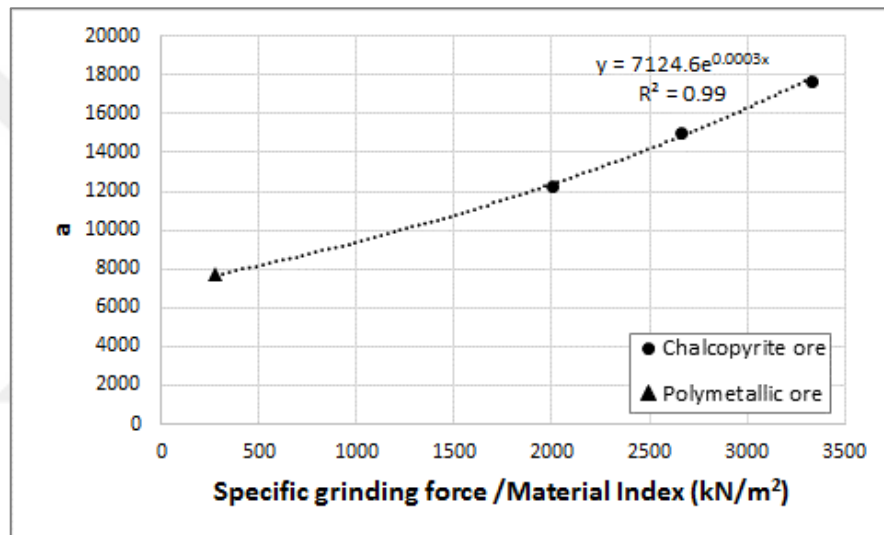


Figure 5.6 Relationship between normalized specific grinding force and “a” parameter

In the second part of the modelling of grinding operation, “ θ ” parameters were investigated. “ θ ” parameter defines the slope of breakage rate in the model (Equation 5.2.).

In vertical roller mill modelling, particle size distribution of the material bed is represented by “ θ ” parameter similarly to HPGR model developed by Dundar et al. [104]. Specific surface area was used to define the size distributions of the material bed. Specific surface area was calculated theoretically and correlated with “ θ ” parameter. Relationship between specific surface area of material bed under the rollers and “ θ ” parameter for chalcopyrite and polymetallic ores are presented in Figure 5.7.

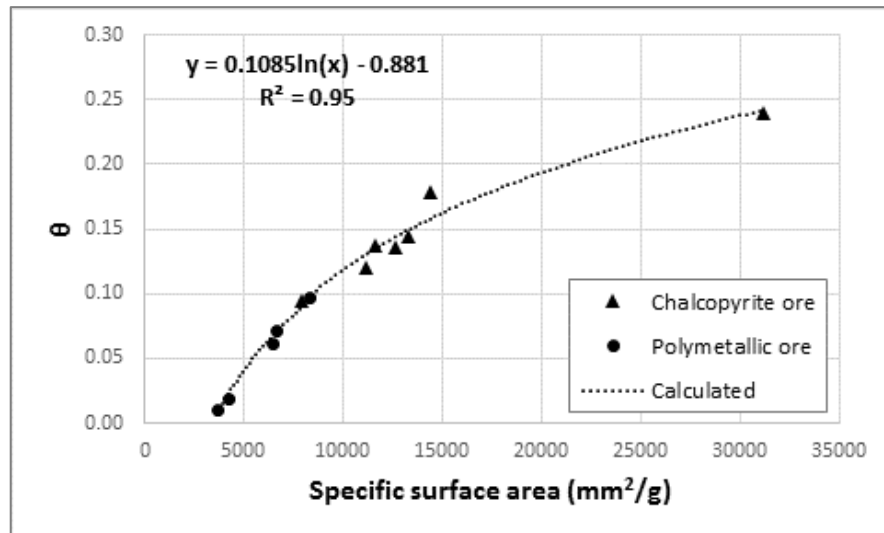


Figure 5.7 Relationship between theoretical specific surface area and “θ” parameter for chalcopyrite and polymetallic ore

Size distribution of the material bed affects the grinding efficiency because applied load under pressure during breakage operation is transferred to the material through the surrounding particles. Finer table feed affects the bed stabilization and improve the breakage. This effect can be observed with “θ” parameter. Decrease in the table feed size increases the “θ” parameter.

5.1.1. Application Of Grinding Model To Industrial Scale Data

Model development studies were carried out by the data obtained from the pilot scale tests. In this section, applicability of the developed model of grinding operation to industrial scale data were investigated. Within this context, model parameters “θ” was calculated using defined equation given in Section 5.1. “a” parameter was back calculated by using table feed and table product size distributions and flowrates. Specific grinding force is 816 kN/m² for two test. Estimated product size distributions of clinkers are given in Figure 5.8. The results showed that the presented modelling concept was applicable for the modelling of grinding operation in industrial scale vertical roller mills.

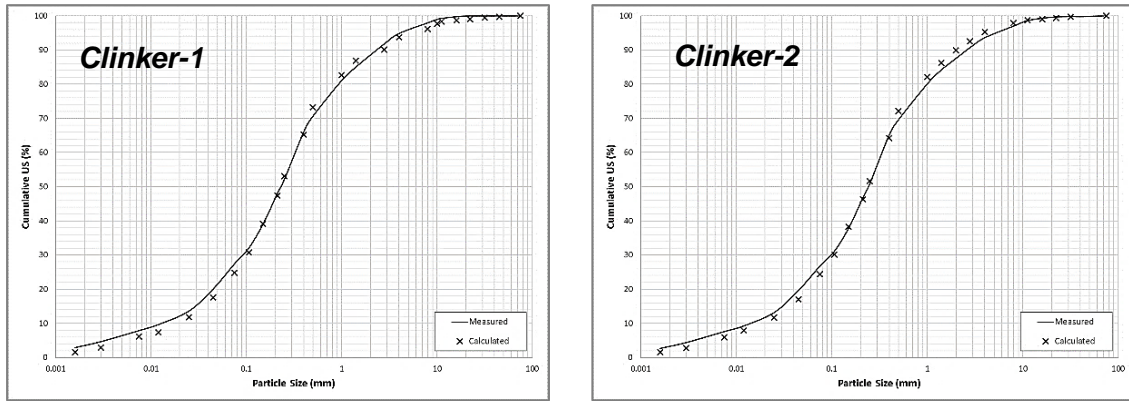


Figure 5.8 Measured and estimated product size distributions for clinkers
 Calculated model parameters for two clinker samples are given in Table 5.2.

Table 5.2 Calculated model parameters for industrial scale data

	a	θ
Clinker-1	31141.28	0.238
Clinker-2	26320.83	0.286

It is observed that there is a big difference between calculated “a” parameters for pilot and industrial scale tests (Figure 5.9). Implementation of the industrial scale test data into the developed approach is a preliminary work, it is necessary to develop a scale up procedure by more industrial scale data as a future work.

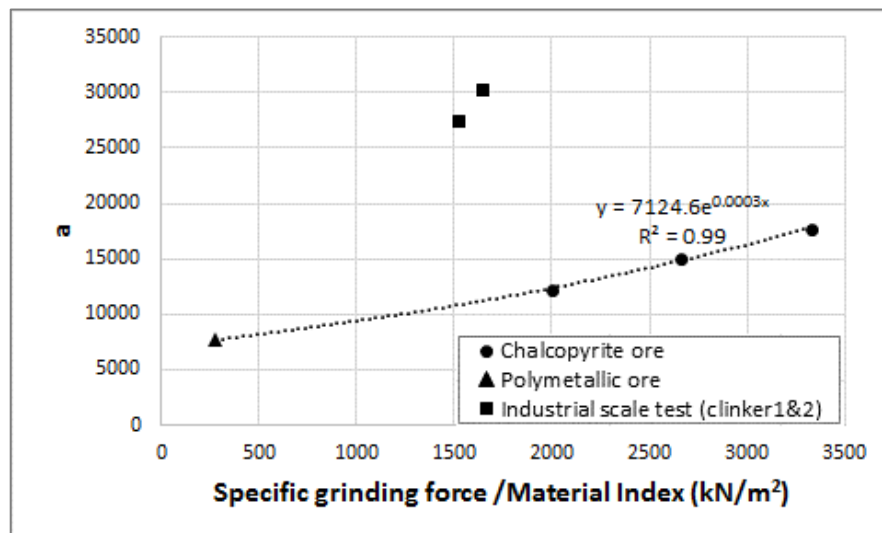


Figure 5.9 Integration of the industrial scale “a” parameter to the pilot scale model

5.2. Modelling of Separation Section

In this part of the study, modelling studies were performed for dynamic air classifier. It was aimed to calculate the flowrates and the particle size distributions around the high efficiency dynamic air classifier. Within this context, modelling approaches were investigated and efficiency curve approach was applied to develop a model structure for high efficiency air classifier. Among the efficiency curve approaches [105-110], Whiten's approach [103] was preferred because of its success of fit with high accuracy at finer sizes. The mathematical expression of Whiten's approach is given in Equation 5.4.

$$E_{oa} = C \left[\frac{(1 + \beta \beta^* X)(e^\alpha - 1)}{e^{\alpha \beta^* X} + (e^\alpha - 2)} \right] \quad (5.4.)$$

where,

- E_{oa} : The actual efficiency to overflow
- C : Fraction subjected to real classification; (100-bypass)
- B : Parameter that controls the initial rise of the curve in fine sizes (fish-hook)
- β^* : Parameter that preserves the definition of d_{50c} ; $d = d_{50c}$ when $E = (1/2)C$
- α : Sharpness of separation
- X : d/d_{50c}
- d : Size
- d_{50c} : Corrected cut size

High efficiency dynamic air classifier data obtained from grinding tests were fitted to Whiten's approach and model parameters were back calculated for chalcopryrite and polymetallic ore grinding tests. Particle size distributions around the classifier obtained by model fitting study and mass balancing were compared to determine the success of model fit of the model. Experimental and calculated particle size distributions are given in Figure 5.10 and Figure 5.11 for chalcopryrite and polymetallic ore, respectively.

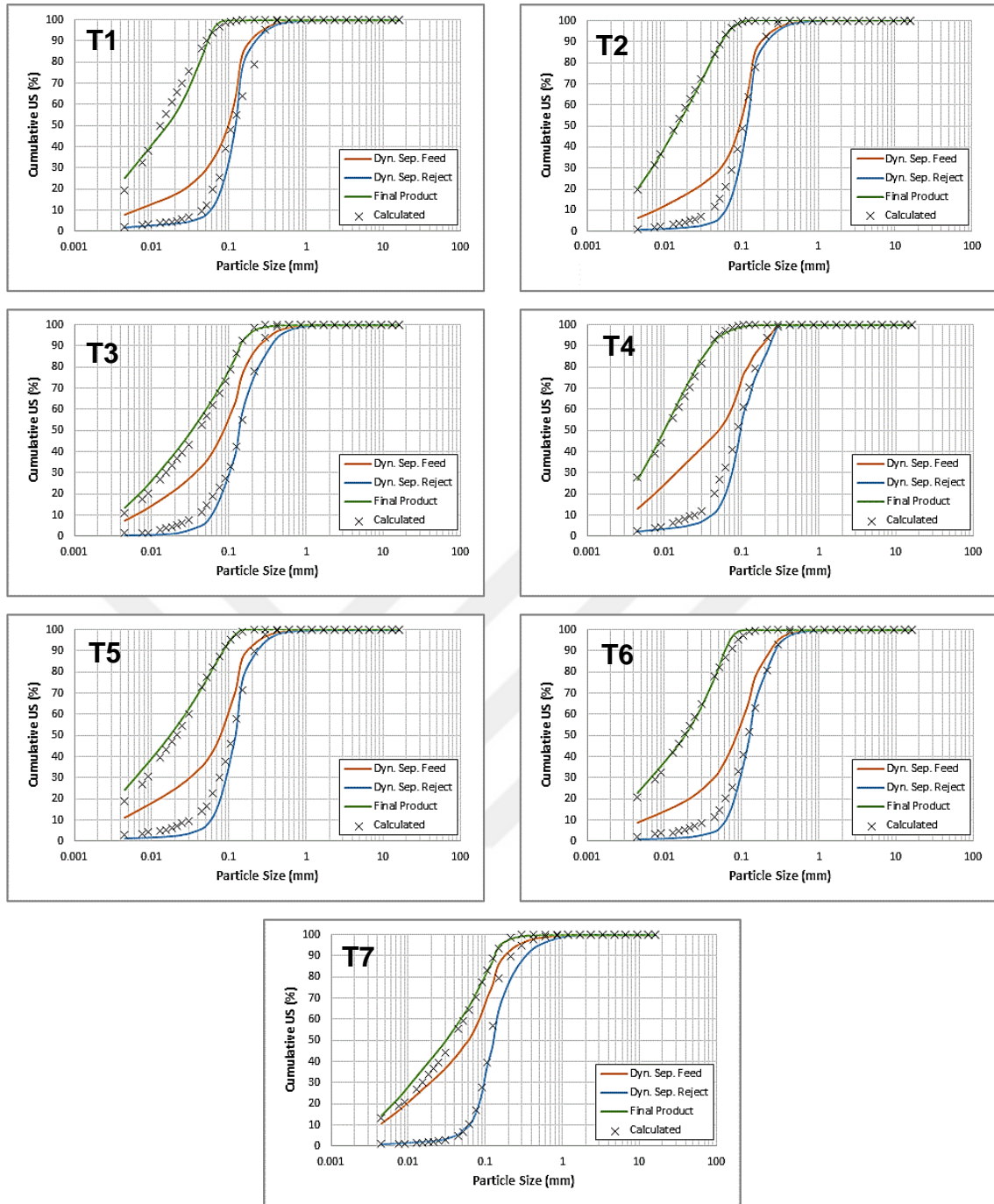


Figure 5.10 Measured and estimated product size distributions for chalcopyrite ore

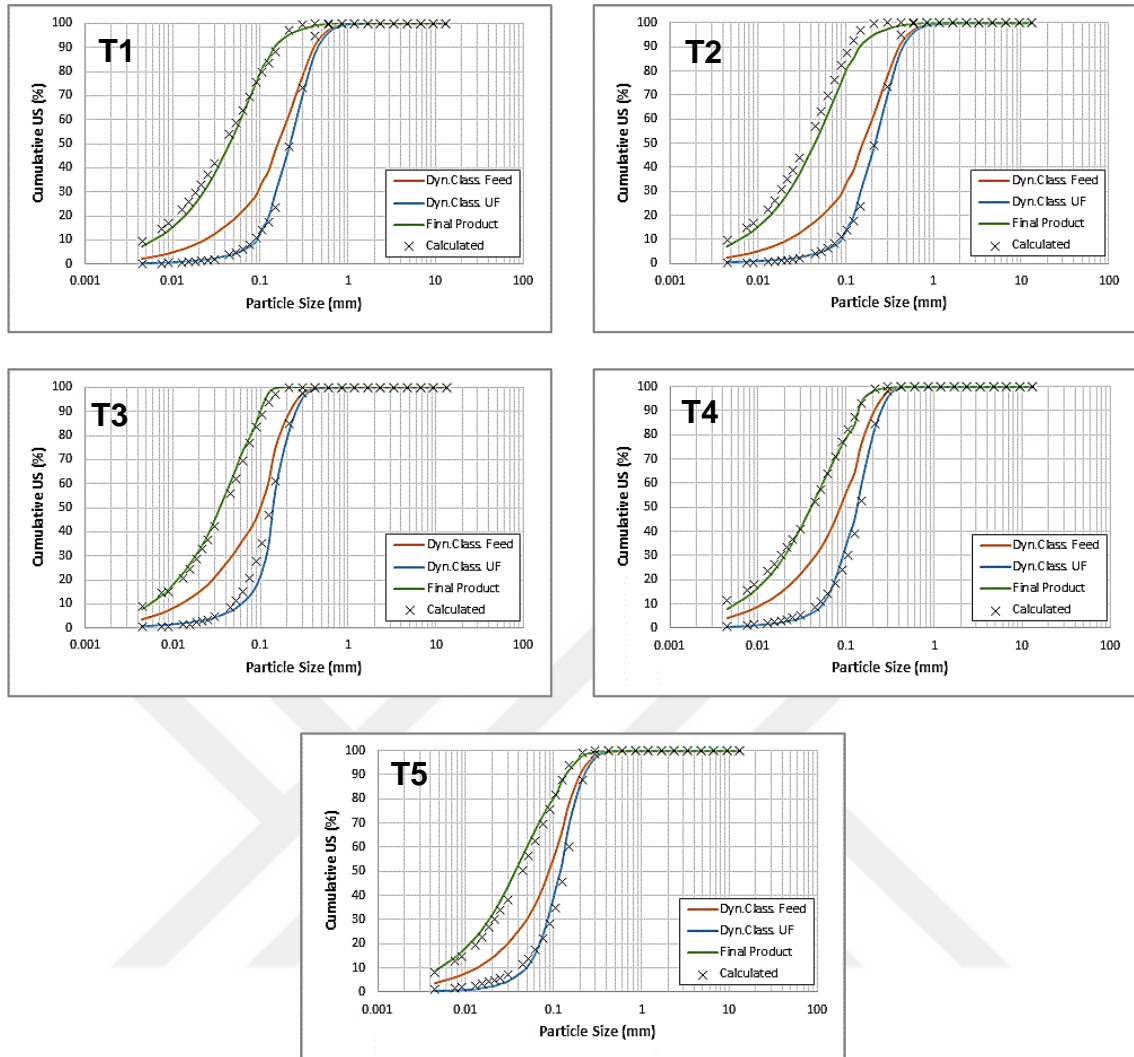


Figure 5.11 Measured and estimated product size distributions for polymetallic ore

After comparison of measured and calculated size distributions, it was decided to use the data for modelling of dynamic air classifier. Calculated parameters for chalcopyrite and polymetallic ore are summarized in Table 5.3.

Table 5.3 Model parameters of dynamic air classifier

		100-C (Bypass)	α	d_{50c}	β	β^*
Chalcopyrite ore	T1	11.65	2.0	0.055	0.10	1.086
	T2	12.70	2.0	0.039	0.10	1.086
	T3	15.90	2.0	0.130	0.10	1.086
	T4	13.30	2.0	0.035	0.10	1.086
	T5	15.00	2.0	0.069	0.10	1.086
	T6	15.80	2.0	0.058	0.10	1.086
	T7	11.30	2.0	0.160	0.10	1.086
Polymetallic ore	T1	2.68	1.4	0.079	0.07	1.000
	T2	4.76	1.4	0.078	0.07	1.000
	T3	3.68	1.4	0.069	0.07	1.000
	T4	7.13	1.4	0.092	0.07	1.000
	T5	11.96	1.4	0.092	0.07	1.000

At the first stage, relationships between fitted efficiency curve model parameters and operational parameters were investigated. Initially, bypass (100-C) which is defines as fine materials in the circulating stream was tried to correlate with operational parameters. It was reported that the bypass fraction is mainly influenced by the dust load of the separator feed [87,93,110]. Based on this, variation of bypass fraction with separator feed tonnage is investigated (Figure 5.12). An increase in the amount of material fed to the classifier results in high bypass fraction.

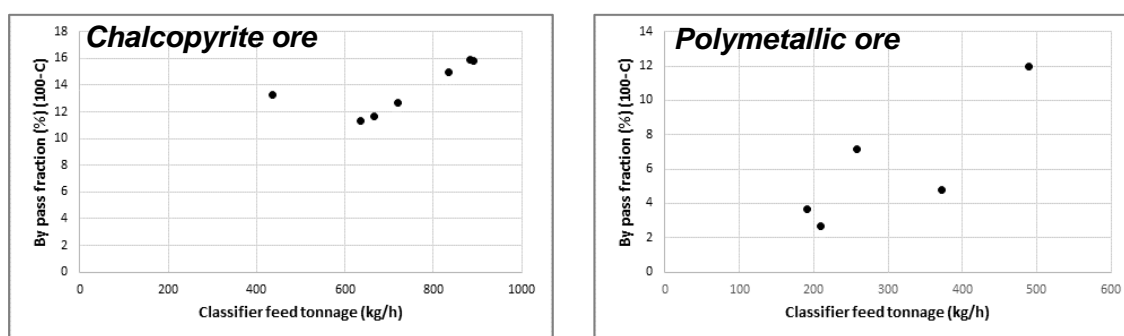


Figure 5.12 Relationship between separator feed amount and bypass fraction

Dust load of the separator feed was correlated with bypass to integrate the air flowrate which is an effective parameter on separator performance. Correlations between dust loading of the separator and bypass fraction is given in Figure 5.13. Dust load and bypass of the separator are directly proportional to each other. Bypass fraction of chalcopyrite and polymetallic ore is different for the same dust load of the separator feed. It is thought that this results from the differences of the

material densities. Chalcopyrite ore which has the highest density (4.1 g/cm³) has the highest bypass value. For this reason, density of the material was correlated with bypass- dust load relationship. The ratio of equation coefficients is equal to ratio of densities of the materials where 4.1 g/cm³ for chalcopyrite ore and 2.8 g/cm³ for polymetallic ore. Derived equation is given in Equation 5.5. This equation allows to calculate bypass fraction of each material.

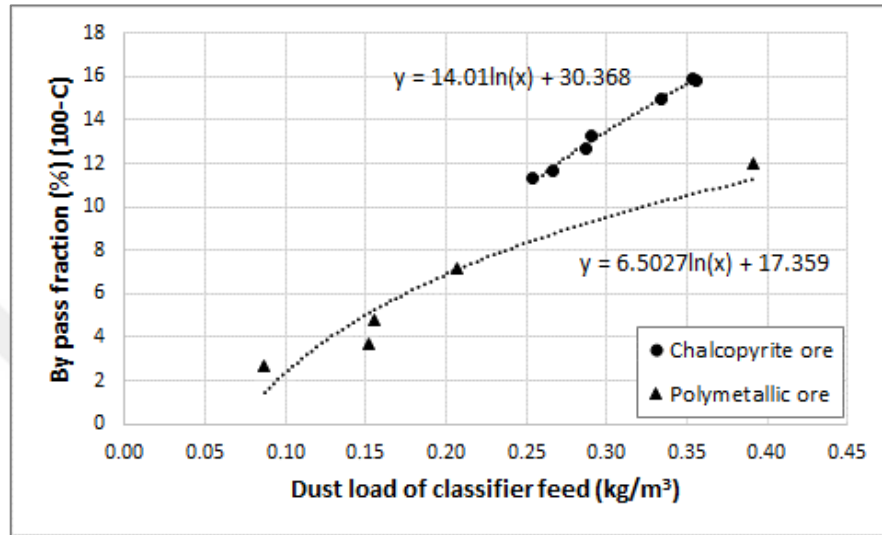


Figure 5.13 Relationship between dust load of the separator and bypass fraction

$$Bypass = 7.8398 * \ln(DL * \rho) + 11.809 \quad (5.5)$$

Where,

ρ : Density of the material (g/cm³)

DL : Dust load of the separator feed (kg/m³)

After defining bypass fraction, corrected cut size (d_{50c}) parameter was investigated. Rotor speed and air speed are effective parameters on the cut size of the separator [111]. Effect of separator rotor speed on corrected cut size is given in Figure 5.14. Rotor speed was converted from rpm to m/s for taking into consideration of separator rotor diameter. There is decreasing trend between rotor speed and d_{50c} as reported in literature [87,91,111]. Increase in rotor speed increases the centrifugal force and possibility of particle reporting to the coarse product.

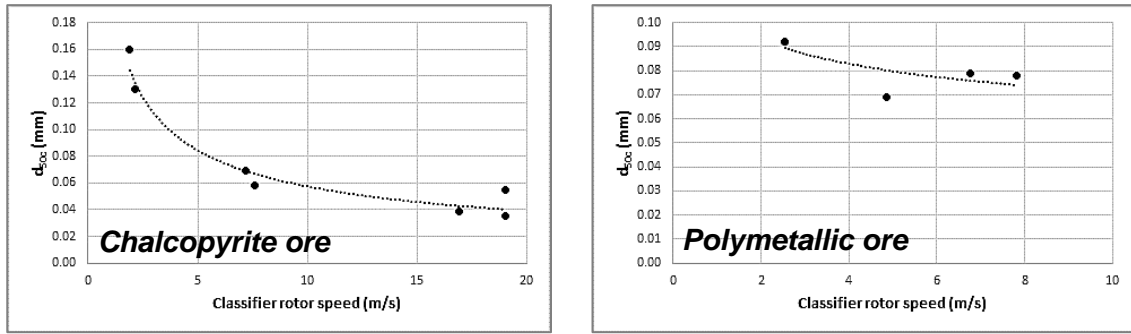


Figure 5.14 Relationship between separator rotor speed and d_{50c}

An improved correlation was obtained when the ratio of air speed and rotor speed was correlated with corrected cut size. Air speed was calculated by dividing air flowrate by the separator rotor area. This relationship is illustrated in Figure 5.15.

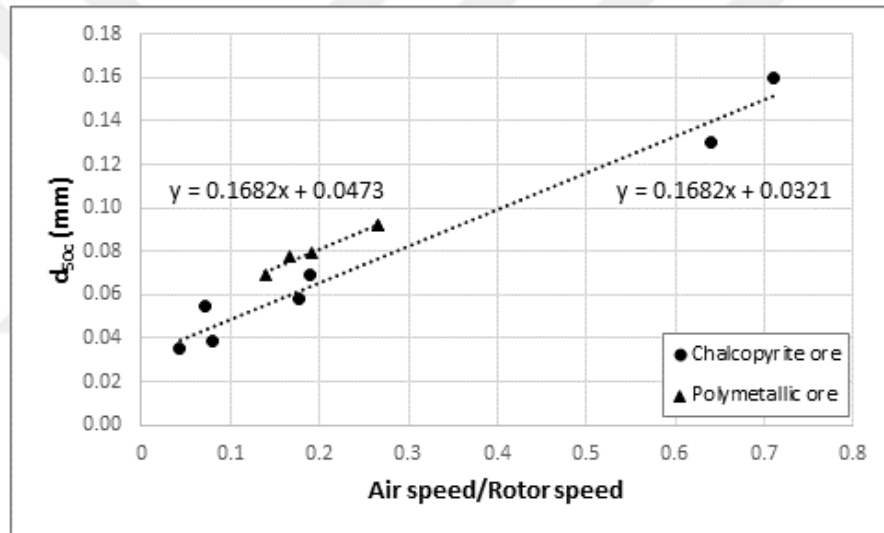


Figure 5.15 Relationship between dust load of the separator and bypass fraction

Air speed-rotor speed ratio and d_{50c} is directly proportional to each other. Also, density effect can be seen from the Figure 5.15. Density effect on cut size was also confirmed by literature studies [112,113]. Cut size of the separator is low for the denser feed. Derived equation for d_{50c} is given in Equation 5.6.

$$d_{50c} = 0.1682 * \left(\frac{\text{Air speed}}{\text{Rotor speed}} \right) + \frac{0.1324}{\rho} \quad (5.6.)$$

It was assumed that, “ α ” and “ β ” parameters were constant for different operational conditions. These parameters were correlated only density of the material. According to this assumption, developed formulas are given in Equation 5.7. and

Equation 5.8. “ β^* ” parameter is correction factor of the equation and iteratively calculated in the model.

$$\alpha = 0.5 * \rho \quad (5.7.)$$

$$\beta = 0.025 * \rho \quad (5.8.)$$



6. SIMULATION STUDIES

Within the concept of the study, simulation studies were performed for airswept vertical roller mill system by using model equations presented in modelling studies section 5. Simulation studies were aimed to validate the developed modelling approaches. With this aim, data obtained from pilot scale airswept vertical roller mill tests were used. Airswept mill is a compact unit consisting of grinding part and dynamic air separator. Also, a kind of static classification occurs in this system which was explained in Section 3.2. After grinding under the rollers, ground material is transported to the dynamic air classifier. But, coarser material was recycled to the mill by air. This operation is defined as a static separation in the simulation studies. This closed design was converted into a circuit for simulation. Simplified flowsheet of the airswept system used in simulation studies is illustrated in Figure 6.1. In this study, model parameters for static separation section were defined and flowrates, particle size distributions around the vertical roller mill circuit were estimated for chalcopyrite, gold, copper and platinum ores (platinum ore-1, platinum ore-2). Experimental and calculated product size distributions were compared to test the precision of the model estimations.

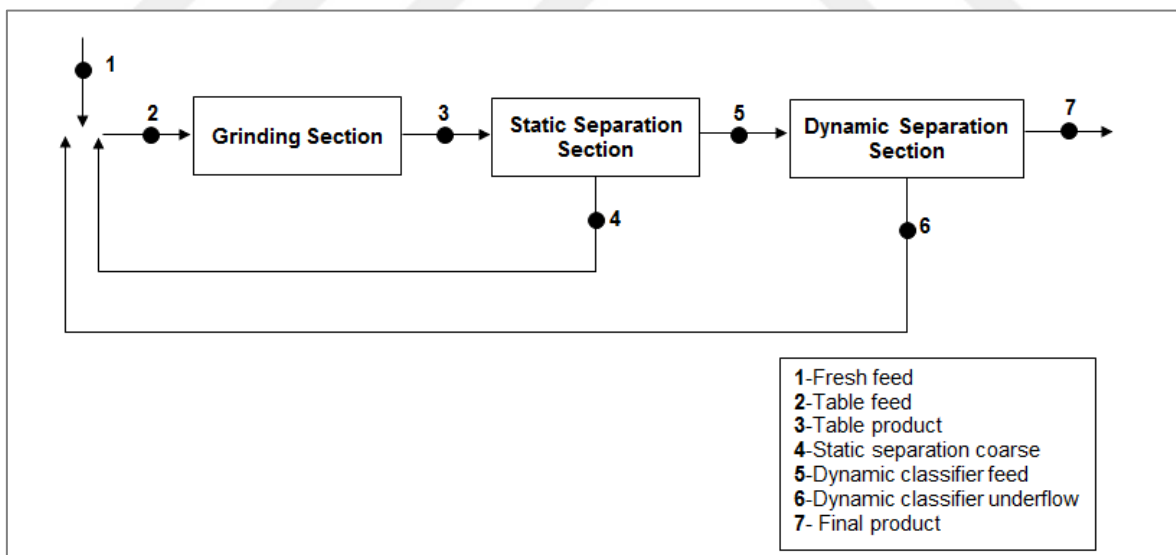


Figure 6.1 Flowsheet of airswept vertical roller mill system

6.1. Simulations for Loesche OGP_{Mobile}

In this part of the study, simulations were carried out for chalcopyrite and gold ore grinding tests in airswept mode. In airswept mode, feed and product streams could be sampled. Calculated model parameters for grinding and separation sections are given in Table 6.1 and Table 6.2. for chalcopyrite ore.

Table 6.1 Grinding model parameters used for simulation for chalcopyrite ore

	Grinding Section	
	a	θ
T1	12245	0.135
T2	12245	0.144
T3	17737	0.152
T4	15074	0.136
T5	15074	0.066

Table 6.2 Separation model parameters used for simulation for chalcopyrite ore

	Static Separation Section					Dynamic Separation Section				
	C	α	d_{50c}	β	β^*	C	α	d_{50c}	β	β^*
T1	90.2	4.0	0.060	0.0	1.0	87.9	2.0	0.045	0.10	1.09
T2	79.0	4.0	0.095	0.0	1.0	79.1	2.0	0.066	0.10	1.09
T3	73.1	4.0	0.130	0.0	1.0	69.2	2.0	0.044	0.10	1.09
T4	79.5	4.0	0.110	0.0	1.0	73.9	2.0	0.067	0.10	1.09
T5	66.0	4.0	0.140	0.0	1.0	64.5	2.0	0.082	0.10	1.09

As a result of this simulation study, flowrates and particle size distributions around the vertical roller mill circuit were estimated. Experimental product size distribution of the final product was compared to the calculated distribution by simulation. Calculated flowrates around the circuit are given in Table 6.3. and particle size distributions are presented in Figure 6.2.

Table 6.3 Calculated flowrates (in kg/h) by simulation for chalcopyrite ore

	Flowrates (kg/h)					
	Fresh Feed	Table Feed	Table Product	Static Class. Coarse	Dynamic Classifier UF	Final Product
T1	189.0	650.4	650.4	381.0	80.5	189.0
T2	480.5	1987.1	1987.1	1210.7	295.9	480.5
T3	765.4	3900.6	3900.6	2294.0	841.3	765.4
T4	682.4	3869.1	3869.1	2593.4	593.3	682.4
T5	921.3	12754.3	12754.3	10517.5	1315.5	921.3

Accuracy of the model on product size estimations are quite high except Test 1. Size distribution of the simulated product is finer than the experimental data. Estimation results of Test 1 is still reasonable despite this deviation.

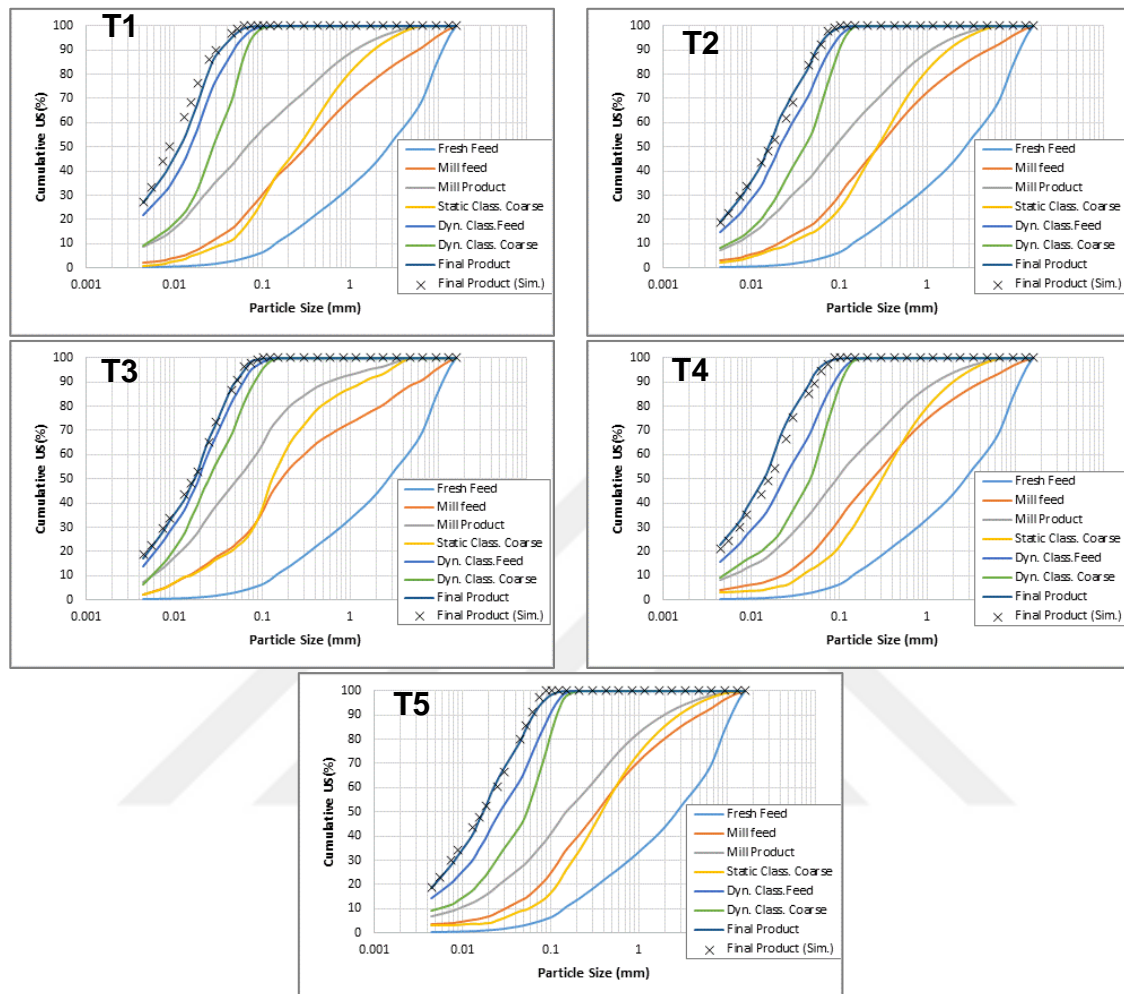


Figure 6.2 Calculated particle size distributions by simulation for chalcopyrite ore. Same procedure was applied to gold ore and model parameters were calculated (Table 6.4 and Table 6.5) for grinding and separation sections.

Table 6.4 Grinding model parameters used for simulation for gold ore

	Grinding section	
	a	θ
T1	7662.8	0.204
T2	7662.8	0.194
T3	7662.8	0.215
T4	7662.8	0.200
T5	7783.3	0.171
T6	7783.3	0.159
T7	7783.3	0.206
T8	8071.9	0.175
T9	8071.9	0.191
T10	8071.9	0.191

Table 6.5 Separation model parameters used for simulation for gold ore

	Static Separation section					Dynamic Separation section				
	C	α	d_{50c}	β	β^*	C	α	d_{50c}	β	β^*
T1	68.4	4.0	0.179	0.00	1.00	83.7	1.4	0.077	0.07	1.093
T2	50.8	4.0	0.260	0.00	1.00	71.4	1.4	0.085	0.07	1.093
T3	54.1	4.0	0.249	0.00	1.00	74.1	1.4	0.094	0.07	1.093
T4	75.0	4.0	0.148	0.00	1.00	94.2	1.4	0.060	0.07	1.093
T5	60.5	4.0	0.201	0.00	1.00	79.5	1.4	0.077	0.07	1.093
T6	54.5	4.0	0.246	0.00	1.00	70.2	1.4	0.086	0.07	1.093
T7	67.2	4.0	0.171	0.00	1.00	86.6	1.4	0.063	0.07	1.093
T8	55.0	4.0	0.260	0.00	1.00	73.3	1.4	0.077	0.07	1.093
T9	55.4	1.4	0.241	0.00	1.00	71.5	1.4	0.086	0.07	1.093
T10	67.5	4.0	0.194	0.00	1.00	86.5	1.4	0.063	0.07	1.093

Flowrates and particle size distributions around the circuit are estimated by simulation studies. Estimated flowrates and size distributions are presented in Table 6.6 and Figure 6.3.

Table 6.6 Calculated flowrates (in kg/h) by simulation for gold ore

	Flowrates (kg/h)					
	Fresh Feed	Table Feed	Table Product	Static Class. Coarse	Dynamic Classifier UF	Final Product
T1	315.0	1771.4	1771.4	1102.3	354.1	315.0
T2	392.6	8544.5	8544.5	7371.2	780.7	392.6
T3	453.5	6069.9	6069.9	4699.5	916.9	453.5
T4	137.0	467.4	467.4	224.7	105.7	137.0
T5	349.0	3020.5	3020.5	2118.7	552.9	349.0
T6	468.2	9892.3	9892.3	7995.8	1428.3	468.2
T7	188.0	1231.0	1231.0	773.2	269.8	188.0
T8	431.6	6650.9	6650.9	4984.7	1234.7	431.6
T9	540.5	8411.5	8411.5	6472.5	1398.6	540.5
T10	213.8	1244.4	1244.4	734.5	296.1	213.8

Product size distributions obtained mass balancing and simulation were compared to evaluate the estimation performance of the developed model. Estimated and product size distributions are in good agreement. Some part of the predictions is finer than actual distribution under 500 micron. It is thought that this difference results from the breakage distribution function determined by piston-die tests. For further studies, breakage distribution function can be calculated by combination of two different test method because shear forces are effective besides compression forces. On the other hand, size distributions of mill feed and product are acceptable because reduction ratio of the grinding part is low as expected.

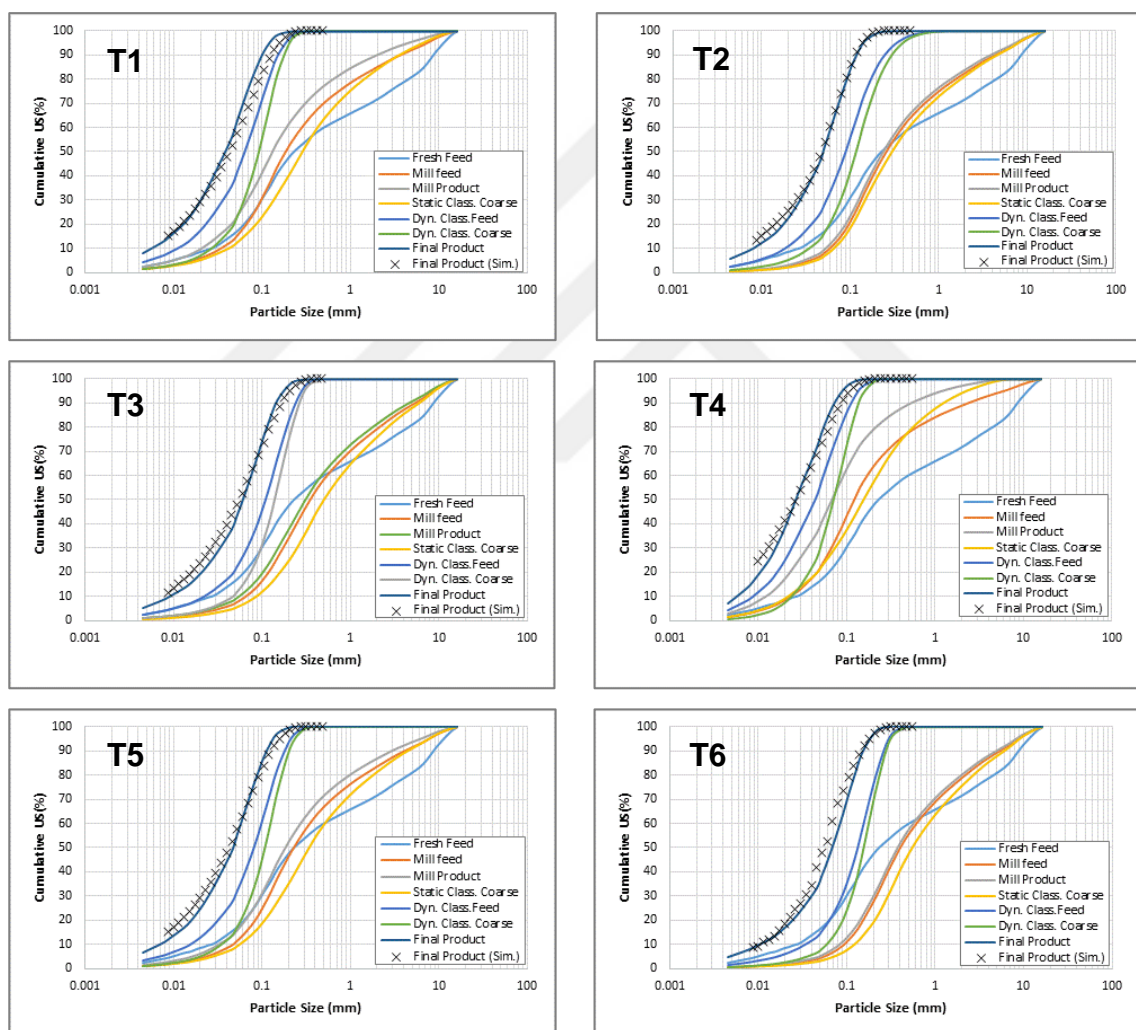


Figure 6.3 Calculated particle size distributions by simulation for gold ore

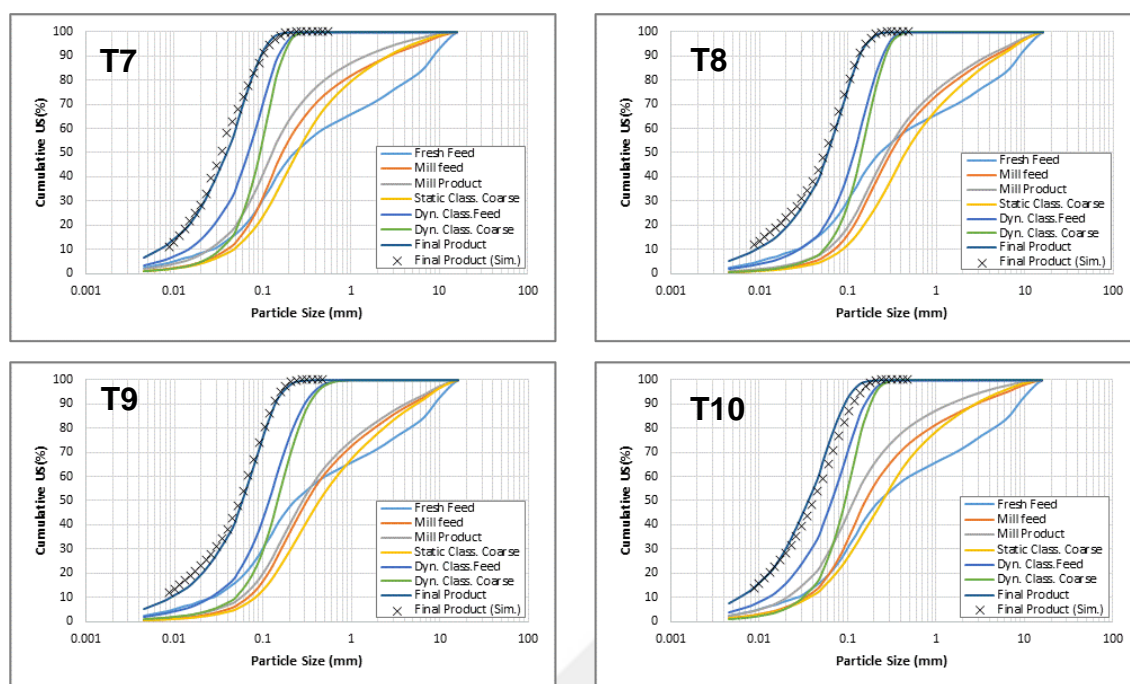


Figure 6.3. (continued)

6.2. Simulations for LM 3,6

In this part of the study, simulations were carried out for two different platinum ores and copper ore by LM 3,6 which is a conventional air-swept vertical roller mill. The main objective of this simulation is to test the precision of the model for different sized vertical roller mills. Calculated model parameters for grinding and separation sections are given in Table 6.7 - Table 6.12.

Table 6.7 Grinding model parameters used for simulation for platinum ore-1

	Grinding section	
	a	θ
T1	7394.4	0.114
T2	7394.4	0.110
T3	7394.4	0.095
T4	7394.4	0.107
T5	7394.4	0.126

Table 6.8 Separation model parameters used for simulation for platinum ore-1

	Static Separation section					Dynamic Separation section				
	C	α	d_{50c}	β	β^*	C	α	d_{50c}	β	β^*
T1	75.0	4.0	0.137	0.0	1.0	83.2	1.9	0.065	0.095	1.095
T2	66.8	4.0	0.170	0.0	1.0	76.9	1.9	0.070	0.095	1.095
T3	65.3	4.0	0.185	0.0	1.0	72.8	1.9	0.073	0.095	1.095
T4	63.2	4.0	0.190	0.0	1.0	71.5	1.9	0.079	0.095	1.095
T5	65.2	4.0	0.181	0.0	1.0	73.7	1.9	0.089	0.095	1.095

Table 6.9 Grinding model parameters used for simulation for platinum ore-2

	Grinding section	
	a	θ
T1	7394.4	0.114
T2	7394.4	0.110
T3	7394.4	0.095
T4	7394.4	0.107
T5	7394.4	0.126

Table 6.10 Separation model parameters used for simulation for platinum ore-2

	Static Separation section					Dynamic Separation section				
	C	α	d_{50c}	β	β^*	C	α	d_{50c}	β	β^*
T1	60.2	4.0	0.180	0.0	1.0	71.7	1.9	0.074	0.095	1.095
T2	58.0	4.0	0.230	0.0	1.0	64.8	1.9	0.077	0.095	1.095
T3	59.9	4.0	0.205	0.0	1.0	67.1	1.9	0.079	0.095	1.095
T4	70.9	4.0	0.159	0.0	1.0	77.7	1.9	0.067	0.095	1.095
T5	60.1	4.0	0.214	0.0	1.0	65.5	1.9	0.091	0.095	1.095

Table 6.11 Grinding model parameters used for simulation for copper ore

	Grinding section	
	a	θ
T1	9435.2	0.0983
T2	9435.2	0.0857
T3	9435.2	0.0925

Table 6.12 Separation model parameters used for simulation for copper ore

	Static Separation section					Dynamic Separation section				
	C	α	d_{50c}	β	β^*	C	α	d_{50c}	β	β^*
T1	76.1	4.0	0.119	0.0	1.0	75.4	2.0	0.062	0.1	1.095
T2	71.4	4.0	0.138	0.0	1.0	70.8	2.0	0.073	0.1	1.095
T3	68.1	4.0	0.152	0.0	1.0	67.1	2.0	0.082	0.1	1.095

After simulation studies, flowrates of the streams defined in the vertical roller mill system were calculated. Simulated flowrates are given in Table 6.13 - Table 6.15 for tested ores.

Table 6.13 Calculated flowrates (in kg/h) by simulation for platinum-1 ore

Flowrates (kg/h)						
	Fresh Feed	Table Feed	Table Product	Static Class. Coarse	Dynamic Classifier UF	Final Product
T1	181.0	881.4	881.4	542.5	157.9	181.0
T2	231.0	1968.7	1968.7	1422.0	315.7	231.0
T3	263.0	3335.7	3335.7	2593.8	478.9	263.0
T4	319.0	3922.8	3922.8	3063.6	540.2	319.0
T5	423.0	2949.5	2949.5	1987.9	538.6	423.0

Table 6.14 Calculated flowrates (in kg/h) by simulation for platinum-2 ore

Flowrates (kg/h)						
	Fresh Feed	Table Feed	Table Product	Static Class. Coarse	Dynamic Classifier UF	Final Product
T1	305.0	3503.7	3503.7	2692.6	506.1	305.0
T2	319.0	8449.1	8449.1	7396.9	733.2	319.0
T3	329.0	6318.9	6318.9	5205.4	784.6	329.0
T4	187.0	1638.4	1638.4	1175.0	276.4	187.0
T5	414.9	7703.3	7703.3	6404.3	884.1	414.9

Table 6.15 Calculated flowrates (in kg/h) by simulation for copper ore

Flowrates (kg/h)						
	Fresh Feed	Table Feed	Table Product	Static Class. Coarse	Dynamic Classifier UF	Final Product
T1	166.0	2222.9	2222.9	1763.1	293.8	166.0
T2	222.0	4017.3	4017.3	3334.9	460.4	222.0
T3	262.0	6473.3	5572.3	6473.3	639.0	262.0

Estimated particle size distributions are presented in Figure 6.4 - Figure 6.6. It was observed that there is an acceptable small difference between experimental data and its simulated precision when all simulation results were evaluated. Model estimations of product size distributions are finer than measured. It can be concluded that developed modelling approaches is valid for LM 3,6 pilot scale mill.

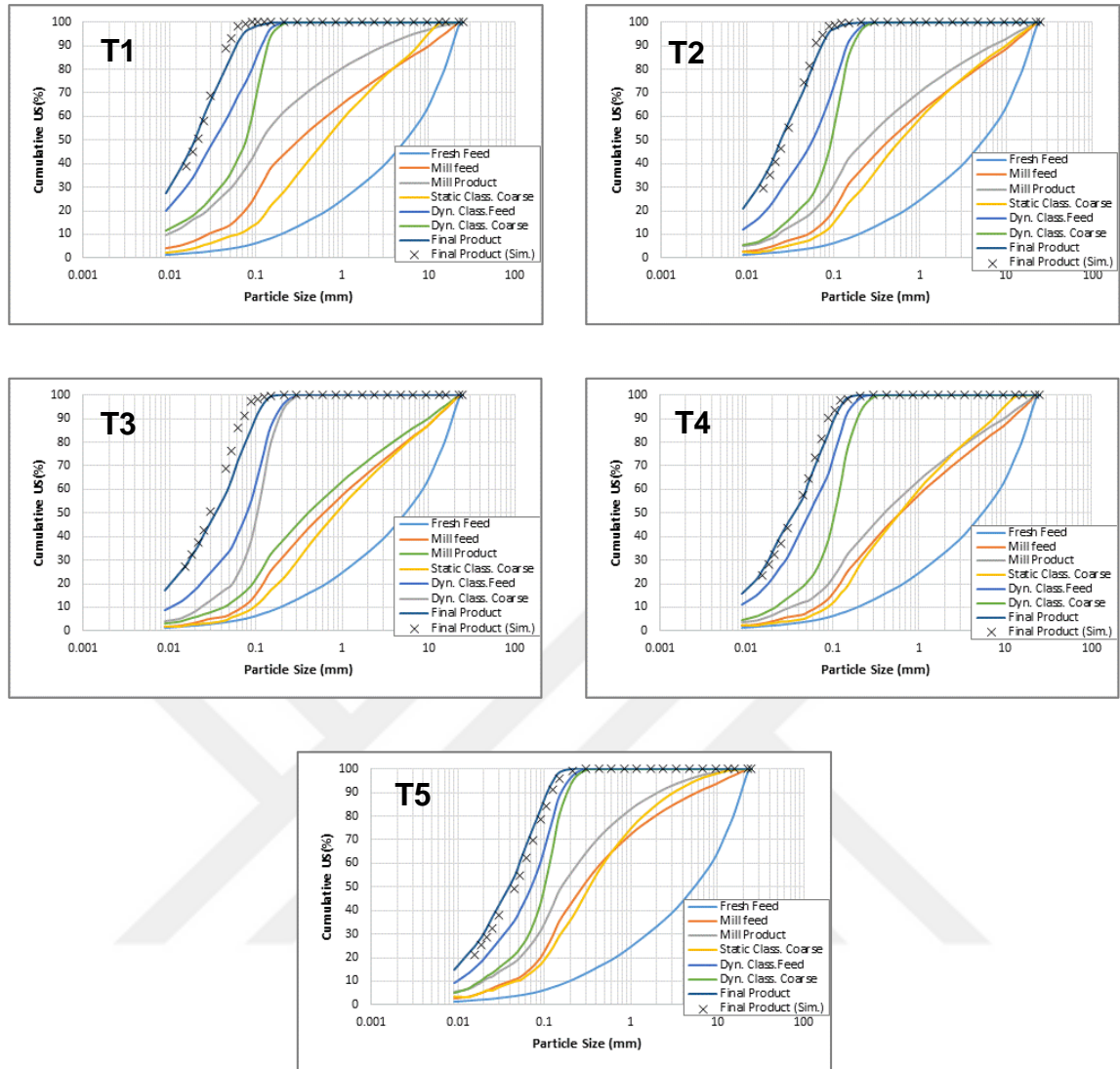


Figure 6.4 Calculated particle size distributions by simulation for platinum ore-1

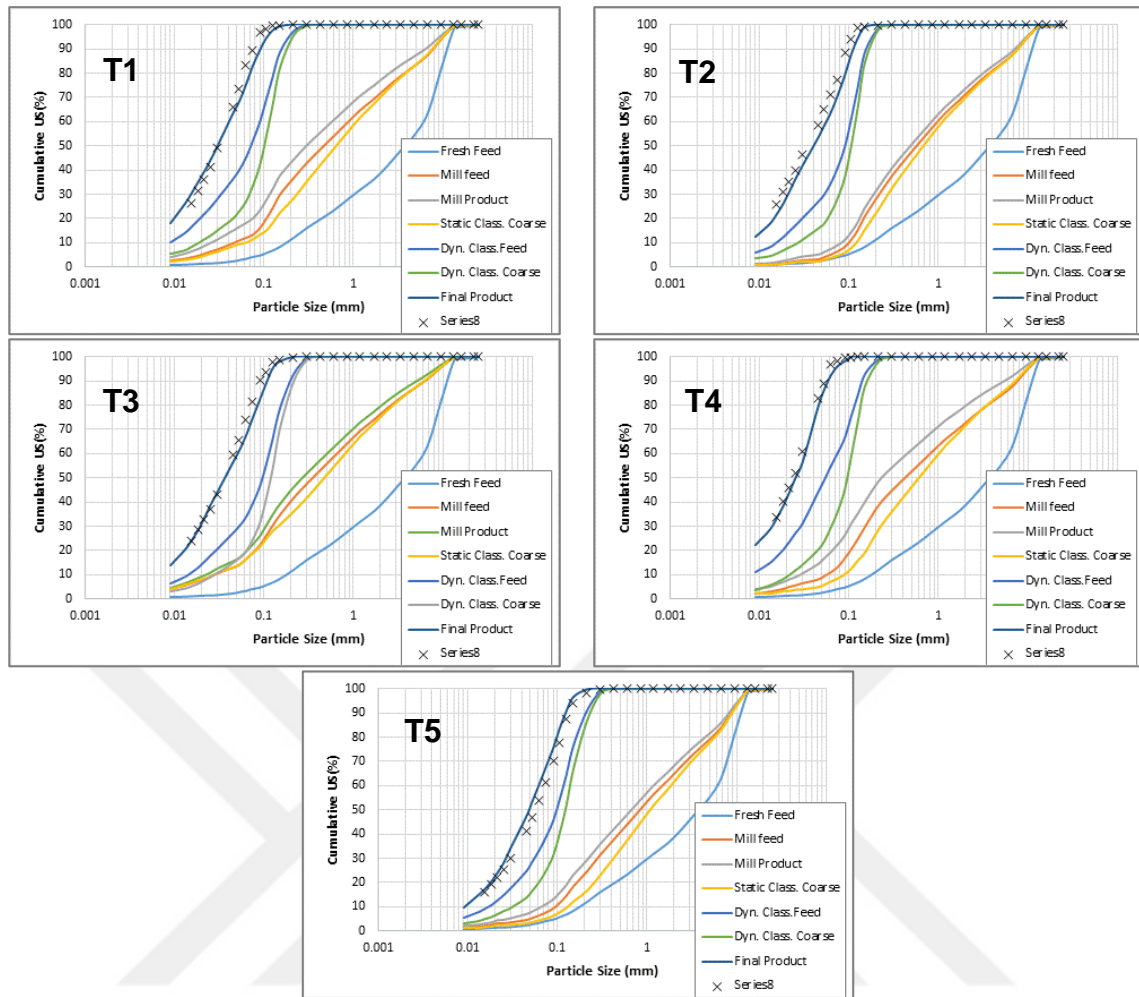


Figure 6.5 Calculated particle size distributions by simulation for platinum ore-2

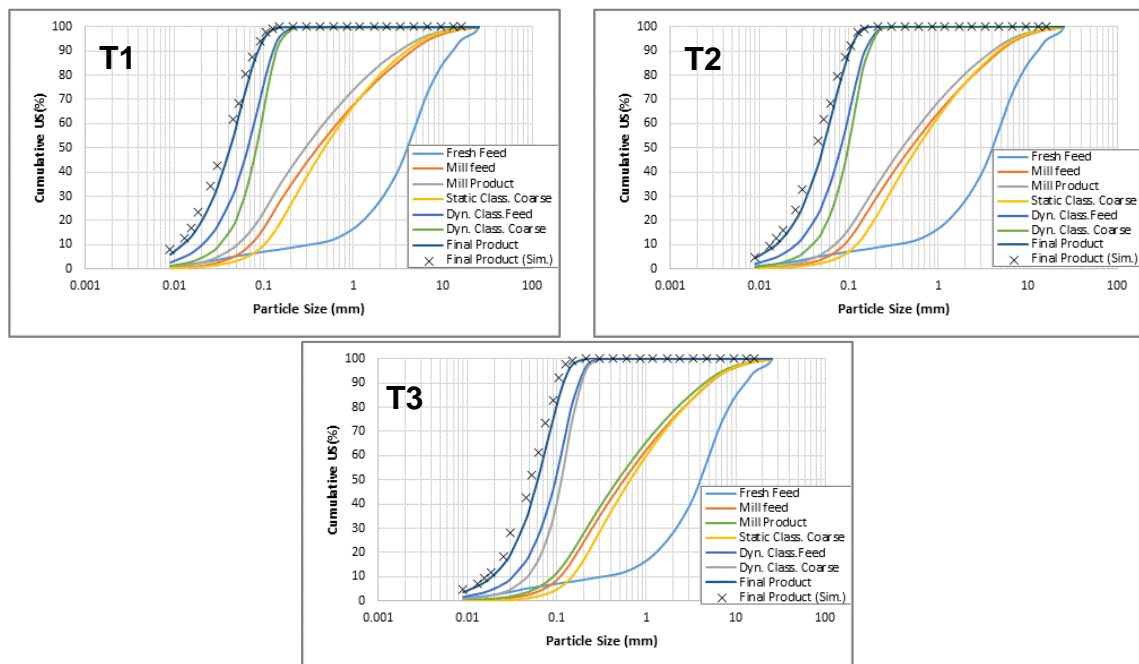


Figure 6.6 Calculated particle size distributions by simulation for copper ore

7. RESULTS AND DISCUSSION

In this study, a modelling approach was developed for vertical roller mills. Within the context, pilot scale and industrial scale tests were performed successfully. New concept mobile vertical roller mill unit Loesche OGP_{mobile} manufactured by Loesche GmbH was used in this study. Operation of this system in overflow and airswept modes provide an advantage to analyze the system in detail. It enables to collect samples around the grinding and classification sections. Also, it is possible to obtain two products as coarse and fine in one test. Mechanical external circulation system of overflow mode reduces the energy consumption. Comparison of energy consumptions of airswept and overflow modes for chalcopyrite ore is given in Figure 7.1. In pilot scale tests, such a remarkable difference couldn't be observed. It is thought that, overflow mode operation would be more beneficial for industrial scale applications. Because, pressure drop of the conventional airswept mode will be higher in industrial scale mill because of the increasing fan power.

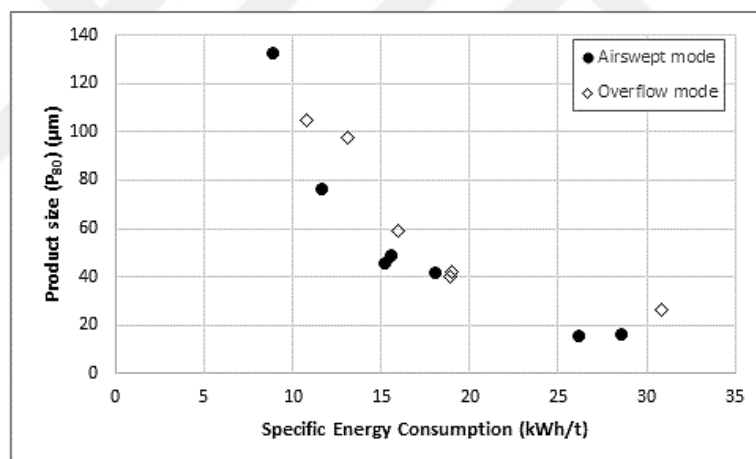


Figure 7.1 Specific energy consumptions of grinding operation for different product sizes

Additional to the grinding energy the classifier motor and the fan motor are consuming energy in the system. The specific energy consumption of the classifier and the fan are determined by a separate scale up procedure and can't be directly taken over from pilot plant.

A comparison was made between two grinding modes on the basis of product quality in terms of shape of the particle size distribution curve. As an example, particle size distribution of two products having similar P₈₀ values are presented in

Figure 7.2. Shape of the size distributions were compared by using Rosin-Rammler-Sperling-Bennet (RRSB) equation [114]. “n” parameter which refer to the steepness of distribution was calculated for airswept and overflow model products. “n” parameters of the airswept and overflow modes are 1.08 and 1.04, respectively. Significiant difference wasn’t observed between two products although product of airswept mode was steeper.

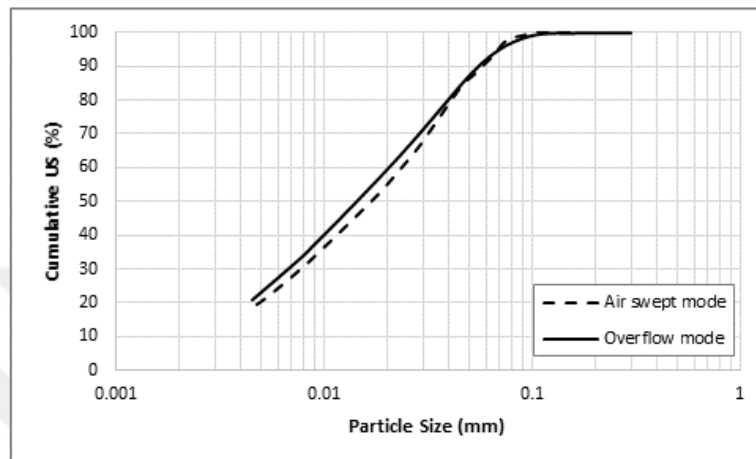


Figure 7.2 Comparison of product particle size distributions of two grinding modes. As stated in previous sections, overflow mode has two-stage air classification system. This system enables to decrease the amount of material fed to the dynamic air classifier. In conventional airswept mode, amount of material in the separator feed is higher and this increases the dust loading of the separator feed. Dust loading of the separator affects the separation performance adversely. In parallel with this increment, by pass fraction increases.

As a supplementary part of this study, industrial scale tests were performed. A new sampling technique developed by Aydogan [99] was applied to industrial scale tests. Grinding table was sampled by the help of this technique. Care should be taken in during sampling at grinding table. It is important not to mix the material outside the roller diameter. Because, suspended particles and material in classifier fall down onto the table after crash stop.

Collected fresh feed samples from pilot and industrial scale tests were subjected to material characterization tests. Characterization of the material plays a crucial role in modelling studies. Compressed bed breakage test was preferred to define the breakage behavior of material under compression force. Size dependent breakage

distribution function was determined by using breakage model developed by Eksi et al. [100]. More reliable definition of breakage was aimed by using this method.

In addition to breakage distribution function, a material index conformably to Bond work index was created to define the resistance of material against the compression forces. Disappearing rate of the material was correlated with specific comminution energy and particle size. This correlation was defined by a mathematical equation. Multiplication of this equation parameters was defined as material index. Bond work index of the materials gives an idea about grindabilities of the materials but grindabilities of materials for compression machines are not correlated with Bond Work Indices. Bond work index doesn't represent the energy size relationship of vertical roller mill system. Estimated specific grinding energy consumption to reduce the size of the chalcopyrite ore from 8.7 mm to 75 μm is 12.9 kWh/t according to Bond Index. But in operation the energy consumption is 14.7 kWh/t. Relationship between Bond work index and material index for all tested materials are presented in Figure 7.3. A material with high resistance to impact force are broken easier under compression force. This difference arises from the breakage mechanisms and the components of the tested materials. This variation is limited and only valid for this study. A detailed further study should be carried out to analyze and comment on this output.

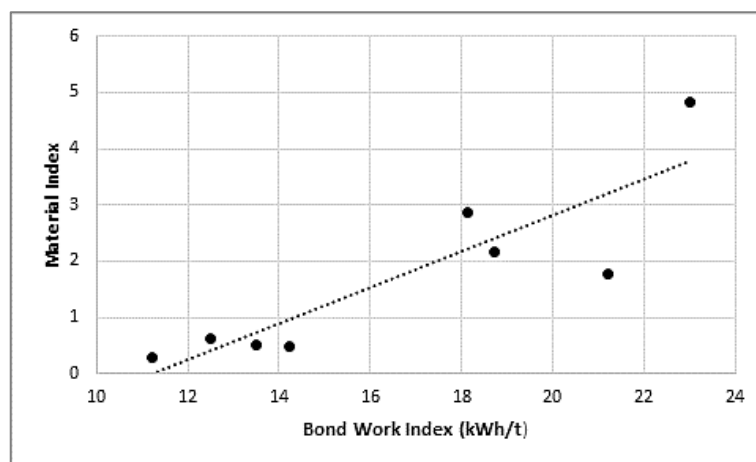


Figure 7.3 Relationship between Bond work index and material index

Mass balance studies were performed for pilot scale overflow mode tests data and industrial test data. Mass balanced data was used for model development. It was expected to estimate the particle size distributions and the flowrates around the grinding and classifying sections. Based on this, vertical roller mill was separated

into the two section as grinding and separation during the modeling studies. For the modelling of the grinding section, population balance model [102] was used based on the simplicity and success of the defining breakage operation of the model. Breakage rate in this model was defined by function developed by Austin et al. [92]. Amount of material inside the mill (s) was represented as material under the grinding rollers. "s" was calculated by using grinding bed height, roller dimensions and density of the material. Nipping angles were chosen 1° and 10° as a standard. Material load on the grinding table has an effect on fineness of the table product. Because of its importance, detailed studies could be performed for calculation of the material amount inside the mill.

By using breakage models, "a" and "θ" model parameters were back calculated. It was observed that "a" parameters are similar for polymetallic ore therewith it was found that specific grinding force is the common point of these tests. Starting from this point, relationships between specific grinding force and calculated "a" parameters of chalcopyrite ore were investigated. It was concluded that "a" parameter is directly proportional to the specific grinding force as expected. Because, an increase in "a" parameter increase the breakage rate and cause finer product as similar as specific grinding force. Another effective parameter on "a" model parameter is material characteristics. Therefore, "a" parameter was correlated with specific grinding force and material index determined by compressed bed breakage tests. By this way, it is possible to determine the "a" parameters for each material at any specific grinding force.

In the model, effect of size distribution of material in the grinding zone was defined depending on the theoretical surface area. "θ" grinding model parameter was represented by specific surface area of the material bed similarly to HPGR model [104]. Obtained specific surface area and model parameter relationships are given for vertical roller mill and HPGR in Figure 7.4. Specific surface area trend of vertical roller mill is logarithmic while trend of HPGR is linear. It is expected that after a saturation point, "θ" parameter will not increase with the increasing specific surface area. Owing to varied product size range of vertical roller mill, limits of the specific surface area-"θ" parameter relationship are wider. Also, these differences could be resulted from the shear forces which is the affected breakage mechanism in vertical roller mills.

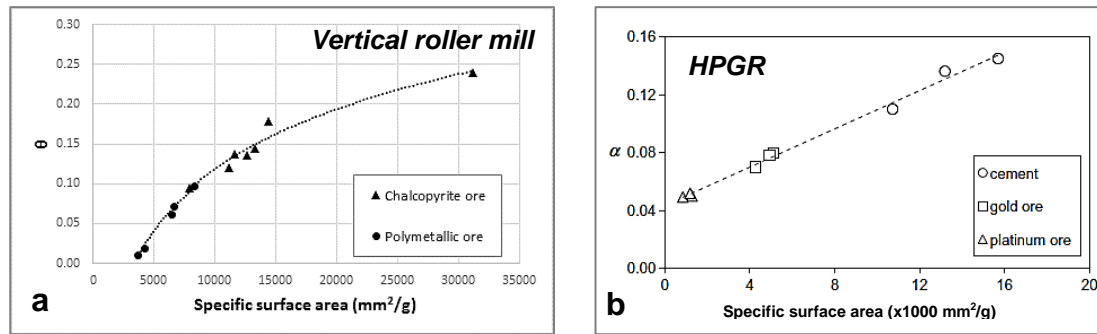


Figure 7.4 Specific surface area & model parameter (" θ " and " α ") relationship for vertical roller mill (a) and HPGR (b) [104]

After modelling studies of grinding section, adaptation of the developed model of grinding operation to industrial scale data were investigated. " θ " parameter was calculated by using correlation used in pilot scale modelling studies. " a " parameter was back calculated for two different clinker and compared to the pilot scale modelling results. There are differences between " a " parameters of pilot and industrial scale tests. Structure of the developed modelling approach is applicable for industrial scale vertical roller mills. Number of industrial scale tests should be carried out for different materials to analyze the reasons of this difference. After evaluation of obtained data, a scale-up procedure could be developed for industrial mills.

For the modelling of separation section, Whiten's efficiency curve approach [103] was used because of the high accurate fit. Model parameters were back calculated and relationships between effective operational parameters were investigated. At first, by pass fraction of the separator and dust loading of the separator feed was investigated. By pass fraction of the separator increases with the increasing amount of material in separator feed. This kind of dependency is also existed in the literature [87,93,110]. From this point, bypass was correlated with dust load of the separator feed. Bypass fraction of chalcopyrite and polymetallic ore differ for the same dust load of the separator feed. Ore with the highest density has the highest by pass value. As a result, by pass fraction was correlated with density and dust load of the separator feed. By pass fraction was correlated with dust load of the separator feed and material density.

Cut size of the separator is another effective parameter. Variation of the cut size with the rotor speed of the separator was investigated in regard to literature

[87,91,111]. A decreasing trend was observed for rotor speed and cut size of the separator. The ratio of air speed and rotor speed was correlated with corrected cut size. Density effect on cut size was confirmed by literature studies [112,113] and this density effect was reflected to the relationship.

“ α ” and “ β ” parameters were assumed constant for different operational conditions. These parameters were correlated with only density of the material.

At the end of the modelling studies, mathematical equations were derived based on obtained relationships between model parameters and operational parameters. Simulation studies were performed for pilot scale airswept grinding tests by using these equations. The purpose of the simulation study is to validate the developed modelling approach.

In the simulation studies, static separation section was implemented. During the studies, efficiency curve parameters for static separation operation was defined. Circulating load in this point was not measured because of the unfavorable conditions inside the mill. Because of this reason, “ α ”, “ β ” and “ β^* ” parameters were accepted as constant for all tests. It is possible to calculate the circulation ratios inside the mill by CFD (Computational Fluid Dynamics) method. This assumption should be confirmed by this method. “C” parameter and dust loading of the static separation feed for tested ores were investigated as similar as in the modelling of dynamic classification. Variation of bypass fraction with dust load is illustrated in Figure 7.5 for different ores. There is a similar increasing trend with dynamic classification modelling results. Curves shifted in parallel. Slope of the curves shows the effect of density on bypass fraction. An equation was derived to calculate the bypass fraction as a function of density and dust load (Equation 7.1).

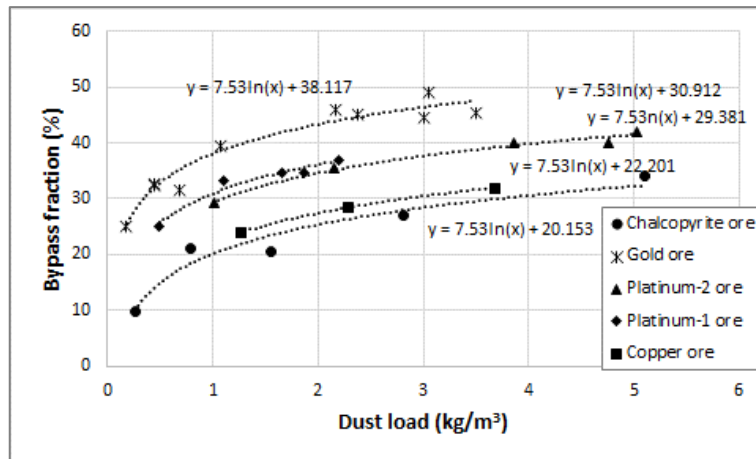


Figure 7.5 Relationship between dust load of the separator and bypass fraction

$$Bypass (100 - C) = 7.53 * \ln(DL) + 138.43 * e^{-0.449*\rho} \quad (7.1)$$

Where,

ρ : Density of the material (g/cm^3)

DL : Dust load of the separator feed (kg/m^3)

After defining bypass fraction for static classification, corrected cut size (d_{50c}) parameter was investigated. Cut size parameter was correlated with bypass fraction. Relationships are given in Figure 7.6. Bypass and cut size is directly proportional to each other. Trends show a change with the variable density of the ores. Derived equation by using these outputs is given in Equation 7.2.

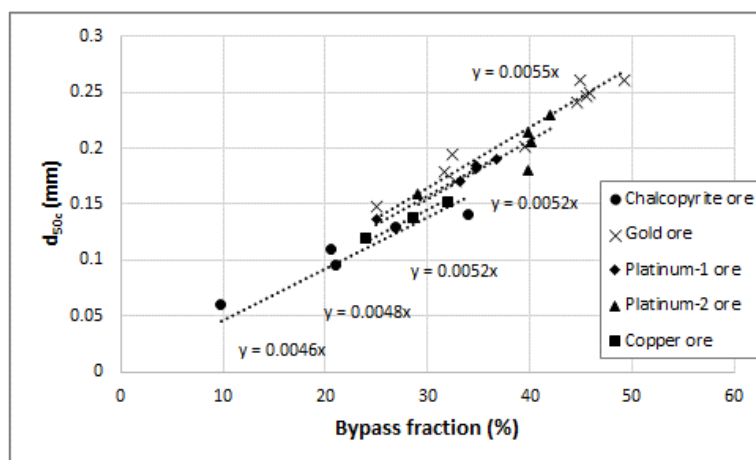


Figure 7.6 Relationship between bypass fraction and cut size (d_{50c})

$$d_{50c} = (-0.0006 * \rho + 0.0072) * bypass \quad (7.2)$$

As a consequence of this study, measured and simulated product particle size distributions were compared. A major part of the estimations is in good agreement with each other. Deviations at fine sizes were observed in some part of the simulations. It was concluded that modelling approach developed is successful in estimation. This model would be upgraded by comprehensive test plan including different dam ring height, table speed and roller type.



8. CONCLUSIONS

In this study, a modelling approach was developed for vertical roller mills. Within the context, pilot scale and industrial scale tests were performed successfully.

- New concept mobile vertical roller mill unit manufactured by Loesche GmbH was used in this study and data obtained from this unit was used for model development studies.
- A new sampling technique developed by Aydogan [96] was applied to industrial scale tests.

Breakage behavior under compression of the materials were investigated by piston-die test equipment.

- Size dependent breakage distribution functions were calculated for each material.
- Disappearing rate of the material was correlated with specific comminution energy and particle size. This correlation was defined by a mathematical equation. Multiplication of this equation parameters were defined as material index.

Mass balance studies were performed for pilot scale overflow mode tests data and industrial test data.

During the modeling studies, vertical roller mill was separated into the two section as grinding and separation.

- For the modelling of grinding section, population balance model [98] was used. Breakage rate in this model was defined by function developed by Austin [88].
- It was observed that “a” grinding model parameter is dependent on specific grinding force and material properties. Therefore, “a” parameter was correlated with specific grinding force and material index determined by compressed bed breakage tests.
- θ grinding model parameter was represented by specific surface area of the material bed similarly to HPGR model [104].

- It was concluded that, developed modelling approach is applicable for industrial scale vertical roller mills. But, it is need to develop a scale-up procedure.
- For the modelling of separation section, Whiten's efficiency curve approach [103] was used. Model parameters were back calculated and relationships between operational parameters were investigated.
- As reported in the literature, by pass fraction of the separator increases with the increasing amount of material in separator feed. From this point, by pass was correlated with dust load of the separator feed.
- Effect of material density was investigated. Ore with the highest density has the highest by pass value. As a result, by pass fraction was correlated with density and dust load of the separator feed.
- Decreasing trend was observed rotor speed and cut size of the separator. The ratio of air speed and rotor speed was correlated with corrected cut size. In addition to this density effect was reflected to this relationship.
- “ α ” and “ β ” parameters were correlated only density of the material.

Simulation studies were performed for pilot scale airswept grinding tests. Measured and simulated product particle size distributions were compared. It was concluded that developed modelling approach is successful in estimation.

9. RECOMENDATIONS

- Dam ring height and table speed are effective parameters on vertical roller mill performance. Developed model could be improved by incorporating these parameters into the model structure. It is recommended to carry out controlled tests to investigate the effects of dam ring height and table speed.
- There is a requirement for a scale-up procedure in industrial vertical roller mill modelling. In this context, it is possible to develop this procedure by increasing number of industrial scale tests.
- Breakage characterization of the materials requires a further study. A new characterization method could be developed combining compression and shear forces.
- During the modelling of static separation section, some assumptions were made. Internal circulation loads should be investigated and determined by the aid of CFD modelling. With this approach, the model could be improved.
- Developed model estimates the size distributions and flowrates. As a further study, per energy modelling of vertical roller mills should be investigated.

REFERENCES

- [1] J. Chadwick, Comminution concerns, *International Mining*, October, 18-29, **2008**.
- [2] R. Batterham, Trends in comminution driven by energy, *Advanced Powder Technology*, 22, 138-140, **2011**.
- [3] F. C. Kersting, Mathematical model of a roller mill for fuel grinding drying in coal fired power stations, *Aufbereitungs Technik*, 10, 563-571, **1994**.
- [4] R. L. Musto, M. R. Dunn, Effect of table speed and geometry on roller mill performance, *Zement Kalk Gips Transactions*, 12, 709-711, **1986**.
- [5] J. Wang, Q. Chen, Y. Kuang, A. J. Lynch, J. Zhuo, Grinding process within vertical roller mills: Experiment and simulation, *Mining Science and Technology*, Vol. 19, 97-101, **2009**.
- [6] K. Schönert, Aspects of the physics of breakage relevant to comminution, *Fourth Tewksbury Symposium*, University of Melbourne, 3.1-3.30, **1979**.
- [7] K. Schönert, O. Knobloch, Cement grinding in the twin-roll mill, *Zement-Kalk-Gips*, 11, 563-568, **1984**.
- [8] H. Kellerwessel, High pressure material bed comminution in practice, *Zement-Kalk-Gips*, 2, 57-64, **1990**.
- [9] F. Feige, Current state of development in high compression, *Zement-Kalk-Gips*, 11, 305-312, **1993**.
- [10] N. Patzelt, High pressure grinding rolls, a survey of experience, *IEEE Cement Industry Technical Conference*, Dallas/Texas, p.180, **1992**.
- [11] P. Reese, Innovation in mineral processing technology, *Proceedings of New Zealand Minerals & Mining Conference*, 29-31 October, 7 p, **2000**.
- [12] B. Parker, P. Rowe, G. Lane, S. Morrell, The decision of opt for high-pressure grinding rolls for the Boddington expansion, *SAG 2001*, III, 93-106, **2001**.
- [13] N. Aydogan, H. Benzer, Comparison of the overall circuit performance in the cement industry: High compression milling vs. ball milling technology, *Minerals Engineering*, 24, 211–215, **2011**.
- [14] FLSmidth, *FLSmidth's High Pressure Grinding Roll (HPGR)*, **2012**.
- [15] I.B. Klymowsky, J. Liu, Modelling of the comminution in a roller press, *Proceedings of the XX Int. Min. Proc. Congress (IMPC)*, Aachen, 141-154, **1997**.

- [16] N.A. Aydogan, Investigation of the Performance of High Pressure Grinding Rolls in Cement Industry. Ph.D. thesis, Hacettepe University, **2006**.
- [17] A. Cordonnier, A New Grinding Process Horomill. In: 8th European Symposium on Comminution, Stockholm, Sweeden, **1994**.
- [18] O. Genç, A.H. Benzer, Horizontal roller mill (Horomill) application versus hybrid HPGR/ball milling in finish grinding of cement, Minerals Engineering, 22, 1344–1349, **2009**.
- [19] Fives FCB, Horomill (Brochure)
- [20] S. Buzzi. The Horomill a new mill for fine comminution. ZKG International Nr. 3, 127–138, **1997**.
- [21] F.A. Huntington, Crushing mill; US 277,134, **1883**.
- [22] A.J. Lynch, C.A. Rowland, The History of Grinding, Society of Mining, Metallurgy and Exploration Inc., Colorado, **2005**.
- [23] H. Louis, A Handbook of Gold Milling, Mc Millan and Company, London, **1894**.
- [24] E.G. Loesche, The roller mill story: Loesche 1906-1981, World Cement, 13, 82-83, **1982**.
- [25] Loesche GmbH, Mills for the world: Loesche's 1906-2006 centenary, ZKG International, 59, 10, 26-34, **2006**.
- [26] H. Brundiek, The roller grinding mill-Its history and current situation, Aufbereitungs-Technik, 10, 609-745, **1989**.
- [27] W.H. Duda, Cement-Data-Book, 1, International Process Engineering in the Cement Industry, French & European, 3rd edition, **1985**.
- [28] K. Sekine, K. Sutoh, M. Ichikawa, I. Hashimoto, S. Sawamura, H. Ueda, Increasing the throughput of grinding plants by using the CKP system, ZKG International, 44, 337-341, **1991**.
- [29] R. F. Miranda, I. Minas, W. T. Yamana, S. Pirapora, V. Cimentos, P. Tete, Brazilian progress in grinding, World Cement, 29, 40-42, **1998**.
- [30] J. Dupuis, C. Rhin , Increased grinding capacity at R.A.K., World Cement, 2, 79-83, **2003**.
- [31] H.U. Schaefer, Loesche mills for grinding of clinker and slag for the production of cement with interground additives, ZKG International, 54, 1, 20-30, **2001**.

- [32] H.U. Schaefer, Loesche vertical roller mills for the comminution of ores and minerals, *Minerals Engineering*, 14, 10, 1155-1160, **2011**.
- [33] P. Jacobs, 15 Years Successful Operation of a Loesche VRM Type LM 50.4 in a Hard Rock Application at Foskor Pty (Ltd) in Phalaborwa, Top Employers Institute, South Africa, **2014**.
- [34] C. Woywadt, Slag grinding with Loesche vertical roller mills, *Global Slag Magazine*, July, 25-29, **2006**.
- [35] Loesche GmbH, Loesche mills for cement raw material (Brochure)
- [36] Loesche GmbH, Loesche mills for cement and granulated blast furnace slag (Brochure).
- [37] E. Y. Reichard, P. Heyd, K. P. Lukas, MPS vertical roller mills for slag and slag cements, *Global Cement Magazine*, November, 22-24, **2007**.
- [38] O. Jung, B. Kraft, High efficiency classifiers for MPS vertical roller mills, *ZKG International*, 58, 6, 55-60, **2005**.
- [39] Y. Reichardt, The use of MPS vertical roller mills in the production of cement and blast furnace slag powder, *Cement International*, 3, 2, 64-69, **2005**.
- [40] Gebr Pfeiffer, Competence in Cement (Brochure).
- [41] C. Woywadt, Operating experience with the Pfeiffer MVR vertical roller mill and the Multidrive, *ZKG International*, 12, 1-8, **2012**.
- [42] Y. Reichardt, The new Pfeiffer roller mill MVR: reliable grinding technology for high throughput rates, *ZKG International*, 11, 40-45, **2010**.
- [43] FL Smidth, Atox Coal mill (Brochure)
- [44] S. W. Jorgensen, Cement grinding-a comparison between vertical roller mill and ball mill, *Cement International*, 3, 2, 54-63, **2005**.
- [45] FL Smidth, OK Vertical roller mill (Brochure).
- [46] T. Tamashige, H. Obana, M. Hamaguchi, Operational results of OK series roller mill, *IEEE Transactions of Industry Applications*, 27, 3, 99. 416-424, **1991**.
- [47] M. Ito, K. Sato, Y. Naoi, Productivity increase of the vertical roller mill for cement grinding, *Cement Industry Technical Conference*, 39. Conference Record, IEEE, 177 – 194, **1997**.
- [48] FL Smidth, OK Vertical roller mill (Brochure).
- [49] ThyssenKrupp AG, The Quadropol roller mill (Brochure).

- [50] ThyssenKrupp AG, Raw material preparation. From the quarry to raw meal feeding into the preheater, (Brochure).
- [51] T. Schmitz, The world's first vertical roller mill with driven rollers, Cement Industry Technical Conference (CIC), 1-5, **2014**.
- [52] ThyssenKrupp AG, QUADROPOL® QMC: Roller mill for the grinding of cement and blast furnace slag, (Brochure).
- [53] S. Fujimoto, Reducing specific power usage in cement plants, World Cement, 7, 25-35, **1993**.
- [54] J.F. Becker, J.W. Sweeney, W.C. Wentzel, The design and manufacture of large vertical roller mills, Zement Kalk Gips, 2, 40-43, **1993**.
- [55] G.R. Roy, Increasing cement grinding capacity with vertical roller mill technology, Cement Industry Technical Conference, 44. Conference Record, IEEE, 205 -211, **2002**.
- [56] M. Simmons, L. Gorby, J. Terembula, Operational experience from the United States' first vertical mill for cement grinding, Cement Industry Technical Conference, IEEE, 241-249, **2005**.
- [57] T. Fahrland, K. H. Zysk, Cements ground in the vertical roller mill fulfil the quality requirements of the market, Cement International, 11, 2, 64-69, **2013**.
- [58] H.U., Schaefer, Slag Grinding: Latest Advances, World Cement, 9, 61-66, **2002**.
- [59] H. U., Schaefer, Experiences in grinding slag and additives, World Cement, February, 26, 58-62, **1998**.
- [60] S. Hashimoto, Evolution of a mill, World Cement, December, 31-36, **2002**.
- [61] W. van Drunick, C. Gerold, N. Palm, Implementation of an energy efficient dry grinding technology into an Anglo American zinc beneficiation process, XXV International Mineral Processing Congress (IMPC) Proceedings, Brisbane, QLD, Australia, 1333-1341, **2010**.
- [62] C. Gerold, C. Schmitz, M. Stapelmann, F. Dardemann, Recent installations and developments of loesche vertical roller mills in the ore industry, Comminution'12 Proceedings, Cape Town, South Africa, 1-22, **2012**.
- [63] D. Altun, C. Gerold, H. Benzer, O. Altun, N. Aydogan, Copper ore grinding in a mobile vertical roller mill pilot plant, International Journal of Mineral Processing, 136, 32-36, **2015**.

- [64] C. Gerold, C. Schmitz, M. Stapelmann and F. Dardemann, Latest installations and developments of Loesche vertical roller mills in the ore industry, XXVI International Mineral Processing Congress (IMPC), New Delhi, India, 18-29, **2012**.
- [65] J. M. Brugan, State of art raw grinding, Zement Kalk Gips, 1, 9-13, **1993**.
- [66] H. U. Schaefer, Loesche Vertical roller mills for the comminution of ores and minerals, Minerals Engineering, 14, 10, 1155-1160, **2001**.
- [67] H. Brundiek, H. J. Poeschl, Roller mill application for high moisture feed, 39th Cement Industry Technical Conference, 21.4. - 24.4, Hershey, Pennsylvania, 213-225, **1997**.
- [68] H. Brundiek, Drying and grinding of extremely moist cement raw materials in the Loesche mill, ZKG International, 51, 2, 64-71, **1998**.
- [69] S.P. Deolalkar, Handbook for designing cement plants, BS Publications, Hyderabad, India, **2009**.
- [70] R.M. Viljoen, J.T. Smit, I. Du Plessis and V. Ser, The development and application of in bed compression breakage principles, Minerals Engineering, 14, 5., 465-471, **2001**.
- [71] R. Crosbie, C. Robertson, I. Smit and V. Ser, The benefits of inter-particle comminution on flotation, Centenary of Flotation Symposium, Brisbane, QLD, 823-828, **2005**.
- [72] M. Reichert, C. Gerold, A. Fredriksson, G. Adolfsson, H. Lieberwirth, Research of iron ore grinding in a vertical-roller-mill, Minerals Engineering, 73, 109-115, **2015**.
- [73] E. Erkan, S. Umurhan, B. Sayiner, M. Cankurtaran, A.H. Benzer, N. A. Aydogan, H.K. Demir, J. Langel, C. Gerold, Comparison of the vertical roller mill and rod-ball mill circuit on the gold extraction, Proceedings of XIIIth International Mineral Processing Symposium, Bodrum, Turkey, **2012**.
- [74] C. Oesch, B. Jurko, Finish grinding with vertical roller mills-operating data, Cement Industry Technical Conference, 44. Conference Record, IEEE, 187-192, **2002**.
- [75] G. Berk, H. A. Fischer, C. Hackländer-Woywadt, First installed LM 56.3+3 in Turkey-Operating experiences, ZKG International, 60, 10, 51-56, **2007**.
- [76] K. Shimojima, M. Hamaguchi, H. Obana, K. Fukuyama, Newly developed roller mill for cement clinker grinding, World Cement, 15, 7, 78-87, **1984**.

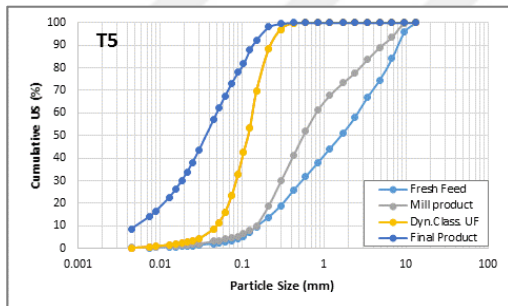
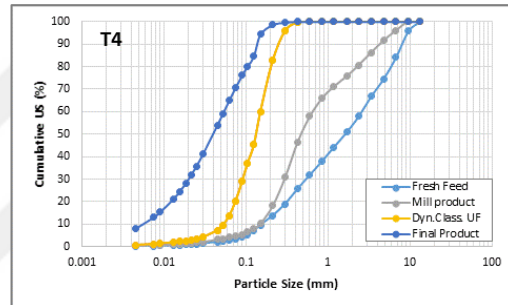
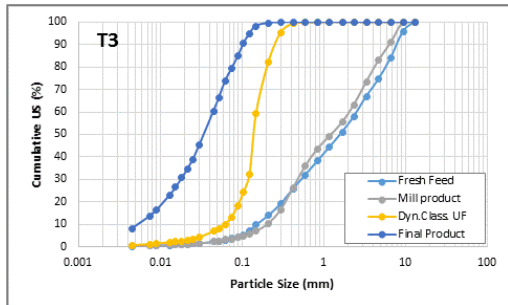
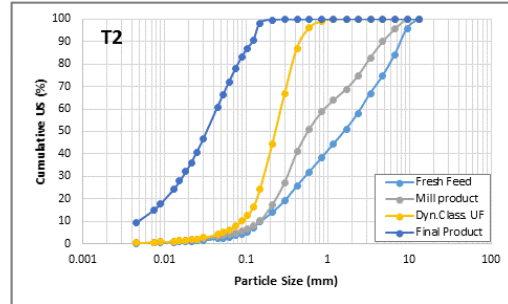
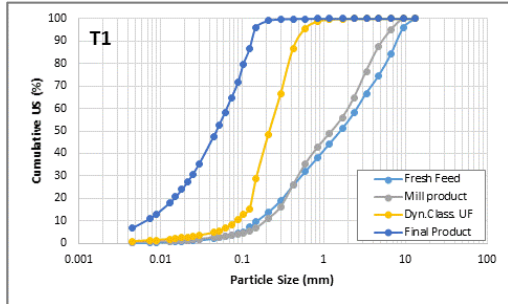
- [77] W. Wahl, Improving the wear protection on the grinding rollers in roller grinding mills, *Zement Kalk Gips*, 6, 167-170, **1994**.
- [78] O. Jung, Wear protection in vertical roller mills, *ZKG International*, 53, 5, 252-260, **2000**.
- [79] O. Velz, F. J. Hülsbusch, New technology to increase wear parts service life in vertical roller mills, *Cement International*, 1, 2, 65-70, **2003**.
- [80] Loesche GmbH, Loesche mills for ores and minerals (Brochure).
- [81] M. Keyssner, P.C. Abraham, A decade of VRM progress for Loesche, *Global Cement Technology*, March, 24-30, **2005**.
- [82] M. Keyssner, Making vertical strides, August, *International Cement Review*, **2006**.
- [83] S.C. Ahluwalia, C. Hackländer-Woywadt, P. C. Abraham Operating experience with the first Loesche mill with the 3+3 system for grinding clinker and blastfurnace slag, *Cement International*, 4, 2, 90-98, **2006**.
- [84] L.T. Schneider, L. Lohnherr, G. Gudat, Roller mills for high capacities and difficult material, *Zement Kalk Gips*, 12, 85, 705-708, **1986**.
- [85] High quality milling, *International Cement Review*, March **2002**.
- [86] S. Strasser, R.A. Somani, A.K. Dembla, Improvements in the production of raw meal and cement by the combined use of roller press and V-separator, *Zement Kalk Gips*, 50, 3, 140-146, **1997**.
- [87] A.L. Pastala, Contribution to the design of air separation equipment for closed circuit grinding systems, *Cement Technology*, 119-1249, **1978**.
- [88] J.F. Becker, J.W. Sweeney, W.C. Wentzel, The design and manufacture of large vertical roller mills, *Zement Kalk Gips*, 2, 40-43, **1993**.
- [89] B.H. Schonbach, High efficiency separators in roller mills, *World Cement*, November, **1988**.
- [90] H. K. Demir, Investigation of effect of operational parameters on vertical roller mill performance, Hacettepe University Msc. Thesis, **2015**.
- [91] D. Altun, H. Benzer, N. Aydogan, C. Gerold, Operational parameters affecting the vertical roller mill performance, *Minerals Engineering* (In press), **2016**.
- [92] L. G. Austin, P. T. Luckie, K. Shoji, An analysis of ball and race milling Part II. The babcock E 1.7 mill, *Powder Technology*, 33, 1, 113-125, **1982**.
- [93] L. G. Austin, P. T. Luckie, K. Shoji, An analysis of ball and race milling Part III. Scale-up to industrial mills, *Powder Technology*, 33, 1, 127-134, **1982**.

- [94] O. Jung, Developments and operational experience with vertical roller mills the cement industry, ZKG International, 8, 452-458, **1999**.
- [95] O. Jung, Rating of vertical roller mills on the basis of grindability tests, Aufbereitungs Technik, 43, 44-50, **2002**.
- [96] O. Jung, Raising the output of vertical roller mills as an alternative to new capital investment, Cement International, 2, 52-57, **2004**.
- [97] K. Sato, N. Meguri, K. Shoji, H. Kanemoto, T. Hasegawa, T. Maruyama, Breakage of coals in ring-roller mills Part I. The breakage properties of various coals and simulation model to predict steady-state mill performance, Powder Technology, 86, 275-283, **1996**.
- [98] K. Shoji, N. Meguri, K. Sato, H. Kanemoto, T. Hasegawa, T. Maruyama, Breakage of coals in ring-roller mills Part 2. An unsteady-state simulation model, Powder Technology, 99, 46-52, **1998**.
- [99] N.A. Aydogan, A simple sampling method for VRMs, ZKG International, 3, 50-55, **2015**.
- [100] D. Eksi, H. Benzer, A. Sargin, O. Genc, A new method for determination of fine particle breakage, Minerals Engineering, 24, 216-220, **2011**.
- [101] H. Dundar, An Investigation of the Performance of the High Pressure Grinding Rolls During the Ore Grinding in the Minerals Industry, Hacettepe University Ph.D. Thesis. (in Turkish), **2012**.
- [102] B. Epstein, The material description of certain breakage mechanisms leading to the logarithmic-normal distribution, Journal of the Franklin Inst., 244, 471-477, **1947**.
- [103] T. J. Napier-Munn, S. Morrell, R. D. Morrison, T. Kojovic, Mineral comminution circuits and their operation and optimisation, JKMRRC monogram series in mining and mineral processing, Brisbane, Australia, p.413, **1996**.
- [104] H. Dundar, H. Benzer, N. A. Aydogan, **2013**, Application of population balance model to HPGR crushing, Minerals Engineering, 50-51, 114-120.
- [105] M. Ito, K. Sutoh, T. Matsuda, Classification efficiency of cage-type air classifier, Zement Kalk Gips, 49, 3, 134-141, **1996**.
- [106] L.R. Plitt, A mathematical model of the hydrocyclone classifier, CIM Bull. 69 (776), 114-123, **1976**.

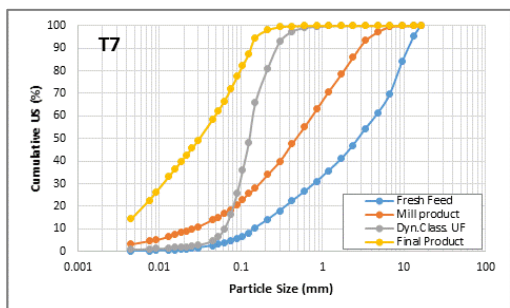
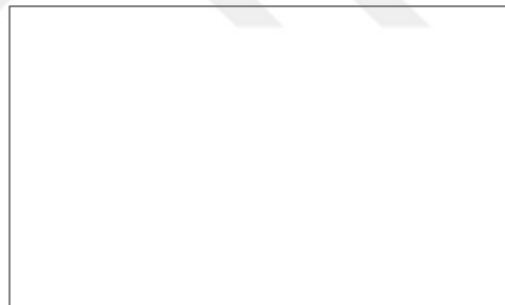
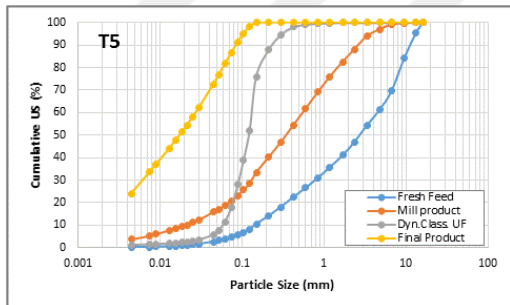
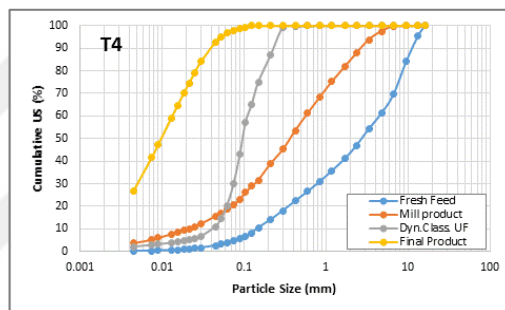
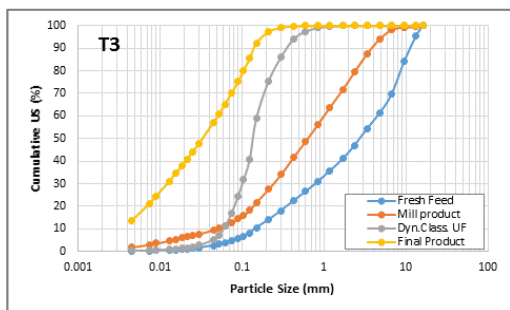
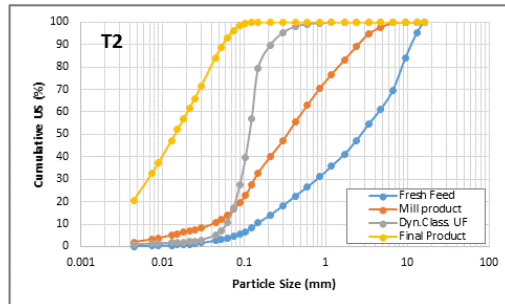
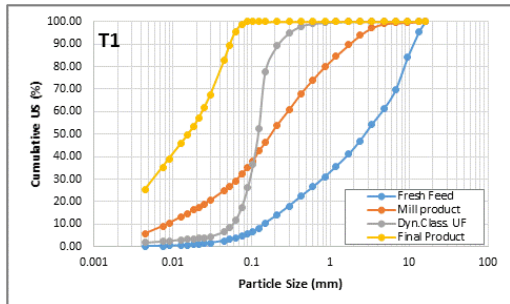
- [107] E. Lippek, D. Espig, Forschungsarbeiten zur Mathematischen, Modellierung von Trockenmahlangen, Freiburger Forschungsheft, 602 77-78, **1978**.
- [108] J.A. Finch, Modelling a fish-hook in hydrocyclone selectivity curves, Powder Technology, 36, 127-129, **1983**.
- [109] Y.M. Zhang, A. Kavetsky, T.J. Napier-Munn, Effects of separator efficiency on clinker grinding circuits, Zement Kalk Gips, 41, 10, 501-505, **1988**.
- [110] E. Onuma, M. Ito, Separators in grinding circuits, Zement Kalk Gips, 47, 9, 535-542, **1994**.
- [111] O. Altun, H. Benzer, Selection and mathematical modelling of high efficiency air classifiers, Powder Technology, 264, 1-8, **2014**.
- [112] H. Benzer, O. Altun, O. Oksuz, E. Uzun, Investigating the Effects of Specific Gravity Difference on Air Classification Performance, SAIMM Conferences, **2008**.
- [113] O. Altun, A. Toprak, H. Benzer, O. Darılmaz, Multi component modelling of an air classifier, Minerals Engineering, 93, 50-56, **2016**.
- [114] J. G. Bennet, Broken coal, Inst. Fuel, 15, 524, **1936**.

APPENDICES

APPENDIX-1: Measured raw particle size distributions of polymetallic ore (Loesche OGPmobile-overflow mode)



APPENDIX-2: Measured raw particle size distributions of chalcopyrite ore (Loesche OGPmobile-overflow mode)



APPENDIX-3: Full circuit model fit results for polymetallic ore

			Fresh Feed	Mill feed	Mill product	V Sep. Feed	V Sep. Reject	Dyn. Sep. Feed	Dyn. Sep. Reject	Final Product
T1	Flowrate (kgh)	Balanced	86.5	2233.5	2233.5	2320.0	2023.9	296.1	209.6	86.5
		Fit	86.5	2233.4	2233.4	2319.9	2024.3	295.6	209.1	86.5
	P₈₀ (mm)	Balanced	5.86	3.94	3.79	3.86	4.18	0.32	0.37	0.10
		Fit	5.86	3.96	3.71	3.86	4.19	0.30	0.34	0.11
T2	Flowrate (kgh)	Balanced	121.9	2893.4	2893.4	3015.3	2746.2	269.1	147.2	121.9
		Fit	121.9	2894.4	2894.4	3016.3	2746.9	269.4	147.6	121.9
	P₈₀ (mm)	Balanced	5.86	3.25	2.99	3.15	3.39	0.29	0.38	0.08
		Fit	5.86	3.04	3.08	2.90	3.20	0.16	0.19	0.08
T3	Flowrate (kgh)	Balanced	85.6	3325.9	3325.9	3411.5	3205.5	206.0	120.4	85.6
		Fit	85.6	3327.9	3327.9	3413.5	3207.5	206.0	120.4	85.6
	P₈₀ (mm)	Balanced	5.86	4.43	4.31	4.36	4.53	0.17	0.21	0.08
		Fit	5.86	4.43	4.28	4.36	4.53	0.17	0.20	0.08
T4	Flowrate (kgh)	Balanced	106.2	2236.0	2236.0	2342.2	2123.5	218.7	112.5	106.2
		Fit	106.2	2236.9	2236.9	2343.1	2124.7	218.4	112.2	106.2
	P₈₀ (mm)	Balanced	5.86	2.58	2.27	2.42	2.74	0.17	0.20	0.10
		Fit	5.86	2.58	2.34	2.42	2.74	0.17	0.20	0.10
T5	Flowrate (kgh)	Balanced	196.1	3734.1	3734.1	3930.2	3441.4	488.8	292.7	196.1
		Fit	196.1	3732.6	3732.6	3928.7	3501.3	427.3	231.3	196.1
	P₈₀ (mm)	Balanced	5.86	3.07	2.68	2.90	3.31	0.16	0.18	0.10
		Fit	5.86	3.07	2.87	2.90	3.26	0.16	0.19	0.10

APPENDIX-4: Full circuit model fit results for chalcopyrite ore

			Fresh Feed	Mill feed	Mill product	V Sep. Feed	V Sep. Reject	Dyn. Sep. Feed	Dyn. Sep. Reject	Final Product
T1	Flowrate (kgh)	Balanced	198.0	2818.6	2818.6	3016.7	2350.5	666.2	468.1	198.0
		Fit	198.0	2818.6	2818.6	3016.7	2349.3	667.4	469.4	198.0
	P₈₀ (mm)	Balanced	8.70	1.17	0.86	1.08	1.54	0.14	0.16	0.04
		Fit	8.70	1.17	0.86	1.15	1.57	0.14	0.22	0.04
T2	Flowrate (kgh)	Balanced	204.1	3234.8	3234.8	3438.9	2720.3	718.5	514.4	204.1
		Fit	204.1	3234.8	3234.8	3438.9	2720.4	718.4	514.4	204.1
	P₈₀ (mm)	Balanced	8.70	1.76	1.45	1.65	2.10	0.14	0.15	0.04
		Fit	8.70	1.76	1.45	1.65	2.10	0.14	0.16	0.04
T3	Flowrate (kgh)	Balanced	475.7	4584.0	4584.0	5059.7	4176.0	883.6	408.0	475.7
		Fit	475.7	4584.0	4584.0	5059.7	4176.0	883.6	408.0	475.7
	P₈₀ (mm)	Balanced	8.70	3.05	2.43	2.81	3.25	0.17	0.25	0.10
		Fit	8.70	3.05	2.43	2.81	3.25	0.17	0.22	0.11
T4	Flowrate (kgh)	Balanced	198.0	2218.4	2218.4	2416.4	1981.5	435.0	236.9	198.0
		Fit	198.0	2218.4	2218.4	2416.4	1843.5	572.9	374.9	198.0
	P₈₀ (mm)	Balanced	8.70	2.05	1.56	1.87	2.27	0.12	0.18	0.03
		Fit	8.70	1.90	1.56	1.87	2.27	0.12	0.15	0.03
T5	Flowrate (kgh)	Balanced	373.1	3821.8	3821.8	4194.9	3359.7	835.2	462.1	373.1
		Fit	373.1	3821.8	3821.8	4194.9	3356.5	838.4	465.3	373.1
	P₈₀ (mm)	Balanced	8.70	2.05	1.51	1.84	2.31	0.14	0.17	0.06
		Fit	8.70	2.05	1.51	1.84	2.31	0.14	0.18	0.06
T6	Flowrate (kgh)	Balanced	312.3	3676.5	3676.5	3988.8	3098.5	890.4	578.1	312.3
		Fit	312.3	3676.5	3676.5	3988.8	3098.1	890.7	578.4	312.3
	P₈₀ (mm)	Balanced	8.70	2.16	1.69	2.00	2.50	0.16	0.21	0.05
		Fit	8.70	2.16	1.69	2.00	2.50	0.17	0.21	0.05
T7	Flowrate (kgh)	Balanced	459.3	3507.7	3507.7	3967.0	3331.4	635.6	176.3	459.3
		Fit	459.3	3507.7	3507.7	3967.0	3331.3	635.7	176.4	459.3
	P₈₀ (mm)	Balanced	8.70	2.48	1.84	2.23	2.60	0.13	0.22	0.10
		Fit	8.70	2.48	1.84	2.23	2.60	0.13	0.15	0.10

CURRICULUM VITAE

Credentials

Name, Surname: Deniz Altun

Place of Birth: Ankara

Marital Status: Married

E-mail: deksi@hacettepe.edu.tr

Address: Hacettepe University Dept. of Mining Engineering ANKARA

Education

BSc. : 2002-2007, Hacettepe University, Dept. of Mining Engineering

MSc. : 2008-2011, Hacettepe University, Dept. of Mining Engineering

PhD. : 2011-... , Hacettepe University, Dept. of Mining Engineering

Foreign Languages

English

Work Experience

2009-... :Research Assistant at Hacettepe University Mining Engineering Department

Areas of Experiences

Performance evaluation, modelling and simulation of comminution circuits

Projects and Budgets

Publications

D. Altun, C. Gerold, H. Benzer, O. Altun, N. Aydogan, Copper ore grinding in a mobile vertical roller mill pilot plant, International Journal of Mineral Processing, 136, 32-36, 2015.

D. Altun, H. Benzer, N. Aydogan, C. Gerold, Operational parameters affecting the vertical roller mill performance, Minerals Engineering (In press), 2016.

Oral and Poster Presentations

Ore grinding practices with Loesche OGP (ore grinding plant) Mobile, ESCC 2013, Germany



HACETTEPE UNIVERSITY
GRADUATE SCHOOL OF SCIENCE AND ENGINEERING
THESIS ORIGINALITY REPORT



HACETTEPE UNIVERSITY
GRADUATE SCHOOL OF SCIENCE AND ENGINEERING
TO THE DEPARTMENT OF MINING ENGINEERING

Date: 31/01/2017

Thesis Title: Mathematical modelling of vertical roller mills

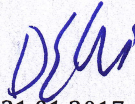
According to the originality report obtained by my thesis advisor by using the *Turnitin* plagiarism detection software and by applying the filtering options stated below on 30/01/2017 for the total of 124 pages including the a) Title Page, b) Introduction, c) Main Chapters and d) Conclusion sections of my thesis entitled as above, the similarity index of my thesis is 1 %.

Filtering options applied:

1. Bibliography/Works Cited excluded
2. Quotes excluded
3. Match size up to 5 words excluded

I declare that I have carefully read Hacettepe University Graduate School of Science and Engineering Guidelines for Obtaining and Using Thesis Originality Reports; that according to the maximum similarity index values specified in the Guidelines, my thesis does not include any form of plagiarism; that in any future detection of possible infringement of the regulations I accept all legal responsibility; and that all the information I have provided is correct to the best of my knowledge.

I respectfully submit this for approval.


31.01.2017

Name Surname: Deniz Altun

Student No: N10248367

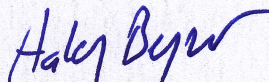
Department: Mining Engineering

Program: Mining Engineering

Status: Masters Ph.D. Integrated Ph.D.

ADVISOR APPROVAL

APPROVED.



Prof. Dr. A. Hakan Benzer